

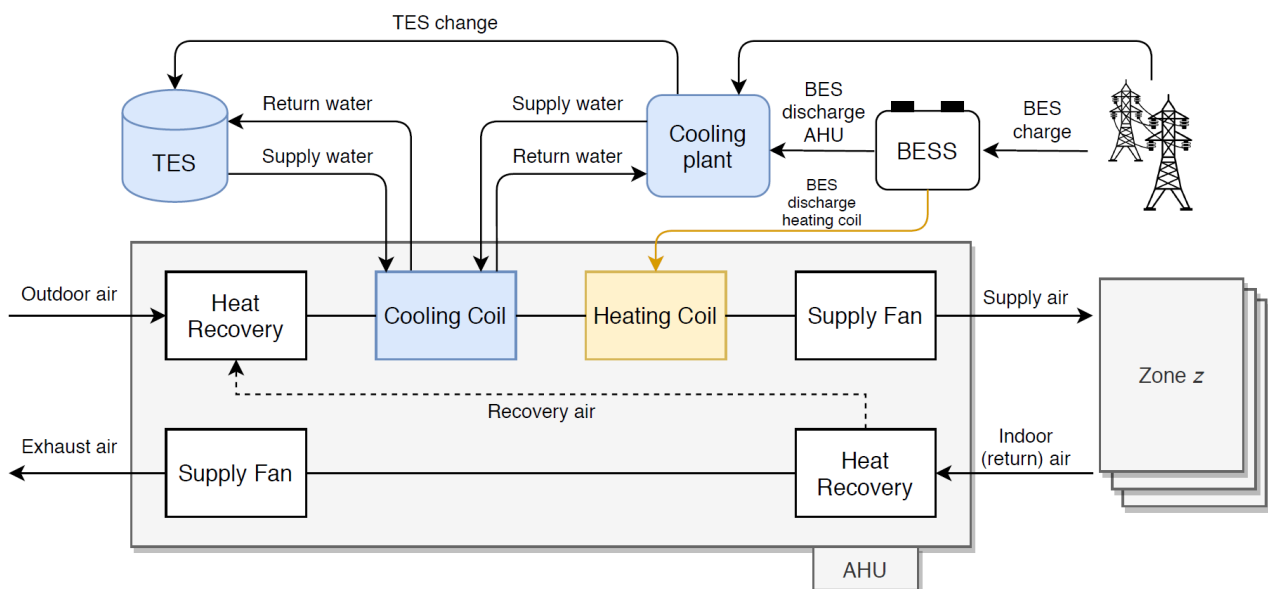


**KTH Industrial Engineering  
and Management**

# Optimization of integrated energy storage for implicit demand-side flexibility

The case study of Singapore office buildings

Tommaso Miori



**Master of Science Thesis**

KTH School of Industrial Engineering and Management

Energy Technology: TRITA-ITM-EX 2020:10

Division of Heat & Power Technology

SE-100 44 STOCKHOLM



KTH Industrial Engineering  
and Management

**Master of Science Thesis in Energy Technology  
TRITA-ITM-EX 2020:10**

**Optimization of integrated energy storage for  
implicit demand-side flexibility**

The case study of Singapore office buildings

Tommaso Miori

Approved 2019-12-12	Examiner Peter Hagström - KTH/ITM/EGI	Supervisor Miroslav Petrov
	Commissioner Technische Universität München TUM-CREATE Ltd. - Singapore	Contact person Sebastian Troitzsch

## Abstract

Demand-Side Flexibility (DSF) is a very attractive option to solve challenges that are emerging from the evolution of modern power systems all around the world. The greater integration of intermittent renewable energy sources into the energy mix creates the need for flexible end-user behavior and demand management. In Singapore, distributed power production grows steadily in the form of rooftop solar PV panels installed on both households and commercial buildings, where the main load demand is cooling and air conditioning. Challenges arise also from the projected rapid increase in the penetration of Electric Vehicles (EVs). The charging routines of EVs could represent a high and potentially dangerous power peak that the current electrical grid is not able to withstand. Providing the ability to shift the demand profile of a large building or a neighborhood with minimum modifications of the electrical grid, DSF is poised to play a central role in solving these challenges during the next 10-20 years.

This study proposes linear mathematical modeling for the optimum utilization of sensible-heat thermal and electrochemical battery energy storage, implemented in the already existing building modelling framework developed by TUM-CREATE, the CoBMo. An optimization problem is defined aiming to minimize the total cost as the sum of operational costs from the electricity consumption of the HVAC system and the investment costs for the energy storage. Financial payback analysis is performed using the CoBMo version improved with the mathematical model to estimate the achievable annual savings. The discounted payback time is considered as an economic indicator to whether the storage would be a valid investment or not depending on the electricity price signal – wholesale and retailer – as well as on the storage operation setup and installation costs, lifetime, efficiency, etc.

The economic analysis shows that both the thermal energy and battery storage options are feasible for office buildings in Singapore considering the investment conditions from year 2020 onwards. While chilled-water thermal energy storage is well established and relatively simple technology, the battery storage displays better economic return when selecting Li-Ion Nickel Manganese Cobalt (NMC) technology. The optimal daily schedule of both storage solutions is presented in this study, showing how the optimization tool leverages the price signals, relying on trade-offs between operational expenditures and investment costs for the energy storage systems.

## SAMMANFATTNING

Den inbyggda flexibiliteten av elkonsument vid slutanvändarna för att jämna ut en varierande tillförsel av elkraft från produktionssidan kallas för "Demand-Side Flexibility" (DSF). DSF är ett attraktivt verktyg för att lösa utmaningarna som uppstår från den växande andelen elproduktion baserad på varierande energikällor såsom solkraft och vindkraft, som utvecklas överallt i världen. I Singapore växer utbyggnaden av solkraft mycket snabbt i form av solceller på byggnaders tak och den större integrationen av förnybara resurser i energiblandningen skapar ett behov av att göra efterfrågan flexibel med tanke på det typiskt stora andelen kyla och luftkonditionering. Utmaningar uppstår också från den förväntade snabba ökningen av antalet elfordon vars laddningsrutiner representerar en hög och potentiellt farlig effekttopp som det nuvarande elnätet kommer snart inte kunna tåla. Därför spelar DSF-tekniken en central roll när det gäller effektiva lösningar för dessa utmaningar inom de kommande 10-20 åren.

Studien härmed föreslår en optimeringsmetod baserad på linjära matematiska modeller för byggnadsintegrerade energilagringssystem i form av både kylvattenlagring och elbatterier. Metoden implementeras i ett redan befintligt program för modellering av byggnadsenergisystem som utvecklats av TUM-CREATE och kallas för CoBMo. Optimeringsmålet definieras för att minimera den totala kostnaden som är summan av driftskostnaderna för VVS-systemet samt investeringskostnaderna för energilagringen. En ekonomisk återbetalningsanalys utförs med hjälp av CoBMo-programmet förbättrad med det härmed utvecklade optimeringsverktyget som utvärderar de årliga besparingarna. Återbetalningstiden betraktas som en ekonomisk indikator på huruvida energilagringen skulle varit en giltig investering eller ej, beroende på en varierande elprissignal – både grossist elhandel och elpriset för småkunder – och även energilagringens användarprofil och effektivitet samt kostnaderna för installation, underhåll, avskrivningar, m.m.

Den ekonomiska analysen visar att både kylvattenackumulator samt elbatterier integrerade i kontorsbyggnader i Singapore kan leverera avkastning med tanke på det förväntade investeringsklimatet från och med år 2020. Även om lagringen av värme och kyla är en beprövad och relativt enkel teknik, studien visar att batterilagring står sig bättre ekonomiskt, särskilt när man väljer Li-Ion Nickel Mangan Cobalt (NMC) tekniken. Den optimala dagliga laddnings- och urladdningsstrategin för vardera energilagringens lösningen presenteras i resultaten från denna studie, vilket visar hur optimeringsmodellen utnyttjar de prissignaler som tillhandahålls och gör en avvägning mellan driftsutgifter och investeringskostnader för energilagringen.

# Contents

<b>Contents</b>	<b>1</b>
<b>List of Figures</b>	<b>4</b>
<b>List of Tables</b>	<b>7</b>
<b>1 Introduction</b>	<b>8</b>
1.1 Energy consumption in buildings . . . . .	8
1.2 Singapore Energy outlook . . . . .	9
1.2.1 Singapore energy imports and exports . . . . .	9
1.2.2 Electricity production mix . . . . .	9
1.2.3 Electricity consumption and customer categorization in Singapore	9
1.2.4 Electricity market structure . . . . .	12
1.2.5 Singapore and Sustainability . . . . .	14
1.2.6 Solar energy . . . . .	17
1.2.7 The role of Storage . . . . .	18
1.2.8 Demand Side Management in Singapore . . . . .	19
1.3 Motivation and Research question . . . . .	20
1.4 Scope of the thesis . . . . .	21
1.4.1 Physical boundaries of the thesis . . . . .	22
1.5 Introducing the Control-Oriented Building Model . . . . .	22
<b>2 Literature Review</b>	<b>24</b>
2.1 Demand Side Flexibility (DSF) . . . . .	24
2.2 Mathematical Programming . . . . .	26
2.3 Model Predictive Control (MPC) . . . . .	29
2.3.1 Building Modelling for MPC . . . . .	29
2.4 Storage and control . . . . .	34
2.4.1 Storage strategies . . . . .	34
2.4.2 Storage and MPC . . . . .	35
2.5 Storage Technologies . . . . .	38

2.5.1	Thermal storage . . . . .	38
2.5.2	Battery energy storage . . . . .	39
2.5.3	Main ageing parameters in BES . . . . .	43
2.6	Storage system modelling approaches . . . . .	45
2.6.1	TES Modelling . . . . .	45
2.6.2	Losses and efficiency in storage tanks . . . . .	48
2.7	Introduction to the Methodology . . . . .	50
<b>3</b>	<b>Mathematical Modelling of Energy Storage</b>	<b>52</b>
3.1	Demand-Side Flexibility in Buildings . . . . .	52
3.2	Control-oriented Building Model . . . . .	56
3.2.1	The thermal model . . . . .	56
3.2.2	Indoor Air Quality (IAQ) model . . . . .	57
3.2.3	State-Space formulation . . . . .	58
3.2.4	Thermal flexibility of buildings . . . . .	60
3.2.5	The thermal model in the CoBMo . . . . .	61
3.2.6	CREATE Tower test case . . . . .	65
3.3	Modelling of TES . . . . .	67
3.3.1	Thermal flows Model . . . . .	67
3.3.2	Single Temperature Tank Model . . . . .	70
3.3.3	Two layers storage model . . . . .	72
3.3.4	Mass flows model . . . . .	77
3.4	Modelling of BES . . . . .	79
3.5	Modelling storage into the CoBMo . . . . .	83
3.5.1	Air-Handling Unit (AHU) . . . . .	84
3.5.2	Terminal Unit (TU) . . . . .	89
<b>4</b>	<b>Optimization Problem</b>	<b>92</b>
4.1	Implementation Approach . . . . .	92
4.1.1	Coding overview . . . . .	93
4.2	Independent framework . . . . .	95
4.3	CoBMo optimization framework . . . . .	101
4.4	Economic Analysis and Optimization . . . . .	104
4.5	Economic Analysis: theory and approach . . . . .	108
<b>5</b>	<b>Results</b>	<b>111</b>
5.1	Cost assumptions of storage . . . . .	111
5.1.1	TES cost assumptions . . . . .	111
5.1.2	BES cost assumptions . . . . .	113
5.2	Price signals . . . . .	117
5.3	Results: Economic Analysis . . . . .	118

---

5.3.1	TES Economic Analysis . . . . .	119
5.3.2	BES Economic Analysis . . . . .	121
5.4	Results: Optimal Scheduling . . . . .	126
5.4.1	Optimal Scheduling: TES . . . . .	126
5.4.2	Optimal Scheduling: BES . . . . .	130
<b>6</b>	<b>Discussion</b>	<b>133</b>
6.1	Economic Analysis . . . . .	133
6.2	Optimal Scheduling . . . . .	134
6.3	Limitations of the Analysis . . . . .	135
<b>7</b>	<b>Future Work</b>	<b>137</b>
<b>8</b>	<b>Conclusions</b>	<b>139</b>
	<b>Acknowledgments</b>	<b>141</b>
	<b>Bibliography</b>	<b>142</b>

# List of Figures

1.1	Singapore electricity mix by fuel (EMA, 2018b) . . . . .	10
1.2	Singapore electricity consumption by sector and by contestability (EMA, 2018b) . . . . .	10
1.3	Overview of the Singapore electricity market (OEM, 2019) . . . . .	12
1.4	Singapore’s Climate Action Plan – framework (NCCS) . . . . .	15
1.5	Singapore’s Climate Action Plan – framework (NCCS) . . . . .	16
1.6	Floating PV pilot in Tengeh Reservoir (MFA, 2018) . . . . .	17
1.7	Physical boundaries of the thesis withing the CoBMo. . . . .	22
2.1	Types of model categories proposed by (McCarl and Spreen, 1997) . . . . .	26
2.2	Using MILP to approximate nonlinear load curve of a chiller with a piecewise linear function (Rawlings et al., 2018) . . . . .	27
2.3	Mapping of thermal modelling approaches for buildings (Atam and Helsen, 2016) . . . . .	29
2.4	(Serale et al., 2018) maps the most critical aspects of an MPC. . . . .	33
2.5	Graphical representation of the different strategies to use storage (Sun et al., 2013). The dotted --- line represents the chiller power. . . . .	35
2.6	Measured temperature inside a the chilled water storage tank in the UC Merced Campus (Ma et al., 2009) . . . . .	36
2.7	Selected and fixed operation profile used by (Ma et al., 2009) . . . . .	37
2.8	Representation of the demand-levelling control of storage to adjust the chiller operation after a fast DR event (Tang et al., 2019) . . . . .	38
2.9	Classification of lithium batteries (Stan et al., 2014) . . . . .	40
2.10	Basic functioning of a of a lithium metal oxide cathode and carbon-based anode Li-ion battery (ISEA, 2012) . . . . .	40
2.11	Representation of the single-temperature model for a typical water tank (Duffie and Beckman, 2013) . . . . .	46
2.12	Representation of two-layers stratified tank for sensible thermal storage. (Rearranged from (Deng et al., 2015)) . . . . .	47
2.13	Sketch of how the methodology is structured, pointing out with a ✓ what was part of the scope of this thesis. . . . .	50

3.1	Possible setups for the operation of an HVAC of a building. The profiles for Load , temperature and tariff are qualitative and they do not reflect any real value. . . . .	54
3.2	Examples of load curves. Detail of Fig. 3.1. Case a) is the non-flexible building, while b) is the flexible one. . . . .	54
3.3	Use-Of-System tariff depending on the voltage connection of the customer (Geneco, 2019) . . . . .	55
3.4	Overview of the CoBMo thermal model. . . . .	57
3.5	Simplified representation of a system including thermal storage. The parts involved are supply, demand and storage. . . . .	68
3.6	Thermal-flows model adapted to the multi-zone modelling approach. . . . .	68
3.7	Sketch of the single-temperature modelling approach . . . . .	71
3.8	Sketch of the two-layer storage tank and the heat. . . . .	72
3.9	Representation of the system in the two-layer modelling approach for TES. . . . .	76
3.10	Sketch of the mass flows model highlighting the charge and discharge loops. . . . .	78
3.11	Sketch of the system with both TES and BES. . . . .	80
3.12	Representation of the AHU model in the CoBMo and the connections with the cooling/heating plant. . . . .	85
3.13	Psychometric chart representing the process of cooling air from the ambient (A) conditions to the zone (Z) conditions supplying air at the AHU conditions. The framework chart is rearranged from Spinelli (2015). . . . .	86
3.14	Addition of storage to the AHU model in the CoBMo. . . . .	88
3.15	Representation of the TU model in the CoBMo and the connections with the cooling/heating plant. . . . .	89
3.16	Addition of storage to the TU model. . . . .	90
4.1	Behaviour of a chiller depending on the operational load. The figure kW/ton is expression of the efficiency and the load is indicated in percentage (%). The curves are parametric with the condensing temperature of the chiller (Blackburn et al., 2019) . . . . .	98
4.2	Hourly electricity tariff from the Singapore wholesale electricity market and demand curve of the CREATE Tower in NUS. . . . .	100
4.3	Flowchart describing the process defining the storage size (optimization algorithm) and evaluating whether installing storage is feasible or not. . . . .	107
4.4	Graphical representation of simple and discounted payback time. . . . .	110
5.1	Linear interpolation of past TES projects in the US (DeForest et al., 2014). . . . .	112
5.2	Snapshot of the IRENA battery cost tool (IRENA, 2017) . . . . .	113
5.3	Representation of the reasoning used to select the battery storage technologies. . . . .	114
5.4	Battery (energy installation) cost and battery efficiency (rearranged from (IRENA, 2017)). . . . .	116

5.5	Battery lifetime (rearranged from (IRENA, 2017)). . . . .	116
5.6	Wholesale and retail price signals from (EMC, 2019c) and (KE, 2019). The peak-to-peak distance is highlighted as a $\Delta$ . . . . .	117
5.7	Framework used to present the results of the BES economic analysis. . . . .	118
5.8	TES Economic Analysis results using an overall efficiency of 80%. Figure (a) is the result using 291 SGD per m <sup>3</sup> as cost. Figure (b) using 407 SGD per m <sup>3</sup> . . . . .	120
5.9	TES Economic Analysis results using an overall efficiency of 92%. Figure (a) is the result using 291 SGD per m <sup>3</sup> as cost. Figure (b) using 407 SGD per m <sup>3</sup> . . . . .	121
5.10	BES Results: wholesale price signal. Discounted payback time. . . . .	122
5.11	BES Results: wholesale price signal. Yearly savings as percentage of baseline operational costs. . . . .	123
5.12	BES Results: retail price signal. Discounted payback time. . . . .	124
5.13	BES Results: retail price signal. Yearly savings as percentage of baseline operational costs. . . . .	125
5.14	BES Results: retail price signal. Break-even evaluation. . . . .	126
5.15	Optimal scheduling – TES – AHU operation. . . . .	128
5.16	Optimal scheduling – TES – TU operation. . . . .	128
5.17	Optimal scheduling – TES – AHU and TU operation; storage level; charge electric power. . . . .	129
5.18	Optimal scheduling – TES – AHU and TU operations; wholesale electricity price; charge electric power. . . . .	130
5.19	Optimal scheduling – BES – AHU operation. . . . .	131
5.20	Optimal scheduling – BES – TU operation. . . . .	131
5.21	Optimal scheduling – BES – AHU and TU operation; storage level; charge electric power. . . . .	132
5.22	Optimal scheduling – BES – AHU and TU operation; retailer electricity price; charge electric power. . . . .	132

# List of Tables

1.1	Comparison of contestable and non-contestable customers. The "Customer" column indicates for who the pricing method is valid – Contestable (C) and Not Contestable (NC) . . . . .	11
2.1	General advantages and disadvantages of Lithium Ion batteries (IRENA, 2017)	41
2.2	Advantages and disadvantages for Lead acid batteries sub-dividing by flooded lead-acid and valve regulated lead-acid batteries (IRENA, 2017) . . . . .	44
3.1	Description of the <i>vectors</i> that appear in the state space formulation . . . . .	59
3.2	Description of the <i>matrix</i> that appear in the state space formulation . . . . .	60
3.3	Thermal model parameters. . . . .	66
3.4	Thermal model linearization parameters. . . . .	66
3.5	Comfort constraints. . . . .	66
3.6	Explanatory table for the elements in the equations eq. (3.26) and eq. (3.27)	75
3.7	Explanatory table for the elements in the equations eq. (3.26) and eq. (3.27)	81

# 1 Introduction

## 1.1 Energy consumption in buildings

Currently, residential and commercial buildings consume about 29 % of the global energy and feed-stock fuels, being second only to the industrial sector. Although this share is projected to remain nearly constant in the next 20 years, the actual buildings energy consumption will keep rising reaching 5'638 Mtoe in 2040 (BP, 2019).

In terms of electricity Total Final Consumption (TFC), the statistics show that residential and Commercial & Public Services account for half of the consumption worldwide in 2016 – being 27% and 22% respectively – with a constant growth in the last 10 years (IEA, 2019).

On a general level, IEA has analyzed and identified where the main opportunities for efficiency improvement are when talking about several sectors, and how the policies worldwide can help the succeed of transforming the nowadays world in a more energy efficient one (IEA, 2018). Since buildings represent a very high share of the total energy consumption worldwide, relevant savings in consumption and emissions can be achieved considering energy efficiency in buildings in different sectors. IEA has framed the Efficient World Scenario (EWS)<sup>1</sup>, which aims to estimate what would be the improvements needed in buildings to reach certain goals. The EWS shows that by 2050 buildings have the potential to become up to 39% more efficient. which would result in a flattening of the energy use in buildings over the years – opposed to what shown above and proposed by (BP, 2019) in case no action is taken. This would require energy intensity (as  $GJ m^{-2}$ ) to decrease at at almost double the pace than it did in the past(IEA, 2018).

Within the scope of energy consumption in building it is of particular interest for this thesis to zoom in and analyze the trends of cooling consumption. Cooling is subjected to forces pushing from different directions and making it a growing share in buildings' consumption worldwide. On one side, the demand for cooling is increasing as economies

---

<sup>1</sup>The Efficient World Scenario (EWS) answers the question of what would happen if countries realised all the available cost-effective energy efficiency potential between now and 2040

become wealthier; simultaneously, the global temperature is increasing, making it more energy demanding to achieve indoor comfort. Although representing only about 6% of the total final energy use in buildings in 2017, the projected increase in cooling activity is more than double in 2040. (IEA, 2018) suggests that "improvements in cooling technology performance are the primary source of energy efficiency gains (accounting for over 90% of the change)" and that 60% of these "are in developed countries that already have significant cooling energy consumption".

## 1.2 Singapore Energy outlook

### 1.2.1 Singapore energy imports and exports

As accurately presented in the reports by the Energy Market Authority (EMA) (EMA, 2018b), Singapore imports are mainly composed of petroleum products and crude oil, which accounted for 63.7% and 30.6% of the whole 2017 imports respectively – a total of 189.3 Mtoe was imported in this year, 7.4% higher than the precedent year.. Natural gas imports are mainly in the form of pipeline natural gas. energy experts are almost completely represented by petroleum products, namely fuel oil and jet fuel kerosene.

### 1.2.2 Electricity production mix

In (EMA, 2018b) statistics on the electricity generation mix are also presented. Singapore has seen an electricity mix totally dictated by natural gas (NG), with a share of 95.2% in 2017 of the 4'435.6 ktoe (52.2 TWh) of total electricity generated. Is interesting to notice how Singapore was able in 2015 to almost completely phase out the use of Fuel Oil thanks to a declined dependency in steam turbine plants, which were substituted by gas-fueled plants. In fact, the installed capacity of Combined Cycle Gas Turbine (CCGT), co-generation (Co-gen) and tri-generation (Tri-Gen) plants – all technologies fueled by NG – has drastically increased in 2015. In the first quarter of 2018 the share of NG technologies for electricity generation was 77.2% of a total of 13'614.4 MW installed for electricity generation, with steam turbine accounting for 18.8% of the electricity generation mix. The breakdown of the electricity mix by fuel in the 2005-2018 time-span is proposed in Fig. 1.1.

### 1.2.3 Electricity consumption and customer categorization in Singapore

In 2017 the electricity consumed in Singapore was 49.6 TWh. Fig. 1.2 shows the breakdown of the consumption by sector and by contestability (EMA, 2018b):

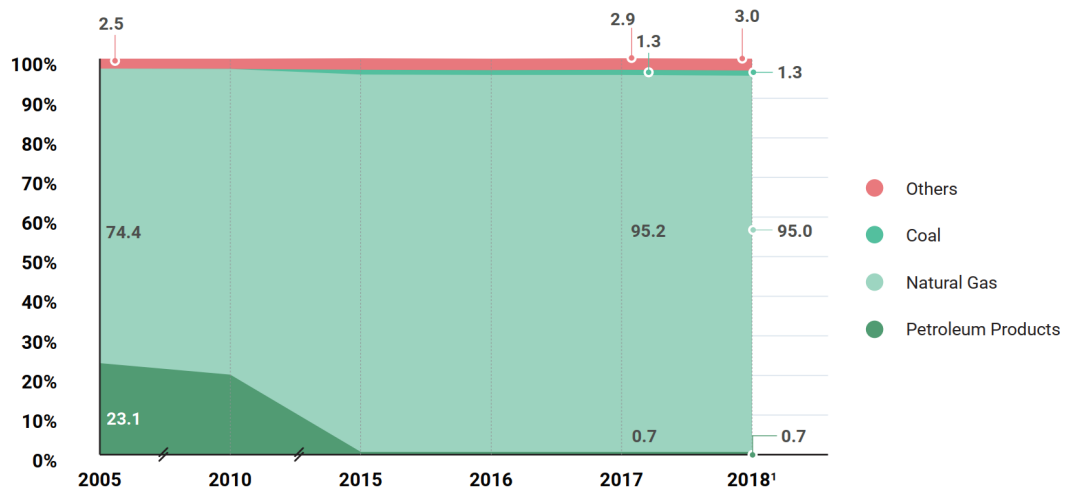


Figure 1.1: Singapore electricity mix by fuel (EMA, 2018b)

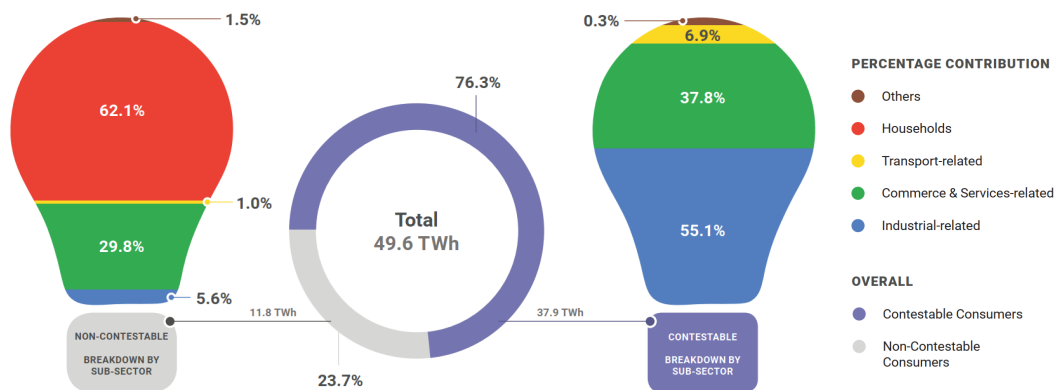


Figure 1.2: Singapore electricity consumption by sector and by contestability (EMA, 2018b)

The contestability of a consumer is a concept that is born with the opening of the Singapore electricity market, action that was started in 2001 by the EMA. Initially, the electricity could be purchased only from the energy utility in Singapore SP Group (SPGroup, a) at the regulated tariff which is subjected to a change every quarter each year<sup>2</sup>. With the beginning of the open electricity market, consumers are divided between contestable and non contestable. The requirement to be eligible as a contestable consumer

<sup>2</sup>The regulated tariff for Q2 of 2019 is 25.92 cents USD per kWh (SPGroup, b)

is to have a monthly electricity consumption of at least 2'000 kWh (which results in a bill of at least 400 SGD per month) (EMA, 2018b). It results that given this threshold, no residential customer is eligible to be contestable in Singapore, while about 90'000 businesses are, which makes up for about 80% of the whole electricity consumption (as visible in Fig. 1.2). The difference between contestable and non contestable when it comes to the purchase of the electricity is underlined in Table 1.1, where the different options available to the two groups are presented.

*Table 1.1: Comparison of contestable and non-contestable customers. The "Customer" column indicates for who the pricing method is valid – Contestable (C) and Not Contestable (NC)*

<b>Customer</b>	<b>Option</b>	<b>Price of Electricity</b>	<b>Buy from</b>
C/NC	Regulated Tariff	Reviewed quarterly	SP Group
C/NC	Electricity Retailer	Depends on retail electricity package offered by retailers. Each retailer has a different offering.	Contestable consumers are those with a monthly consumption exceeding 2'000 kWh. The contestable customer that selects the retailer purchase option can choose from a list of 22 total retailers from which to buy a plan.
C	Wholesale Electricity Market	Half-hourly wholesale electricity prices.	SP Group

Regarding the "ElectricRetailer" purchase option, the list of retailers partly overlap between the two groups of customers. In fact all the 13 retailers available to the non-contestable customers are also in the list of 22 retailers available to the contestable customers<sup>3</sup>.

It is relevant to underline for the scope of this thesis that Commerce and service-related customers make up for the 37.8% of the contestable customers, representing a 28.8% of the global electricity consumption in Singapore – 14.3 TWh.

<sup>3</sup>Find the list of retailers at these online addresses: Contestable: <https://www.openelectricitymarket.sg/business/list-of-retailers#business-consumers-min-2000> | Non-contestable: <https://www.openelectricitymarket.sg/residential/list-of-retailers>

### 1.2.4 Electricity market structure

This section aims to provide a synthetic yet thorough overview of the electricity market structure in Singapore. Fig. 1.3 provides a sketch of the framework highlighting the main stakeholders participating in the market, as well as their interactions (OEM, 2019).

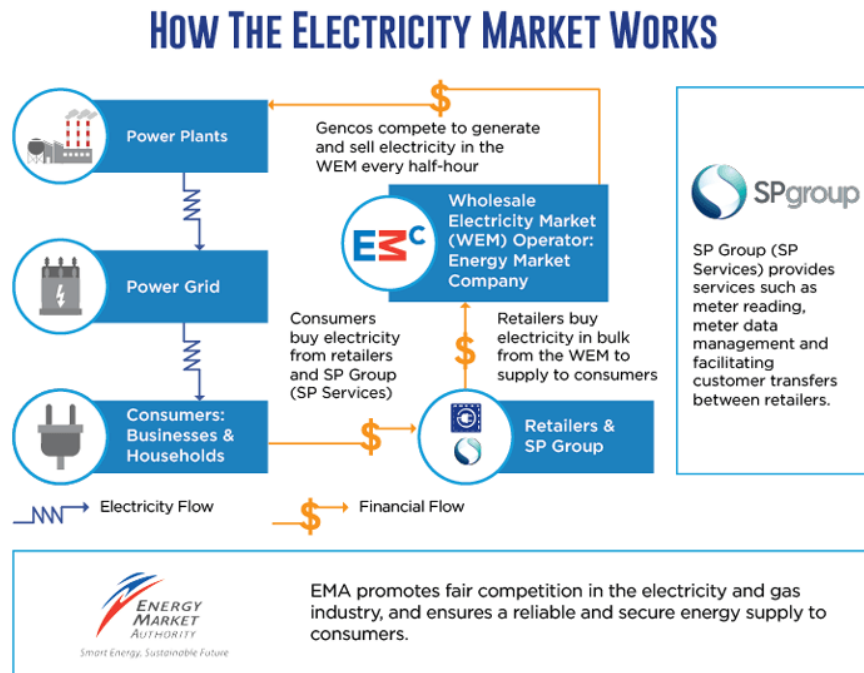


Figure 1.3: Overview of the Singapore electricity market (OEM, 2019)

The market is composed of the wholesale electricity market, where the generation companies compete to sell the produced electricity every half hour, and the retail market, where retailer compete to acquire customers and sell the electricity bought in bulk from the wholesale market.

The proposed market structure suggests that the electricity market in Singapore is designed with the "integrated market" approach. As presented by (Cramton, 2017) this design envisages that a system operator optimizes scheduling and dispatch centrally with two objectives in mind: (i) short run efficiency: meaning making the best use of resources; (i) long run-efficiency: ensuring that the market provides the proper incentives for efficient long-term investment. An excellent detailed review of the electricity market types and their mechanism is given by (Cramton, 2017), though for the scope of this thesis is not of interest to go deeper in each single mechanism and review its functioning.

The stakeholders shown in Fig. 1.3 are (OEM, 2019):

- **Energy Market Authority (EMA):** is the government authority that "ensure a reliable and secure energy supply, promote effective competition in the energy market and develop a dynamic energy sector in Singapore".
- **Power Generation Companies:** they generate electricity and compete to sell it on the wholesale market.
- **Energy Market Company (EMC):** administrates and operates the wholesale market. This is the "central operator" that (Cramton, 2017) refers to.
- **Electricity Retailers:** they buy electricity in bulk from the wholesale market and compete to acquire customers that will buy electricity from them.
- **SP Services (SPS):** it provides services such as electricity meters, management of meter data and facilitation of access to the wholesale market.
- **SP PowerAssets (SPPA):** owner of the grid.
- **SP PowerGrid (SPPG):** appointed by SPPA to maintain and operate the grid.

The market structure described here reflects the direction Singapore has undertaken towards opening the market, where the retailers play an active role and the final objective is to favour the end customers, letting them enjoy a wider choice in terms of pricing plans.

### **The different roles of EMA and EMC**

For the sake of completeness, a more detailed comparison between the two entities EMA and EMC is done hereby.

The Energy Market Authority (EMA) is defined as "a statutory board under the Ministry of Trade and Industry" having the duties of "ensuring a reliable and secure energy supply, promoting effective competition in the energy market and developing a dynamic energy sector in Singapore" (EMA, 2019c). The three key roles it covers are industry developer, industry regulator and system operator (SO). Of particular interest for this thesis is the latter role, because the EMA is both the TSO and DSO in Singapore. While SPGroup owns and maintains the grid – through SPPA and SPPG – is the EMA that operates it from the Power System Control Centre (PSCC), which is defined as "the nerve centre of the electricity generation and transmission system" (EMA, 2019b).

As said above, the Energy Market Company (EMC) is instead the central market operator in Singapore. The EMA defines itself as an entity which "is like the stock exchange for electricity, providing the IT systems, the trading environment and the governance for

the market" (EMC, 2019a). EMC is involved in three main governance activities: rule-making, market surveillance and compliance, and dispute resolution and compensation<sup>4</sup>.

### 1.2.5 Singapore and Sustainability

Singapore has ratified the Paris Agreement (PA) in September 2016, with its intends to decrease carbon emissions being specified in (UNFCCC, 2016). Singapore's goal is to reduce its Emissions Intensity (EI) by 36% by 2030 from 2005 level – going from a level of 0.176 kgCO<sub>2</sub>e/S\$GDP in 2005 to 0.113 kgCO<sub>2</sub>e/S\$GDP in 2030 –, stabilizing its emissions in the period of 2021-2030 and peak in 2030.

Singapore's deployed strategy to tackle climate change is presented in the Climate Action Plan published by the NCCS<sup>5</sup>, released in July 2016. The plan is divided into two publications – "Take Action Today, For a Carbon-Efficient Singapore" (NCCS, 2016b) and "A Climate-Resilient Singapore, For a Sustainable Future" (NCCS, 2016a) – which frame the country's strategy to meet the 2030 PA pledge (NCCS, 2018).

The Climate Action Plan is built on four main macro-areas which represent the pillars of the strategy to reduce GHG emissions; these actions are grounded into one major instrument which Singapore sets as key to achieve the pledged goals: the carbon tax. Figure Fig. 1.4 shows a schematic representation of such framework.

These four set strategies are:

- Improve energy Efficiency: this is done across multiple sectors, like industry, buildings, transport, households and waste & water.
- Reduce carbon emissions in power generation
- Develop and deploy low carbon technologies
- Encourage collective climate action

A schematic of the strategies is shown in Fig. 1.5 where further details are provided

<sup>4</sup>The yearly market reports released by the EMC are available since year 2003 <https://www.emcsg.com/aboutus/publicrelations/marketreports#>

<sup>5</sup>National Climate Change Secretariat (NCCS) – <https://www.nccs.gov.sg/about-us/about-nccs>

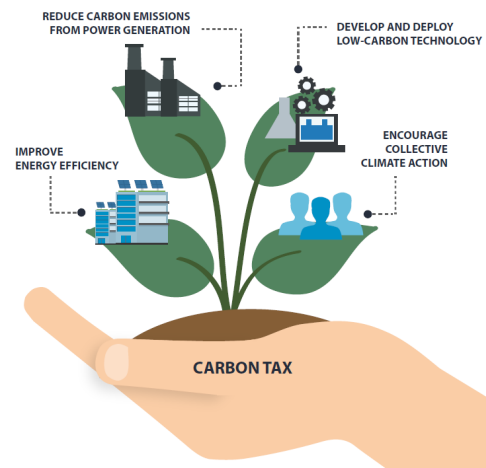


Figure 1.4: Singapore's Climate Action Plan – framework (NCCS)

The carbon tax introduced by the Singapore government has an initial value of 5 SGD/tCO<sub>2</sub>e – approx. 3.8 USD – and will remain so during the period 2019-2023. The tax will be covering all the sectors without exclusion, targeting 80% of the total emissions in the island. The future plan is to review the tax in 2023 and increase it to 10 and 15 SGD/tCO<sub>2</sub>e. The carbon tax is set upstream user, meaning that energy producers and large emitters will be affected by the tax cost and not the end users. Although the carbon tax is a good instrument to reduce carbon emissions especially on the power generation level, (CAT, 2019) propose that the tax is too low to properly set Singapore's energy sector on the correct trajectory to achieve the PA targets. (CAT, 2019) rely on (Warren, 2014) and (CMW, 2017), and in fact the latter suggests that a carbon tax of minimum of 40–80 USD/tCO<sub>2</sub> by 2020 and 50–100 USD/tCO<sub>2</sub> by 2030 is needed to reach the objectives of PA<sup>6</sup>.

<sup>6</sup>(CMW, 2017) in turn refers to (Stiglitz et al., 2017)

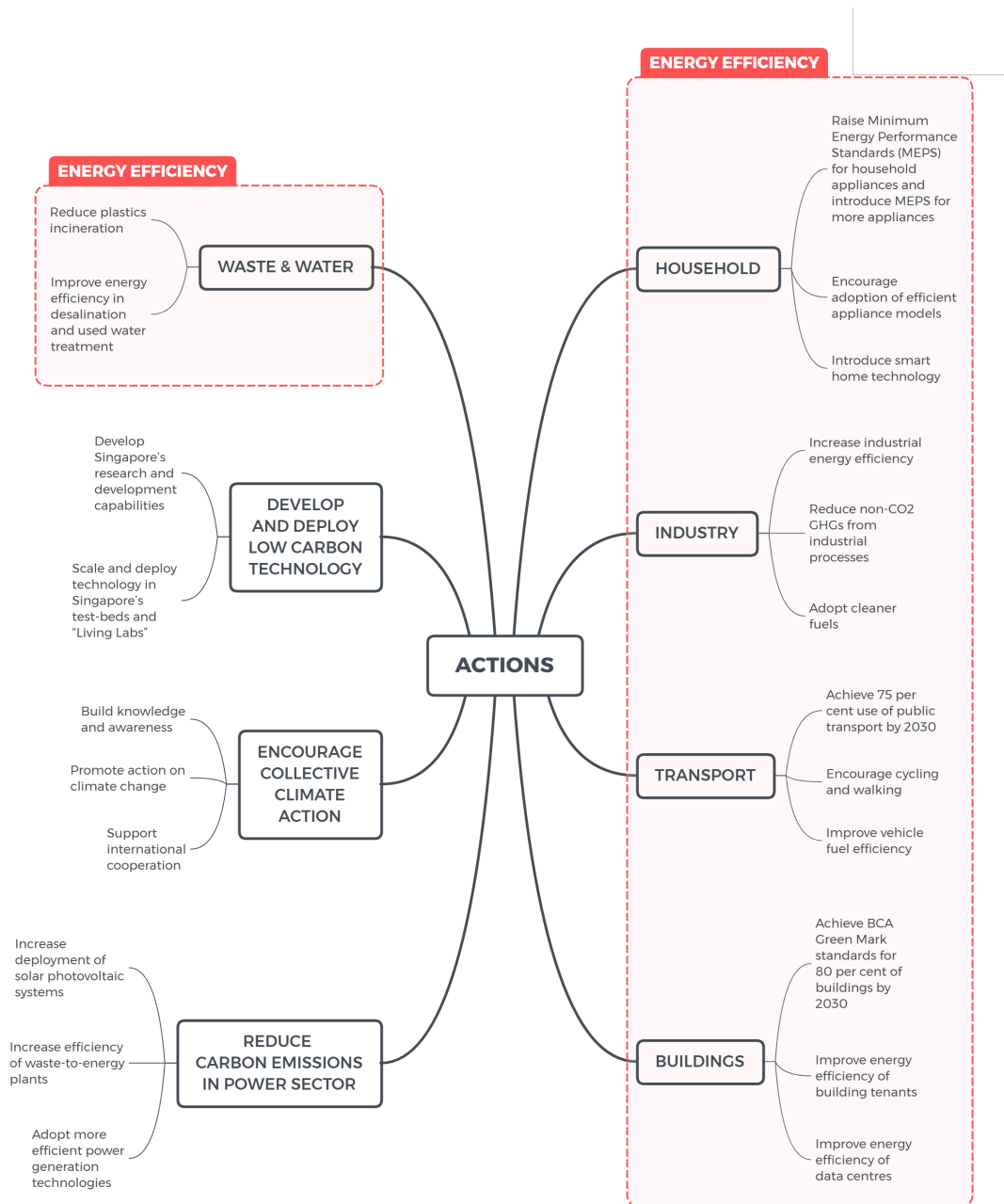


Figure 1.5: Singapore's Climate Action Plan – framework (NCCS)



Figure 1.6: Floating PV pilot in Tengeh Reservoir (MFA, 2018)

### 1.2.6 Solar energy

The statistics proposed in (EMA, 2018b) clearly suggest that renewable energy technologies do not play an important role in the energy sector of Singapore. Although, it is of interest to highlight an example of the evolution of the clean energy sector is the city mentioning the «world's largest offshore floating solar systems», that will be soon be operating in the city-state (ST, 2019). The facility – to be located in Strait of Johor, north of Woodlands Waterfront Park<sup>7</sup> – will provide about 6 TWh of electricity per year (about 0.0121% of the electricity generation in 2017) and reduce the emissions of 2'600 tonnes of CO<sub>2</sub> (5% reduction with respect to the 2014 emissions level of 50.1 MtonsCO<sub>2</sub>, *eq* (Tracker, 2019)). The project is developed by Sunseap Group, whose Co-founder and CEO, Frank Phuan, already in November 2018 had stated the importance of such project to support «Singapore's ambition to be a solar hub for Asia» (SUNSEAP, 2019). A test-bed of floating PV system was launched already in 2016 at Tengeh Reservoir<sup>8</sup>. Singapore aim to scale-up this technology thanks to the successful testing of the pilot and to reach up to 50 MWp at Tengeh (MFA, 2018).

Another example displaying the clear intention of Singapore towards clean energy is the SolarNova programme led by the Economic Development Board (EDB) (Housing and Board). The project aims to increase the PV capacity up to 350 MWp by 2020 and has already called three solar leasing tenders up to date. The goal is to cover about the 5% of total Singapore consumption by 2020. Up until the first quarter of 2018 the total solar installed capacity in Singapore was 114.8 MW<sub>ac</sub>, of which 49.3% in the non-residential private sector, and 41% in town councils & grassroots units. The solar power globally accounted for only 0.8% of the total capacity installed in the island (EMA, 2018b).

Although this figure is noticeable small, what is to be captured from this solar overview

<sup>7</sup> Map position <https://goo.gl/maps/EEQiRnjqfiewjC6p8>

<sup>8</sup> Map position <https://goo.gl/maps/KTXm4Pg45Y26VLQ96>

is that the distributed production is gaining more and more importance in Singapore and this has to be considered in an important factor to be considered when assessing the grid stability and the the grid management by the DSO. Later in the Section 1.3 it will be introduced how the integration or renewable energy technologies (RET) in the current energy systems can create challenges for the system operators and how DSF can be beneficial to smoothly accompany their penetration.

Another interesting option is been considered by Singapore to drastically increase the share of renewable in its mix in the future. This is importing solar electricity in bulk from North Australia with a 3'800 km HVDC<sup>9</sup> underwater cable running through the Indonesian archipelago and reaching the island city-state (Guardian, 2019). The electricity would be produced by the solar park envisaged by the Sun Cable project, a 3-GW and 15'000 hectares installation that promises to be the biggest solar project in the world. The solar array would be constructed close to Tennant Creek<sup>10</sup> and supported by battery storage (SunCable, 2019).

### 1.2.7 The role of Storage

Singapore shows to have a clear understanding of the beneficial impact that storage technologies could have in the current and future energy systems. EMA has dedicated a whole section in its website to address the topic of Energy Storage Systems (ESS) (EMA, 2019a) where the several initiatives undertaken by the Singapore government to push and sustain this technology are reported. Singapore is encouraging industry to adopt storage solutions by way of many means, such as the launch of Intermittency Pricing Mechanism (IPM), a Regulatory Sandbox in partnership with SP PowerAssets (SPPA), and a record of past ESS Initiatives in form of grant calls. Of interest for this thesis is to deeper analyze the lastly published policy paper on ESS (EMA, 2018a) where the storage topic is consistently framed for the Singapore case.

Already back in 2016 the EMA had published a consultation paper to review the regulatory framework for ESS (EMA, 2016b). The feedback from this paper led EMA to conclude that the framework already allowed ESS to participate in the market. ESS can bring many different benefits to the local energy system and these will be shortly review below.

In (EMA, 2018a) it is underlined the importance of storage to reduce the critically of Intermittent Generation Sources (IGS) when they are to be introduced into the current energy systems. As presented in Section 1.2.6 Singapore's distributed solar capacity has drastically increased in the past years and is projected to increase even further, being the only clean technology feasibly implementable in the island. A too high penetration

---

<sup>9</sup>High Voltage Direct Current

<sup>10</sup> Map position <https://goo.gl/maps/NtznEEP1ePKb1NEy5>

of IGS can represent a critical challenge for the system operator – EMA itself – since "insufficient backup reserves or lack of system flexibility to cater for the unexpected loss of IGS output when weather conditions change could lead to severe power system outages" (EMA, 2018a). Although the balance of IGS integration in the grid is a central topic in the discussion on storage it is not the only one. ESS can also provide market services such as frequency regulation and spinning reserves, which are defined as in-front-of-the-meter services, meaning that they favour the network. ESS can also provide benefits the end consumer by allowing to shift the demand from peak to non-peak hours by way of storing electricity in periods of low electricity prices – i.e. low-peak. This concept is the one leveraged in this thesis and can also be defined as "implicit" demand side flexibility. Later in the the thesis more detailed information will be given about this specific topic. Moreover, ESS helps the system operator to defer the cost of upgrading or expanding the grid by helping the system meeting the peak demand. This is something already happening in some Europe countries and can be beneficial to DSOs to save costs. Finally, voltage regulation is another service that ESS can provide by providing or absorbing reactive power to regulate the local network voltage and provide voltage support.

Is worth highlighting some major efforts done by the Singapore government to facilitate the adoption of ESS. The implemented a rule change in the electricity market to allow batteries to participate in the regulation market was implemented in 2015 (EMC, 2015). In 2017 17.8 million SGD were awarded to two Singapore-led consortiums the first utility-scale battery facilities in the city, with an aggregated capacity of 4.4 MWh (EMA, 2017). The performance of two different technologies – redox flow and lithium-ion batteries – will be evaluated in the specific climate of Singapore. These installations have the purpose of understanding the behaviour of this technology in stabilizing the grid and even to couple it with solar forecasting techniques. EMA is also aware of the conflicts of interest that could arise if the grid operator – in this case SP PowerAssets – both owns and operates the storage facility, and the authority will take action implementing proper regulations to asses this conflict.

This section aimed to give an overview on how Singapore perceives and acted on the storage topic during recent times. It will connect with the scope of this thesis later on in the Section 1.4 section.

### 1.2.8 Demand Side Management in Singapore

Demand Side Management (DSM)<sup>11</sup> is a simple yet powerful concept that could allow wide savings on the operation side – electricity consumption – and planning level of the electric grid. Although a broader review of what DSF is and what the benefits it can bring

---

<sup>11</sup>Also Demand Side Flexibility or Demand Side Response

are, in this section we briefly analyze what is the DSR current scenario in Singapore, as this information is needed to formulate the motivation of this work.

DSR is a subject that Singapore has well identified as an opportunity, with many initiatives related to the topic proposed by the government. (EMA, 2015) states that achieving peak reduction would have a huge potential for Singapore, with some studies showing up to \$1.6 million savings every MW reduced, as Professor Frank A. Wolak affirmed. The clear sign of the direction taken by Singapore towards DSR is for example the launch of the OptiWatt project in 2006, which puts together multiple stakeholders and aims to demonstrate the viability of DSR in Singapore. Red Dot power, an independent electricity retailer, is an example of player that took part in the project cooperating with EMA (Red Dot Power, 2016). The OptiWatt project has led to several success stories. Among them there is the shift in 0.3 – 0.4 MW of load by The Agency for Science, Technology and Research (A\*STAR) adjusting the operational time of washers and sterilizers; or Air Liquide partnering Diamond Energy to offer 2.2 MW Interruptible Load in the electricity market; or the Direct Demand Response Aggregator enhancement by EMA that allows customers to participate to DR by way of demand aggregation.

With a specific document (EMA, 2016a) EMA has clearly defined the boundaries of the eligibility for DR participation. Consumers can directly participate in the DR Programme if they have an aggregate curtailable load of at least 0.1 MW. Alternatively, in case of consumers with curtailable load of less than 0.1 MW, the participation is allowed in an indirect mode, via retailers or DR Aggregators.

It is clear with these examples that Singapore already in 2016 has started setting up the foundation for the proper development of a complete model of DR. This is important to be highlighted with regard to this thesis, since the work aims to assess the potential of applying DSF(DR) to commercial buildings in Singapore.

### **1.3 Motivation and Research question**

This thesis aims to assess the potential of DSF in commercial buildings in Singapore when considering the distributed installation of storage at the building level. The potential is in terms of economic savings that come from the flexibilization of a buildings' HVAC consumption thanks to the addition of storage. As will be shown in Section 3.2, the storage extends on an already existing flexible potential that a building has by nature thanks to its thermal inertia. This thesis will investigate the savings generated on the operation of the HVAC system in a building, which relates to the use of electricity in periods of low-price tariffs allowed by the presence of the storage and a non-flat rate price signal.

The reason of focusing the study on buildings is connected to the work that was done

in the past in TUM CREATE on the modelling of building systems. The approach used is numerical optimization, which is developed remaining in the linear domain. The flexibilization of a building is done setting up an optimization problem which could be used in an MPC – Model Predictive Control – in the future. Part of the motivation of this work comes from the fact that although MPC has greatly evolved in the last years (Section 2.3, Section 2.4), its commercial development has not took off yet, and several studies have shown the need of fast and computationally inexpensive MPC formulations that allow also for distributed control (Troitzsch et al., 2018).

A gap in the literature was noticed when it comes to integrated and linear models for storage to be used for DSF applications in buildings. Giving the possibility of estimating the impact of storage when using multiple storage technologies at the same time – thermal, mechanical, electricchemical, etc – is fundamental for evaluating the most suitable technology for a specific case. Several authors developed MPC strategies to control the HVAC system in a building including thermal storage, but the implementation of these is in most cases based on MILP – Mixed Integer-Linear Programming – which is less efficient than LP – Linear Programming.

Finally, looking at the Singapore energy outlook proposed in Section 1.2 it is clear that the city is not only pushing towards DSF, but that it will rely more and more on solar resources to meet the sustainability goals that were pledged in the Paris Agreement (UNFCCC, 2016). On top of this, even more critical is the penetration of EVs into the grid. To this end, storage will on one side be beneficial for pushing DSF by allowing peak demand shift; on the other hand, distributed storage can also support the smooth penetration of renewable generation at the building level – e.g. solar PVs installed on buildings’ rooftops.

The research question can the be stated as follows:

#### Research Question

When implementing storage on the distributed level to improve DSF in buildings using optimal control strategies, are storage technologies economically feasible in the current Singapore scenario, and how relevant are the benefits that the storage can produce to this regard?

## 1.4 Scope of the thesis

This section aims to clearly define the scope of the thesis, showing what contribution this work brought to TUM CREATE’s ESTL (Electrification Suite & Test Lab) and drawing the physical boundaries withing which the analysis of this work was limited .

### 1.4.1 Physical boundaries of the thesis

During this thesis linear mathematical models of thermal and battery storage were implemented and integrated into the CoBMo. The CoBMo is calculating the thermal demand of the building depending on the comfort requirements and the disturbances acting of the building system, as explained in Section 3.2. The combination of the storage models with the CoBMo allows to evaluate the extended flexibility potential of a building when considering the electricity price as an input. Hence, the market side of DSF is not considered in this thesis, as only implicit DSF<sup>12</sup> is included in this work. Fig. 1.7 shows a representation of the physical boundary.

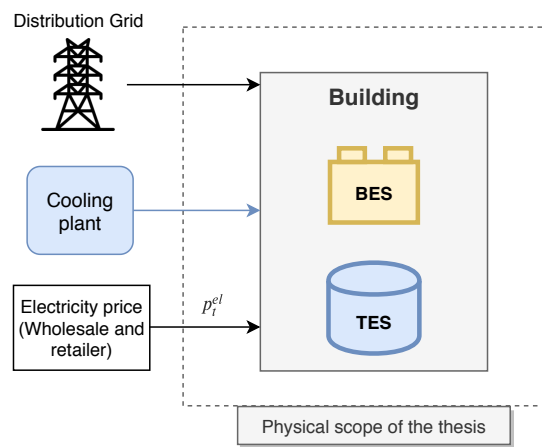


Figure 1.7: Physical boundaries of the thesis within the CoBMo.

## 1.5 Introducing the Control-Oriented Building Model

A quick introduction to the Control-oriented Building Model (CoBMo) developed in TUM CREATE is provided here to allow the reader to more easily follow the Literature Review. While The CoBMo will be discussed more in detail in Section 3.2, it is important to name it here because its presence influenced some choices during the analysis and scouting of the literature.

The first point is that the CoBMo is a linear model, a lot was searched on this topic and the possibility to model the storage for the use of a MILP problem was excluded early in the thesis. The reason for keeping the CoBMo linear is to develop a model which can be used to run a fast and distributed MPC, for which convex problems are needed.

<sup>12</sup>It is that type of flexibility that is not sold on any market and is performed for the only final consumer's benefit (EUETS, 2006)

The CoBMo is also modeled with a white-box approach. As it will be shown in the literature Section 2.3.1, white-box models involve an explicit modelling by writing the equations that reflect the physics of the system. This method is the only one that can be used to model systems which do not exist yet, meaning in their *planning-phase*.

## 2 Literature Review

### 2.1 Demand Side Flexibility (DSF)

Demand Side Flexibility (DSF) can be defined as the capability of changing the electricity consumption pattern by an end-user in response to a price signal (EUETS, 2006). The price signal can be a time-variable price of electricity or an agreement between a customer and an aggregate to provide a certain amount of flexibility – i.e. change in consumption pattern – compensated by a reward. Looking at the network value of DSF from the DSO (Distribution System Operator), this exists in the form of "reduced or deferred investments, better system reliability or other system cost reductions" (NCM, 2017). DSF can be of two types (EUETS, 2006):

- **Implicit:** is that flexibility that is performed for the only end-user's benefit and is not sold on the market. This type does not need any trading process and can be launched at any time and by the consumer.
- **Explicit:** this flexibility is sold as a product on the market, and thus need a specific control. As an example, in Singapore customers with a curtailable power of at least 0.1 MW directly participate in a DR Program Section 1.2.8.

This division can be expanded with also the definition used by (NCM, 2017), which labels explicit DSF as the one that is mobilized in real time and with short notice, while implicit DSF as the one related to a long-term change in consumption pattern. These two definitions are coherent, as only a flexibility that is able to be quickly supplied can be sold and purchased on the market.

Some key enablers are needed to allow DSF of both types to take off and develop completely and properly (SEDC, 2016). For the explicit case, what is needed is that all the market segments (wholesale, capacity, balancing and ancillary services) are open and that no discrimination is done against demand response, distributed generation or storage due to product definitions. Fairly competition shall also be ensured, letting for example third party aggregators participate to the market without energy retailers or balance

response parties – both aggregators’ competitors – prior agreement. Concerning the implicit DSF, a fundamental enabler is to allow customers to access retailing electricity pricing, such as hourly or period (peak and off-peak) pricing. This is necessary to let the consumers react to a price signal and adapt the consumption to the system condition. To make variable pricing possible, smart meters are a necessary condition, since the time-dependent consumption of a consumer has to be tracked and matched with the day-variant electricity price.

Since this thesis focuses on implicit DSF, a deeper review of implicit DSF services will be hereby provided<sup>1</sup>. Four are the main services that can be offered to a prosumer<sup>2</sup> by an ESCo (Energy Service Company) (USEF, 2018).

- ToU (Time of Use) optimization: the consumer has the opportunity of reducing the operational costs by partly of totally shifting the loads to low-price time intervals during a day. The price schedules must be known in advance – day-ahead – and the consumption of prosumer has to be tracked using smart meters.
- In-home self-balancing: is a service that prosumers that also generate electricity can enjoy. The value is achieved by optimizing the different prices combinations of buying, generating and selling electricity at different times in the day.
- Control of maximum power: current price tariff schemes often include a component which bills consumers depending on their maximum power (the peak) they consume. Moving part of the load consumed and performing peak shaving can allow to reduce the bills of prosumers thanks to avoiding being charged the peak share.
- Emergency power supply: Emergency power supply is an additional service that consumers can purchase. DSF can enable islanding and eliminate the need of such service. To do so, an additional and relevant investment cost is needed on the prosumer side for storage and synchronization systems.

---

<sup>1</sup>(USEF, 2018) include also an excellent review of the services related to the explicit DSF.

<sup>2</sup>A prosumer is a consumer who is both consuming and producing a product.

## 2.2 Mathematical Programming

Before digging further into the literature review is worth giving an overview to the reader about what are the main and typical methods used for mathematical programming and their features. Mathematical programming can be defined as a mathematical representation which "concerns the optimum allocation of limited resources among competing activities, under a set of constraints imposed by the nature of the problem being studied" where these constraints "could reflect financial, technological, marketing, organizational, or many other considerations" (McCarl and Spreen, 1997). This discipline aims to allocate in the best way possible a certain amount of limited resources within a defined system and conditions.

Modelling can be divided into broad categories depending on different parameters. In Fig. 2.1, four main categories are proposed by (McCarl and Spreen, 1997): operational exercise, gaming, simulation and analytical models. From left to right, the models grow in degree of abstraction and speed, and the involvement of a human decision maker is only in the first two types. From right to left the degree of realism and the cost increase.

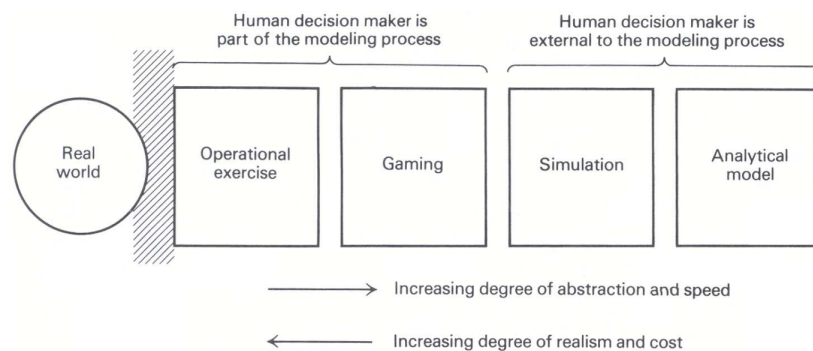


Figure 2.1: Types of model categories proposed by (McCarl and Spreen, 1997)

Since this thesis considers analytical models, this category will be further described, although it is relevant to quickly underline the difference between simulation and analytical methods. The first one is empirical and often run on computer programs which involve arithmetic operations. Simulations assess the performance of alternatives which are identified upfront by a human decision maker. One can run simulations as long as the comparison between the different input combinations is satisfying and draw conclusions from the results. Instead, analytical models are constructed completely in mathematical terms and in programs that seek to maximize or minimize a defined objective function, constraining the problem with mathematical equations which reflect the nature of the system which is represented as well as its conditions.

The most relevant mathematical programming models will be summarized below (McCarl and Spreen, 1997):

- Linear Programming (LP) has been since the '80s for sure the most used and analytical model to perform optimization. LP is a method that is expressed by linear a optimization function and linear constraints.
- When the functions describing the constraints and/or the objective function become non-linear, the Non-Linear Programming (NLP) takes shape, In NLP, the nonlinear functions have to be well-behaved in order for the model to reach a satisfying computational efficiency. The certainty of finding a global maximum or minimum when pursuing an optimum in NLP is not a trivial matter and can represent a bareer to the proper development of mathematical modelling with this method. Since NLP is not envisaged in this thesis, the reader is referred to the reference for a deeper understanding of NLP.
- When some but not all the variables in a mathematical problem are integers, the method is called Mixed Integer programming. When the objective function and constraints are linear and integer variables are used, the method is called Mixed Integer Linear Programming (MILP). Among other things, MILP can be very useful to approximate nonlinear functions with linear, piecewise functions. Giving, this can be very useful to represent the behaviour of a chiller, as done in (Rawlings et al., 2018) (Fig. 2.2).

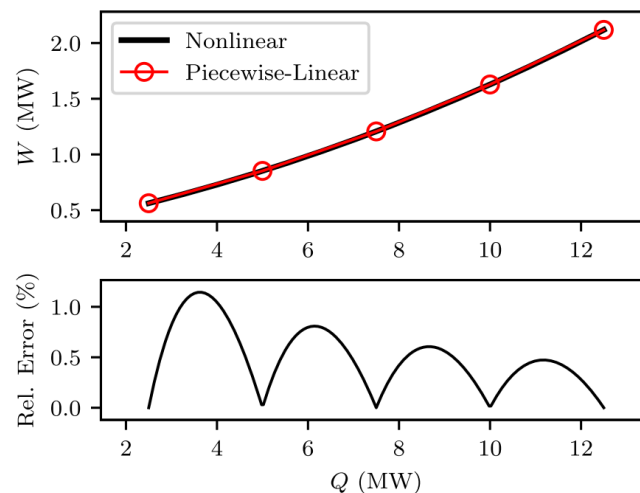


Figure 2.2: Using MILP to approximate nonlinear load curve of a chiller with a piecewise linear function (Rawlings et al., 2018)

In this thesis, LP is used as mathematical model approach for the reasons that were presented in Section 1.3.

To deepen the subject of mathematical modelling, the reader can also refer to (Abdmouleh et al., 2017) for a review designed specifically for optimization techniques used in the distributed integration of renewable energy resources.

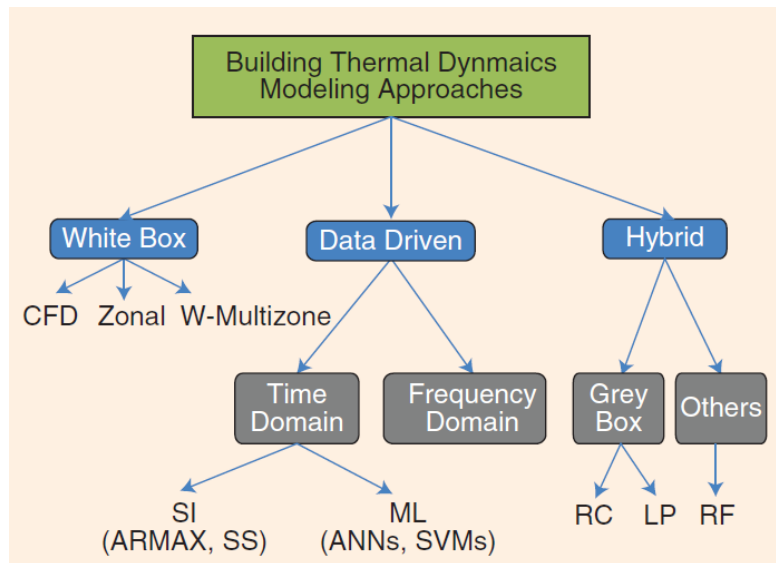


Figure 2.3: Mapping of thermal modelling approaches for buildings (Atam and Helsen, 2016)

## 2.3 Model Predictive Control (MPC)

### 2.3.1 Building Modelling for MPC

Many approaches can be considered for modelling the thermal behaviour of buildings, and particularly of interest for this thesis is to review the “intelligent HVAC control methods”. (Atam and Helsen, 2016) provide an extensive review on the control-oriented approaches to model the dynamic thermal behaviour of multi-zone buildings. The approaches are divided into three categories: white-box, data driven and hybrid. Fig. 2.3 shows a breakdown of the approaches with details about their sub-groups.

The white-box is based on modelling explicitly the physical parts of the building and implementing it in computational language. This results in implementing many differential equations that include several parameters describing properties of the building’s geometry and characteristics. Three sub-categories of white-box can be defined. CFD approach, which has very high complexity and is not suitable for control purposes. Zonal approach, which divides the zones into cells less fine than a CFD mesh, alleviating this way the computational power. Still this approach formulates the modelling problem in a way not efficient enough for control purposes. And W-multizone approach, which further simplifies the modelling by dividing the building into layers (air zones) which have uniform characteristics. Each layer in this case is defined by a state variable.

The Data-driven approach is the opposite than white-box as it does not rely on any knowledge of the physics of the system but only on available data. Usually these methods are used in the time-domain and can be divided into System Identification (SI)

and Machine-Learning (ML) types. SI is a method purely based on input-output data, without requiring any modelling on the physical system. ML is sharing the same features and results particularly useful to accurately predict temperature changes when several nonlinear characteristics are considered.

Hybrid approaches, as the name suggests, are a combination of the white-box and data-driven. Hybrids are further divided into Resistance-Capacitance (RC) and Lumped parameter (LP) modelling. The Resistance-Capacitance (RC) method is an example of grey-box approach. RC starts from an analogy between the current flow in circuits and the heat transfer in building components. The building is formulated as a number of capacitance and resistances which are interconnected and that depend on the materials and geometry of the building's section. The analogy can be expressed as

$$I = \frac{\Delta V}{R_{el}} \quad \dot{Q} = \frac{\Delta T}{R_{th}} \quad (2.1)$$

Where  $I$ ,  $\Delta V$  and  $R_{th}$  are the current flow, the voltage potential and the electric resistance of a circuit, while  $\dot{Q}$ ,  $\Delta T$  and  $R_{th}$ . In both cases, a potential generates a flow, which is impeded by a resistance. The thermal resistances are of mainly four kinds: advective, convective, conductive and radiative. These differ as they are related to different heat transfer mechanisms<sup>3</sup>. These four mentioned resistances are defined in eq. (2.2).

$$R_{adv} = \frac{1}{c\dot{m}} \quad R_{cnv} = \frac{1}{kA} \quad R_{cnd} = \frac{1}{h_c A} \quad R_{rad} = \frac{1}{h_r A} \quad (2.2)$$

- $c\dot{m}$  is the product between the air specific heat and the mass flow flowing into a zone. Advective heat flow is in fact given by the movement of air from a location characterized by a temperature to another at a different temperature.
- $k$  and  $A$  are the thermal conductivity of a solid material (walls in the case of a building) and  $A$  is the cross-section area of the solid body (perpendicular to the heat flow direction). This resistance is involved in conductive heat transfer happening between two solids (or throughout the two surfaces of a single one).
- $h_c$  is the convective heat transfer, which depends on many parameters, among which the type of fluid and its speed. This resistance is involved in convective heat transfer, which happens between a fluid and a solid.
- Finally  $h_r$  is the radiative heat transfer coefficient. Radiative heat transfer is due to electromagnetic radiation leaving a body and striking another.

<sup>3</sup>The several heat transfer mechanisms will not be explained here, while reference is made to the excellent textbook by (Lienhard, 2011) for a deeper understanding of the subject.

The RC model is very useful as it can be used for both grey and white-box approaches. In the first case, the RC values of capacitances and resistances can be estimated from data, making up for the data-side of the hybrid model. Instead, if construction data about the building are available, these can be directly input into the RC model, making it actually a white-box approach. As will be shown in Section 3.2, the RC model used in white-box setup is the case of CoBMo.

Considering the fact that this work has to take into account an already existing multi-zone building modelling framework (Section 3.2), the multizone modelling approach will be further deepened. (Prívarová et al., 2011) present a novel approach to overcome the barriers encountered to model large detailed problems for buildings when the modelling is intended for MPC (Model Predictive Control). Referring to the expressions used by (Atam and Helsén, 2016), the grey-box approach is not suitable for fitting of parameters of differential equations. On the other hand, data-oriented approaches show poor performance for the presented case because some important assumptions are violated during building's normal operations and real data are not available. Hence, the authors propose a different approach which can be useful for modelling multizone buildings based on coupling together different modelling softwares. The Building Controls Virtual Test-bed (BCVTB) is used as middle-ware tool used to couple different simulation tools. However, as suggested by (Gorecki et al., 2015) these tools have a limitation consisting in the need of having knowledge of EnergyPlus on one side, and not addressing the issue of modelling of the other. An example of overcoming this barrier can be found in (Corbin et al., 2013), who use EnergyPlus as prediction engine for the MPC controllers. Unfortunately, this approach inevitably falls back into the need of black-box modelling approaches (i.e. data-driven) which make the modelling complicated and slow. (Gorecki et al., 2015) provide a solution via the OpenBuild, a toolbox to design, test and validate various types of controllers, doing so with the creation of linear models as state-space formulations. OpenBuild aims to leverage simultaneously the computing power of Matlab and accuracy of EnergyPlus. The toolbox collects disturbance input data such as weather and internal gains, making OpenBuild suitable for MPC controllers. The advantage of the approach proposed by the authors lies in the fact that HVAC systems are implemented in Matlab and that the user can add additional modules without a specific knowledge of EnergyPlus (US DoE, 2019a).

It is worth giving a general introduction of EnergyPlus (US DoE, 2019c) as this framework represents very often the industry benchmark when it comes to multizone building modelling. In (US DoE, 2019a) EnergyPlus is categorized as a Building Energy Modelling (BEM). BEM "is the practice of using computer-based simulation software to perform a detailed analysis of a building's energy use and energy-using systems. The simulation software works by enacting a mathematical model that provides an approximate representation of the building. [...] [EnergyPlus] also guides existing building projects to optimize operation or explore retrofit opportunities." (US DoE, 2019a)". Moreover, this

framework is defined as “a whole building energy simulation program that engineers, architects, and researchers use to model both energy consumption for heating, cooling, ventilation, lighting and plug and process loads and water use in buildings.”. EnergyPlus is an open source tool which has been first released in 2001 with the idea (which is still the core proposition today) of creating a tool understandable by multiple professionals who have to perform calculations about buildings and also need to communicate between each others. EnergyPlus can serve in a very wide number of modelling approaches, such as integrated, simultaneous solution; sub-hourly, user-definable time steps; heat balance based solution; and many others (see (US DoE, 2019b) for extensive documentation).

(Sandoval et al., 2017) and (Gelazanskas and Gamage, 2014) underline also the importance of MPCs when it comes to the future evolution of peak-shaving and increased distributed generation. As solar PVs increase their penetration at the household level for example, the flexibilization of the HVAC systems of buildings becomes a fundamental problem to face in order for a smooth integration of distributed resources in future smart distribution grids. MPCs play a great role in this context as they allow effective and smart energy management of at the building level.

(Serale et al., 2018) proposes an excellent review of MPC designs and defines a framework to clearly breakdown and explain this recent control strategy. In first instance, the authors propose a broad scheme where the critical elements involved in MPC are summarized (Fig. 2.4). When assumed the design an MPC, one has to select a design strategy by combining multiple elements, such as the linearity or non-linearity of the problem, the modelling approach of the building, the disturbances model, the objective function, and so on.

The MPC formulation can for example involve both a real controlled environment, or a surrogate one which replaces the real building. In both cases disturbances and problem constrains are applied. In the case of the surrogate model, the presence of a highly-accurate model is preferred to make the results of the MPC simulation as reliable as possible. When a surrogate model is used, two options are usually available. If no data about the building is available, the MPC is tested on a building archetype<sup>4</sup> and the analysis concludes with insights about the MPC performance for a specific building category. Otherwise, when real case studies are present, the MPC can be designed in relation to a one building case, selecting one of the modelling approaches presented in Fig. 2.3. As will be presented in Section 3.2.6, this will be teh case for the CoBMo. The MPC can also be setup as including both HVAC system and building, or only one of the two. Online and offline predictions can be used, the first requiring an internet connection

---

<sup>4</sup>Building archetypes are theoretical buildings created by a composite of several characteristics found within a category of buildings with similar attributes. Therefore an archetype is a virtual representation of a number of buildings that share similar characteristics in the stock (SOUSA MONTEIRO et al., 2015)

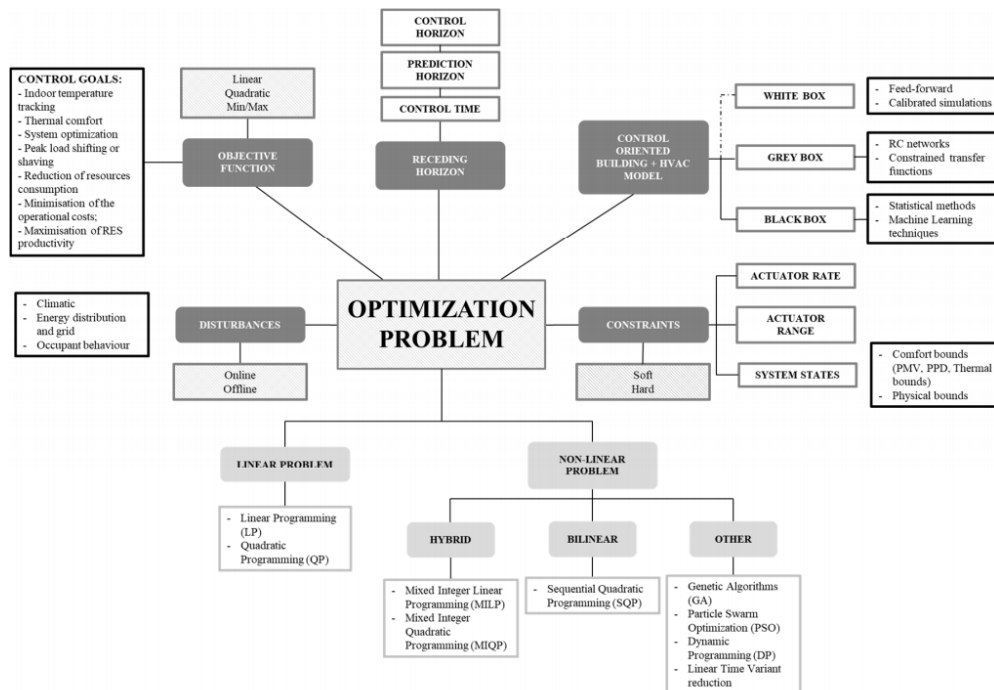


Figure 2.4: (Serale et al., 2018) maps the most critical aspects of an MPC.

and often relying on third party modelling, while the second relies only on measured data and prediction models for disturbances.

In his work, (Kramer et al., 2016) presents the design of an MPC to optimally control the operation of heat pumps in the heating case – heat supply needed by a building during winter. This case shows the potential savings when using the building as a flexible load without any storage technology implemented. As for the building model, a state space formulation is adopted. The MPC is fed with offline data forecasts and tested with a surrogate Model in Matlab. Prices from the spot market are considered. The problem is set up as an optimization of either the comfort conditions or the energy costs. When the second one is selected, an additional constraint is set to ensure that the average temperature over the whole prediction horizon meets the reference zone temperature (22 °C). The results clearly show how the economic benefits come from exploiting the variable electricity prices, both in the comfort end energy costs optimization cases. Another interesting outcome is the increase in savings when allowing a lower level of comfort in the building, performing an energy-costs-wise optimization and ignoring at the same time the average temperature constraint just mentioned. In this case, the optimization squeezes the zone temperature against the lower boundary (22 °C) further increasing the economic savings at the expenses of a large increase of discomfort index

(353,9 °C<sup>2</sup>h<sup>5</sup> compared to the 6,09 when the constraint was active).

The same authors then expand their work with the design of a Distributed MPC (DMP) of a discrete-time, linear model system (Jambagi et al., 2016). The study proves the increase of self consumption in a four-building setup with two case studies. In one, three buildings are provided with battery storage and one with PVs. The objective of the control problem is to coordinate the four houses to increase as much as possible the use of PV energy. The second case considers still one house with a PV installation, but the other three provided with heat pumps instead of batteries. In this case, the building is modeled with an RC single-zone model. The authors show how heat pumps perform overall better than storage in adapting self consumption. The key point of such study is that DMPC can be scaled up without particular increase in computational burden, as the central controller is not running the optimization problem. Adding more buildings to the problem would just add more distributed MPCs which will run independently. This shows huge benefits compared to centralized optimization. Continuing with the work by (Risbeck et al., 2017), the thermal storage is modeled as a two layers tank, with the bottom and top temperature of the two layers equal to the supply and return temperatures of the chiller. Moreover, the losses towards the environment are neglected as much smaller than the losses between the layers. The approximated stratified tank model is taken again from (Ma et al., 2009) and linearized.

Ultimately, it is widely recognized that control-oriented modelling of building thermal dynamics is a key challenge in developing effective and efficient MPC controllers for multizone buildings (Atam and Helsen, 2016). These intelligent control strategies have the potential of creating big savings on the operation of HVAC systems, but the design of fast controllers is fundamental for their real commercial application.

## 2.4 Storage and control

### 2.4.1 Storage strategies

When considering the installation of a storage facility, the sizing of such is a topic that has to be faced. Different sizes of storage can be chosen depending on the strategy that is selected about how to use the storage. Three main strategies can be identified (Ibrahim and Marc A., 2010). To help the reader picturing the different storage strategies described below, Fig. 2.5 is used to represent them (Sun et al., 2013).

- Full-load storage (Fig. 2.5a): the storage in this case is designed to supply the whole facility's load, whether it is thermal (heating and/or cooling) or electric. The

<sup>5</sup>The °C<sup>2</sup>h discomfort unit comes from the definition of the discomfort function that the authors give:  

$$J_{discomfort} = \sum_{k=1}^{N_p} (T_{z,k} - T_{ref,k})^2 \cdot \Delta t$$

storage can shift the whole peak of the demand to another time in the day. This strategy is the one that requires the biggest storage size.

- Demand-limiting partial storage (Fig. 2.5b): the goal of this strategy is to lower a certain amount of the demand of a building, even though that demand is within the design conditions. The size of the storage system in this setup is higher than the load-levelling one and the operation of the storage requires real-time monitoring of the demand and of the storage conditions.
- Load-levelling partial storage (Fig. 2.5c): the storage in this setup supplies part of the demand and has the goal operating when the demand exceeds the design conditions. In this case what is optimized is the size of the storage, in order to keep at the minimum the investment cost, while the operational savings are at the least of the three strategies.

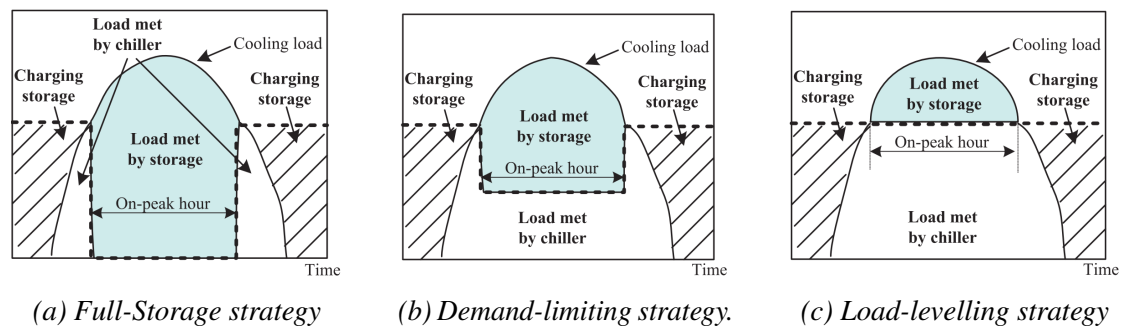


Figure 2.5: Graphical representation of the different strategies to use storage (Sun et al., 2013). The dotted - - - line represents the chiller power.

## 2.4.2 Storage and MPC

(Ma et al., 2009) proposed the design of an MPC to minimize the energy consumption of a campus (UC Merced Campus) while cooling demand constraints of buildings by including a sensible thermal storage. The authors noticed that the non-optimized operations of the storage were leading to additional losses, decreasing this way the overall efficiency of the campus. By introducing a simplified model of the system – chiller, load and storage – the results have shown that 24.5% of daily savings on the electricity bill can be achieved using MPC for the system in case. The storage tank is modeled as a two-layer tank where the mixing losses are minor. The total mass of the storage remains constant as inlet and outlet mass flows are considered to be equal for both charge and discharge. The bottom and top temperatures of the storage layers are set to 277K and

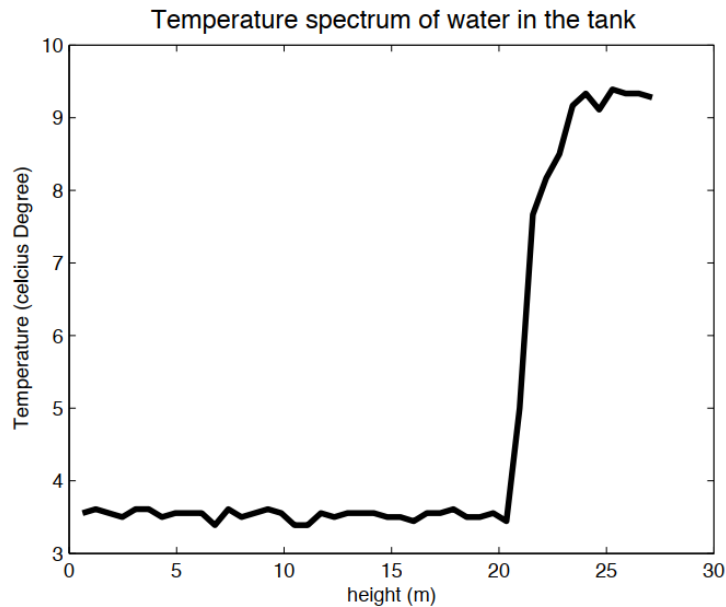


Figure 2.6: Measured temperature inside a the chilled water storage tank in the UC Merced Campus (Ma et al., 2009)

285K respectively, assumption that is backed up by a comparison with measurement data of the storage tank in the campus. The temperature spectrum clearly shows the formation of a thermocline as a thin layer characterized by high temperature and density gradients (Fig. 2.6). The tank operation is modeled by two modes, charge and discharge, which are switched via an integer variable. Given the switch variable for the tank operations, the problem is formulated as a Mixed Integer Linear Programming, which is characterized by a high complexity and high computation burden. To overcome the latter, the problem is then solved by the authors as a branch and bound, first choosing an operation mode of the tank, and then fixing this and solving a Non Linear Problem (NLP) which requires less computational power. The results coming from this study used a fixed tank operation profile which is shown in Fig. 2.7.

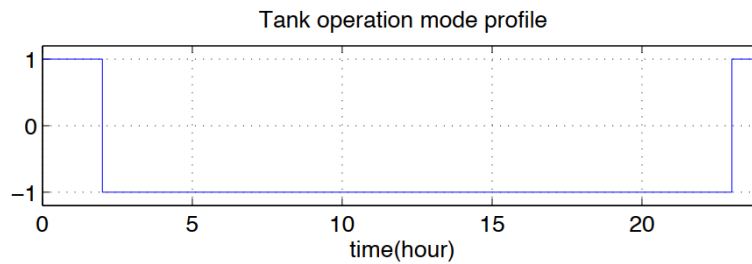


Figure 2.7: Selected and fixed operation profile used by (Ma et al., 2009)

In their work, (Risbeck et al., 2017) set up an optimization problem which aims to minimize the economic cost of operating the HVAC system equipped with thermal storage, respecting the comfort constraints inside the building. The input to the model is the forecast of the ambient condition, the electricity prices and the building occupancy. The problem would need the solution of a MINLP. The integer side is given by the switching constraints – e.g. storage charge/discharge – and the non-linearities come from the modelling of the HVAC and building system. The way the authors overcome the MINLP burden in this case is by linearizing the non-linear physical behaviours with a piece-wise linear approach. In this way the problem can be solved as a MILP. To this regard, a remark has to be done regarding the convexity of MILP problems for HVAC system optimization. In his study about economic MPC for real-time decision making of HVAC systems, (Rawlings et al., 2018) suggests again that the non-convexity of MILP – i.e. the difficulty of having a proven optimal solution – can be overcome for models involving central chiller plant within 5 minutes of computational time. The authors point back to (Risbeck et al., 2016) for reference. It appears very clear that using MILP formulations for optimal control of HVAC systems brings to the table a non-trivial issue of ensuring the convexity of the solution.

Another situation where MPC can be applied to control of storage is for example during fast demand response events in a smart grid. (Tang et al., 2019) investigates the potential of using and MPC to control the discharge operation of a PCM thermal storage allowing the chiller to operate at partial load. This is an example of demand-levelling strategy presented in Section 2.4.1 (Fig. 2.5b). In this study the goal is to achieve a stable power reduction of the chiller, while no price signal is taken into consideration into the optimization problem. The use of an optimal control strategy such as MPC can assist in scheduling the discharge of the storage in order to keep the shape of the reduced chiller operation (---) coherent with the nominal one (—) before the DR event Fig. 2.8.

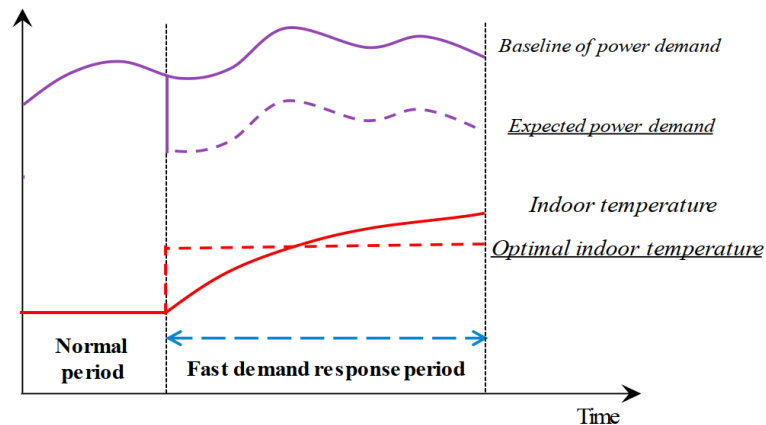


Figure 2.8: Representation of the demand-levelling control of storage to adjust the chiller operation after a fast DR event (Tang et al., 2019)

It is interesting to notice how the indoor temperature is not kept constant when flexibility occurs. Instead, the constraint on the temperature is softened the value is kept between a lower and upper bounds. Eventually, when the flexibility of a building is "called" – required either by an aggregator or by an optimal controller that optimizes the operational cost – the temperature will increase to reach the upper bound, since this condition both satisfies the indoor thermal comfort conditions *and* optimize the chiller operation.

## 2.5 Storage Technologies

In this thesis we analyze two types of storage: Thermal Energy Storage System(s) (TESS); and Battery Energy Storage System(s) (BESS)<sup>6</sup>. For the sake of brevity, the acronyms will be used from now on.

### 2.5.1 Thermal storage

In this thesis the thermal storage is considered to be a water tank, hence this is defined as a sensible thermal storage system.

The TES stores thermal energy by increasing/decreasing the temperature of the storage substance, and releases the thermal potential again via a change in temperature ( $\Delta T$ ). Whilst the  $\Delta T$  represents the thermal potential, the total amount of energy stored depends on other two factors, namely the specific heat capacity of the storage medium ( $c_p$ )

<sup>6</sup>In some occasions the naming will be abbreviated as TES – thermal energy storage – and BES – battery energy storage.

(dependent on the material type) and the mass of the medium ( $m$ ) (Cabeza, 2014). The stored heat in a TES can be expressed as:

$$Q = m \cdot c_p \cdot \Delta T \quad (2.3)$$

Where  $m$  is in [kg],  $c_p$  is in [ $\text{J kg}^{-1} \text{K}^{-1}$ ],  $\Delta T$  in [K] and  $Q$  in [J].

For heating purposes, nowadays water is the material by far most used in sensible thermal storage. The reason for this is that water displays very good physic characteristics when it come to storage density, both per volume and mass unit (Furbo, 2015). The configuration of the storage can vary, but usually water is contained in a tank made of steel, stainless steel, concrete or plastic or envelopes made of watertight materials.

For the use sensible storage in cooling, as for the case of heating, water is very much used. In fact, as underlined by (Li et al., 2012) is very favourable due to its efficient coupling with traditional water chillers. Having a suitable cold storage temperature between 4–6 °C makes water sensible storage perfect to be operated with conventional chillers and distribution systems, allowing for a low-investment efficient solution.

## 2.5.2 Battery energy storage

### Lithium-ion technology

The importance of Lithium-ion batteries (Li-ion) has constantly increased since their introduction in 1990s by Sony corporation, and their application can vary a lot (IRENA, 2017). A straightforward yet accurate breakdown of this technology can be found in (Stan et al., 2014)<sup>7</sup>. Lithium batteries can be categorized depending on the anode material and on the electrolyte; from here comes the division between Lithium-metal and Lithium-ion batteries Fig. 2.9.

For this thesis is interesting to deeper review only the Li-ion technology with liquid electrolyte. The reason for this is on one side that a liquid organic solvent mix is the most common and spread electrolyte nowadays within Li-ion (Scrosati and Garche, 2010). While the choice of investigating Li-ion is given by observing in the literature that this is the most used solution for stationary applications – which this thesis is focusing on – as proposed in the review of use cases by (Malhotra et al., 2016); here it emerged that Li-ion technology represented more than half of the projects (62.6%).

The working principle of Li-ion batteries is based on the exchange of lithium ions between anode (negative electrode  $\ominus$ ) and cathode (positive electrode  $\oplus$ ). The electrodes are made from lithium intercalation compounds and the material specifications affect the characteristics of the battery, hence its application type (IRENA, 2013). For instance,

<sup>7</sup>This source is used in (IRENA, 2017)

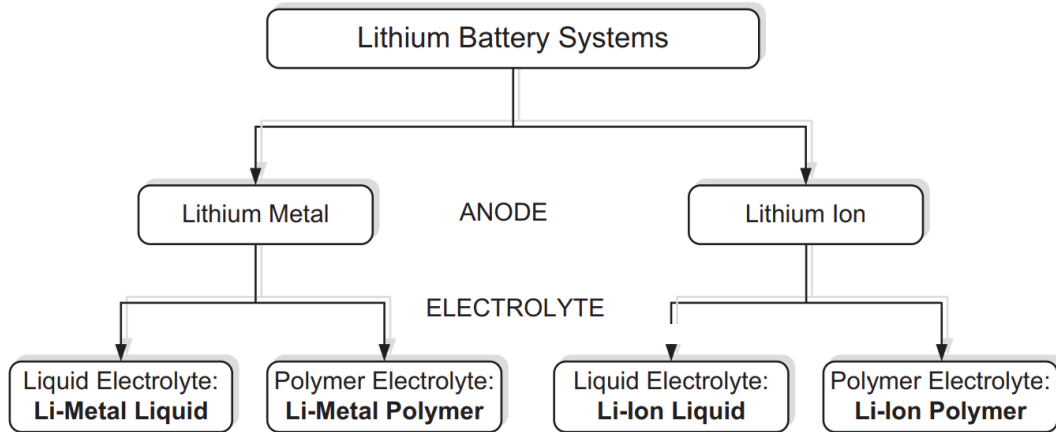


Figure 2.9: Classification of lithium batteries (Stan et al., 2014)

the Li-ion typical cathode is made of lithium metal oxide (LiMEO<sub>2</sub>) and the anode of graphite. Fig. 2.10 shows the basic working principle of this configuration (ISEA, 2012).

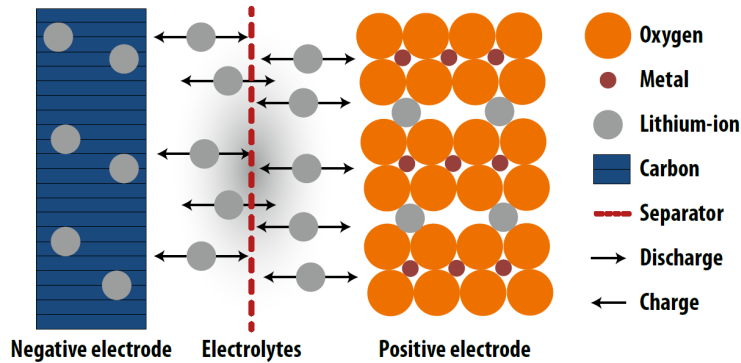


Figure 2.10: Basic functioning of a of a lithium metal oxide cathode and carbon-based anode Li-ion battery (ISEA, 2012)

In Table 2.1 are summarized the general advantages and disadvantages of Li-ion batteries. It has to be underlined that these considerations are formulated for the Li-ion technology as a whole, while various materials combinations can lead to different behaviours, hence features, of the battery.

Table 2.1: General advantages and disadvantages of Lithium Ion batteries (IRENA, 2017)

<b>Advantages</b>	<b>Disadvantages</b>
+ High specific energy and high energy and power densities compared to other technologies	- Fire risks related to chemical reactions releasing oxygen when cathodes overheat.
+ High power discharge capability	- Necessity of a integrated thermal management system
+ Excellent round trip efficiency	
+ Relatively long lifetime	
+ Low self discharge rate	

In terms of performance, depth of discharge (DOD) varies between 80% and 100% in Li-ion batteries, and the round-trip efficiency between 92% and 96%. The operating temperature has a non negligible influence on the performance of the cells and a rule of thumb is that every 10°C increase a 50% decrease in efficiency is observed. Connected with the safety disadvantages of Li-ion technology related to temperature increase (Table 2.1), in hot climates a cooling system is often to be part of the BESS (IRENA, 2017).

The cost of battery systems has kept decreasing during the last years. Nevertheless, in the literature can be found vary diverse cost breakdowns for a BESS, where for instance the cell varies in importance on the whole system cost of the whole system. (IRENA, 2017) has aggregated several studies showing that in Li-ion the main cost contributor is the cathode, which can account for up to 40% of the total material cost – and up to 23% of the whole system. It is observed that as the system size increases, the cell costs weight less on the overall cost, as the power electronics and periphery costs increase their relevance. On a general level, the energy installation costs for Li-ion can vary between 473 and 1'260 USD/kWh as proposed by (IRENA, 2017), with differences between chemistries.

### **Lead Acid technology**

Lead acid has been the first battery technology to be developed more than a century ago and has been deployed in a large and diverse number of applications, such as starters for cars, power supply systems, traction system for golf carts, off-grid and

solar home systems application (IRENA, 2017). Lead acid batteries are available in two designs: flooded and valve-regulated. Firstly, the main functioning principles of lead-acid technology will be explained. Then a brief explanation of the two designs will be presented and a summarizing table will be proposed showing the advantages and disadvantages of the two solutions.

As presented by (Bullock, 1994) in lead-acid technology both the positive and negative electrodes involve the same reactions. The cathode (positive electrode  $\oplus$ ) is made of lead dioxide ( $\text{PbO}_2$ ), the anode (negative electrode  $\ominus$ ) of metal lead (Pb) and the electrolyte is sulfuric acid ( $\text{H}_2\text{SO}_4$ ). During the discharge phase, at the cathode the lead dioxide reacts with the sulfuric acid to form lead sulfate ( $\text{PbSO}_4$ ), while at the anode the metallic lead reacts with sulfate ion ( $\text{SO}_4^{2-}$ ) to form lead sulfate. The net reaction is called double sulfate reaction. When the battery is charged the reactions are inverted and the electrodes and the electrolyte are brought back to their initial state.

In flooded lead-acid batteries the electrodes are immersed in liquid sulphuric acid. This design will lead to the loss of water from the battery during charging on a continual basis, hence the need to compensate this leakage by replacing water. Sulphation – or "acid stratification" – occurs in lead-acid batteries when sulphuric acid separates from the electrolyte and forms lead sulphate. This process accelerates the aging of the batteries and in the flooded is addressed by equipping the BESS with small pumps that circulate air inside the electrolyte to achieve uniform acid density.

Valve-regulated lead-acid batteries prevent electrolyte losses thanks to the use of a valve that regulates the maximum over-pressure. In this design leakage of gasses occurs only when the pressure goes beyond the limit imposed by the valve. Thanks to its self-regulating characteristic this design can last up to 10 years without maintenance. In valve-regulated design sulphation is addressed with a gel or absorbent immobilizing the electrolyte.

(IRENA, 2017). Table 2.2 summarizes the main advantages and disadvantages of the two designs <sup>8</sup>.

Although lead-acid is the most mature technology among batteries and the cost represents one of the advantages of this technology, the evolution and development of Li-ion technology during the last years has procured non negligible competitive pressure to lead-acid manufacturers. Improvement in performance and further reduction in costs are key to keep the technology up to the pace of Li-ion technology and further investment is required for this (IRENA, 2017). Examples of recent advances in lead-acid batteries can be found in the literature, where for instance the management strategy of the battery which includes operation in a partial state of charge can lead to notable improvement in efficiency (Büngeler et al., 2018).

<sup>8</sup>Akinyele and Rayudu, 2014; ISEA, 2012; Linden and Reddy, 2002.

### **2.5.3 Main ageing parameters in BES**

An example can be given citing the findings of (Omar et al., 2014), who provided an empirical relationship correlating the number of cycles in lithium iron-phosphate based batteries with the DoD. The relationship was derived with least-square fitting method and is found to be exponential.

Table 2.2: Advantages and disadvantages for Lead acid batteries sub-dividing by flooded lead-acid and valve regulated lead-acid batteries (IRENA, 2017)

<b>Flooded lead-acid batteries</b>	
<b>Advantages</b>	<b>Disadvantages</b>
+ Low cost compared to other rechargeable battery technologies	- Low cycling times (up to 2'500)
+ High reliability and round-trip efficiency (70-90%)	- Low energy density (50 to 100 [W h L <sup>-1</sup> ])
+ Ample manufacturing and operational experience	- Poor performance at low or high ambient temperatures (need for thermal management system)
+ Can be implemented in large-scale storage applications	- Needs periodic water replacement
+ Good temperature performance	- Sulphation, if stored long-term in discharge condition
+ Easy state-of-charge indication	- Asymmetrical charging and discharging capabilities
+ Established recycling and high recovery rate of materials	
<b>Valve-regulated lead-acid batteries</b>	
<b>Advantages</b>	<b>Disadvantages</b>
+ Very low maintenance and no water addition required	- More sensitive to higher-temperature environment than flooded lead-acid systems
+ Non-flooded electrolyte design allows for operation in areas without the need for special ventilation	- Should not be stored in discharged state
+ No special ventilation required	- Safer because of reduced spillage risk
+ Established recycling and high materials recovery rate	- Shorter lifetime than flooded design
	- More sensitive to over and under charging

## 2.6 Storage system modelling approaches

Another important part of the literature that has been done is relative to the methods that can be used to model thermal storage systems. In this section we present an overview of some relevant modelling approaches that were found in the literature.

### 2.6.1 TES Modelling

#### Single temperature model for TES

(Duffie and Beckman, 2013) models a storage tank providing the energy balance for the no-stratified case, where the dynamic behaviour of the temperature over time is considered. Here we split the expressions for cooling eq. (2.4a) and heating eq. (2.4b) cases, being the signs the only difference.

$$(mc_p)^{st} \cdot \frac{dT^{st}}{dt} = Q^{spp \rightarrow st} - Q^{st \rightarrow ld} - (UA)^{st} (T^{st} - T^{amb'}) \quad (2.4a)$$

$$(mc_p)^{st} \cdot \frac{dT^{st}}{dt} = -Q^{spp \rightarrow st} + Q^{st \rightarrow ld} + \underbrace{(UA)^{st} (T^{st} + T^{amb'})}_{Q_{loss}} \quad (2.4b)$$

The term  $(UA)^{st} (T^{st} - T^{amb'})$  represents the thermal losses of the tank towards the surrounding environment, which is represented in Fig. 3.5 by  $\dot{Q}^{loss, st}$ .  $T^{st}$  is the storage temperature;  $m$  and  $c_p$  are the mass and specific heat of the storage respectively (in kg and  $\text{J kg}^{-1}$ ) and their product results in the capacity of the storage tank in  $[\text{J K}^{-1}]$ ;  $U$  is the overall heat transfer coefficient of the storage (in  $\text{W m}^{-2} \text{K}^{-1}$ ) and  $A$  is the storage surface area where the heat transfer takes place (in  $\text{m}^2$ );  $T_a'$  is the ambient temperature for the tank, which is defined separately from the outside ambient temperature since the two can differ (the thermal storage tank could be positioned in a zone where the temperature is different than the outside one);  $\dot{Q}^{spp \rightarrow st}$  and  $\dot{Q}^{dchrg}$  are the same heat contributions presented in eq. (3.19) and eq. (3.20).

In the heating case an input of hot stream in the storage is charging the tank by making the temperature of the storage rising; the losses dissipate thermal energy towards the ambient cooling down the storage. Whilst in the cooling case an input of thermal flow cools down the storage, improving the cooling potential it can release to the load; the losses warm up the storage.

Using simple Euler integration (Duffie and Beckman, 2013) suggests a non differential form of eq. (2.4a) which can be used to determine the long term performance of a storage unit. Here we indicate with  $t$  the timestep at which the temperature is considered within a time horizon. The expression below is valid regardless how many step compose the

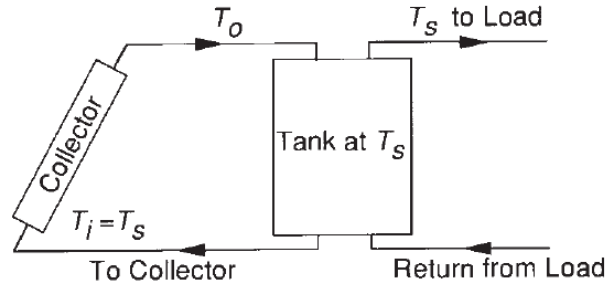


Figure 2.11: Representation of the single-temperature model for a typical water tank (Duffie and Beckman, 2013)

horizon. The expression will be show for the heating case only and can be easily drawn for the cooling case looking at equation eq. (2.4b)

While for the cooling case as:

$$T_{t+1}^{st} = T_t^{st} + \frac{\Delta T}{(mc_p)^{st}} \cdot \left[ Q^{spp \rightarrow st} - Q^{st \rightarrow ld} - (UA)^{st} (T_t^{st} - T^{amb'}) \right] \quad (2.5)$$

### Double-temperature model for TES

For the modelling of the two layers stratified tank (Deng et al., 2015) has been taken as main reference – consider that this modelling approach goes actually back to (Ma et al., 2009), and was also adopted by (Chandan et al., 2012). The authors present a mathematical model to define the dynamic behaviour of a tank which has two parts: a (top) and b (bottom). For modelling the system in this way there is the need to differentiate the mass flows flowing through the system. Find representation of this model in Fig. 2.12. For this model the explanation will be done for the cooling case only in order to remain coherent with what the authors did and for the sake of brevity. The heating case can be easily deduced by substituting the chillers with heaters and changing the direction of the flows.

Although the authors propose optimal scheduling with Mixed Integer Linear Programming (MILP) which differs from the approach used in this thesis, it is useful to consider the physical modelling of the two-layers storage tank as the authors did. Particularly, in this work we use the differential equations for the system dynamics proposed by the authors, and we bring them in non-differential form as done for the single temperature model (as proposed by (Duffie and Beckman, 2013)).

We divide the description of the system dynamics into charging and discharging processes .Notice that the terms  $c_w$  and  $\rho$  are the specific heat and density relatively and refer to water for all the expressions.

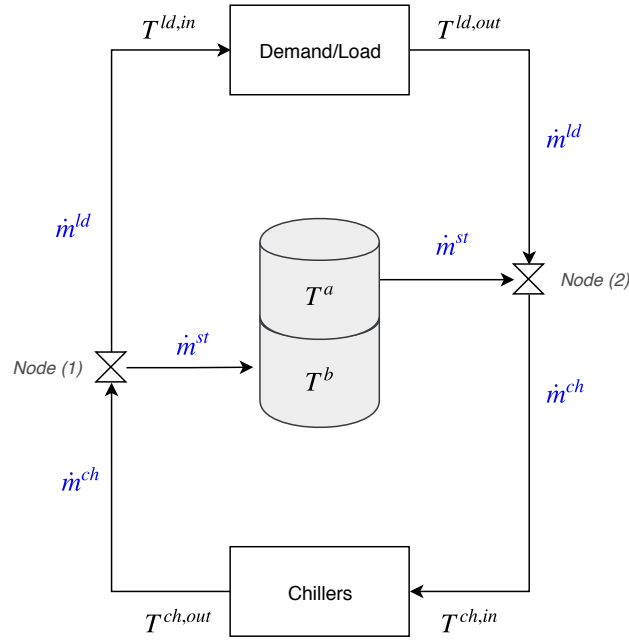


Figure 2.12: Representation of two-layers stratified tank for sensible thermal storage. (Rearranged from (Deng et al., 2015))

For the charging sequence, the mass balance is done at *Node (2)* and the balances can be written as:

$$T^{ld,in} = T^{ch,out} \quad (2.6a)$$

$$m^{st} = m^{ch} - m^{ld} \quad (2.6b)$$

$$m^{ch}T^{ch,in} = m^{st}T^a + m^{ld}T^{ld,out} \quad (2.6c)$$

$$\rho c_w \frac{dT^a}{dt} = \dot{m}^{st} c_w (T^b - T^a) + UA(T^b - T^a) \quad (2.6d)$$

$$\rho c_w \frac{dT^b}{dt} = \dot{m}^{st} c_w (T^{ch,out} - T^b) + UA(T^a - T^b) \quad (2.6e)$$

For the discharging sequence, the mass balance is done at *Node (1)* and the balances

becomes:

$$T^{ld,out} = T^{ch,in} \quad (2.7a)$$

$$m^{st} = m^{ld} - m^{ch} \quad (2.7b)$$

$$m^{ld}T^{ld,in} = m^{st}T^b + m^{ch}T^{ch,out} \quad (2.7c)$$

$$\rho c_w \frac{dT^a}{dt} = \dot{m}^{st} c_w (T^{ld,out} - T^a) + UA(T^b - T^a) \quad (2.7d)$$

$$\rho c_w \frac{dT^b}{dt} = \dot{m}^{st} c_w (T^a - T^b) + UA(T^a - T^b) \quad (2.7e)$$

$T^a$  and  $T^b$  are the temperatures of the top and bottom layers respectively [ $^{\circ}\text{C}$ ];  $\dot{m}^{st}$ ,  $\dot{m}^{ch}$  and  $\dot{m}^{ld}$  are the mass flows going to the storage, chiller and load [ $\text{kg s}^{-1}$ ];  $U$  represents the inter-layer overall heat transfer coefficient [ $\text{W m}^{-2} \text{K}^{-1}$ ].

### 2.6.2 Losses and efficiency in storage tanks

Mainly three kind of losses happen in thermal storage tanks (ARANER, 2018a):

- Losses due to heat exchange between the fluid and the external environment through the tank.
- Conductive heat transfer happening between the warm and cold layers of the tank and flowing throughout the thermocline.
- Losses due to mixing between the hot and cold level.

It is found that the first two items can be often neglected in well designed storage tanks. Losses outwards the environment are avoided thanks to application of insulation layers. Intro-layer conduction losses are demonstrated to be small and negligible. Mixing represents the largest loss in tanks.

Acknowledged the difference in importance of these three losses types, a methodology to estimate an overall efficiency of the tank is needed. (Bahnfleth and Musser, 1998) reviews different efficiencies approaches that can be used when accounting for losses in storage tanks. (Wildin and Truman, 1985) proposed that a cycle thermal efficiency could be defined as the ration between discharged thermal power over the thermal power absorbed by the storage over a complete charge cycle. When accounting for discrete measurements over the charge cycle, the efficiency can be written as in eq. (2.8).

$$\eta = \frac{[\sum_{t \in \mathcal{T}} \dot{m}_t c \cdot (T_{in} - T_{out}) \Delta t]_{discharge}}{[\sum_{t \in \mathcal{T}} \dot{m}_t c \cdot (T_{out} - T_{in}) \Delta t]_{charge}} \quad (2.8)$$

Where  $\dot{m}c$  is the mass flow at each time step;  $c$  is the specific heat of water;  $T_{in}$  and  $T_{out}$  are the inlet and outlet temperatures from the tank and  $\Delta t$  is the time step, for each  $t \in \mathcal{T}$  where  $\mathcal{T}$  is the set of time steps forming the time horizon. This efficiency definition derives from experimental analysis of the tank in question and depends on the measured mass flows and inlet and outlet temperatures of the tank. Both numerator and denominator come from experimental results.

It was noticed that this efficiency definition accounts only for losses towards the environments and neglect the mixing losses, which as was seen from (ARANER, 2018a), are the dominant ones in the industry case. Maxing losses depend basically on two different phenomena, which are described by two dimensionless numbers: the Reynolds number and the Froude number. the Reynolds number expresses the ration between inertia and viscous forces in a fluid, while the Froude number the one between inertia and buoyancy forces<sup>9</sup>. Globally, is very important when introducing water in a storage tank to keep the inertia of the fluid as low as possible to both the viscous and buoyancy forces since mixing is propositional to inertial forces, hence to the speed of the fluid. Introducing the fluid carefully into the tank can lead to a proper formation of the thermocline, which is a layer much thinner than the warm and cold layers which separates this two. In the thermocline – which can be defined as a mixed body of water – a large temperature and density gradients are experienced. In order to ensure the formation of the thermocline and the minimization of mixing losses, water has to be introduced in the tank both on the cold (bottom) and warm (top) parts with the use of diffusers. Diffusers, which can have different designs – radial disk or octagonal slotted-pipe for instance – are installed inside the tank and used as said for a smooth introduction of water into it.

A different type of performance accounting for mixing losses and for internal conduction was proposed by (Tran et al., 1989). This performance is called the Figure Of Merit (FOM) and is lower than the cycle thermal efficiency shows in eq. (2.8). The FOM is expressed as:

$$FOM = \frac{[\sum_{t \in \mathcal{T}} \dot{m}_t c \cdot (T_{in} - T_{out}) \Delta t]_{charge}}{Mc(\bar{T}_h - \bar{T}_c)} \quad (2.9)$$

Where  $M$  is the total mass that is cycled through the tank; and  $\bar{T}_c$  and  $\bar{T}_h$  are respectively the mass averaged discharge inlet temperature and the mass averaged inlet temperature during previous charge cycle.

The FOM is also dependent on the diffusers design, hence from Reynolds and Froude numbers as shown before. Again, (Bahnfleth and Musser, 1998) provides different

<sup>9</sup>Since it is not in the scope of this thesis to investigate the fluid dynamics inside a storage tank, it is chose to not provide further details about these dimensionless numbers that were found in the literature. For further reference one could refer to (Rieutord, 2014)

examples found in the literature where the FOM was calculated for several tank sizes. The values of FOM span from 75% up to 95%, depending on the diffusers size.

(Bahnfleth and Musser, 1998) then introduces a new quantity to allow more accurate measures of the performance of a storage tank: the lost capacity. The assumption is that this measure can be used only in tanks with little bulk temperature changes far from the thermocline. The reason why the lost capacity is more accurate than the FOM is that it measures the lost capacity close to the thermocline. Being the thermocline only 10% of the tank height, the lost capacity can be measured using fewer measurements, thus improving the accuracy. The lost capacity is different for charge and discharge cycle, being the former more efficient than the latter. The experiments run in this study involved a Froude number well below the unity (recommended value) and a Reynolds number at the diffusers increased up to five times above the recommended values. Nevertheless, the results have shown a lost capacity of 2% during charge and 6% during discharge<sup>10</sup>, making up for an FOM of 92% in total.

## 2.7 Introduction to the Methodology

The methodology of this thesis is divided in two parts, the mathematical modelling of the storage (Chapter 3) and the implementation of the optimization problem to calculate the optimal storage scheduling (Chapter 4). The results are finally analyzed (Chapter 5).

Fig. 2.13 presents a sketch of how the methodology can be broken down.

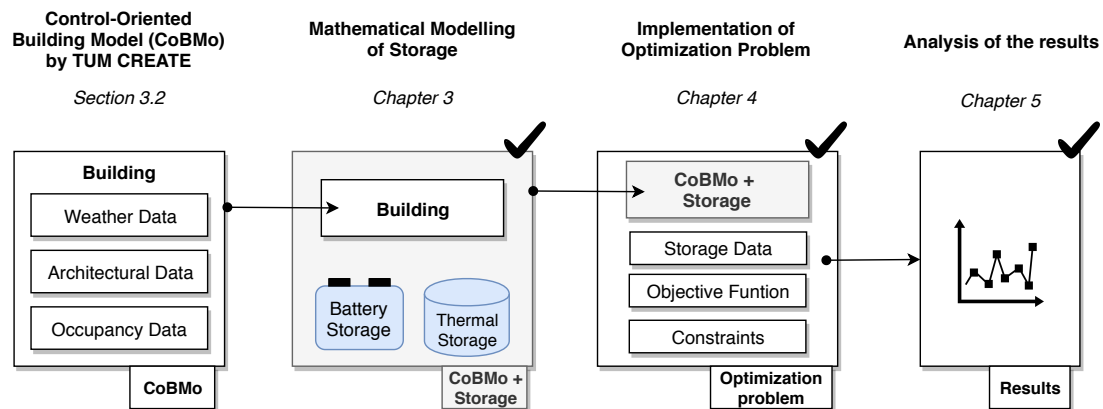


Figure 2.13: Sketch of how the methodology is structured, pointing out with a ✓ what was part of the scope of this thesis.

<sup>10</sup>This suggests that mixing in the top layer free surface might have a big impact on mixing losses.

The thesis started with analysing and understanding the CoBMo framework developed in TUM CREATE. The framework models the behaviour of a building with a white-box approach and requires the weather, architectural and occupancy data to be provided as an input. The CoBMo was then expanded by including the storage models into it, both for thermal and battery storage. The first part of the methodology will present how the storage is modelled as in relation with the building model. An optimization problem is defined and solved to find the optimal daily scheduling of the storage which minimizes cost. The mathematical modelling was developed "on paper", meaning that the mathematics that governs the behaviour of storage have to be defined. The implementation is then done in the form of code, where the equations are transported. Finally, the results are analyzed and commented.

# 3 Mathematical Modelling of Energy Storage

This chapter presents the first part of the methodology of this thesis. This is the mathematical models that were implemented to describe the behaviour of the storage, both thermal and battery. The Control-oriented Building Model (CoBMo) is presented at first, detailing what mathematical approach is followed for its development. This is a model implemented in TUM CREATE.

The modelling of the storage is then presented in a chronological manner, following the real steps that were done during the thesis. Especially for thermal storage, a higher complication of the model was achieved during the course of this work, going from a simple model accounting only for thermal flows to a two-layers storage tank model where water mass flows are calculated.

The battery storage model is more simple than the thermal one. The battery storage is considered to be a black box, hence the internal behaviour of the storage is not modeled. The battery type then influences only the efficiency and the lifetime parameters input in the model. It is part of the future work to improve the model of the battery storage by including a model of the inside of the battery cell. This could be done by integrating other modelling frameworks developed in TUM CREATE to expand the CoBMo.

## 3.1 Demand-Side Flexibility in Buildings

In this section it is explained at a high level how a building can be flexibilized. In other words, how the operation of the HVAC system in a building can be shifted from some hours of the day to others. Refer to Fig. 3.1 for the following explanation where a qualitative representation of the load, temperature and electricity tariff profiles is provided.

The operation of an HVAC in a building can be of three types:

- Currently, most office buildings in Singapore – and worldwide – are operated by

fixing a setup temperature which reflects the conditions of comfort in the zones. For instance, the CREATE tower has a setup temperature of 21°C in each zone. With this approach the building represents a fixed electrical load. The demand depends on the external disturbances – i.e. temperature, humidity, irradiation, etc. – and the physical characteristics of the envelope. This is case a) of Fig. 3.1.

- When the temperature inside the zones is allowed to vary within a defined range the operation of the building becomes flexible. This is possible thanks to the thermal inertia of the building intrinsic in its envelope and the air inside it. In this case the HVAC can be operated at hours of low demand, cooling down the air below the comfort conditions. The air will gradually warm up reaching the comfort conditions during the peak demand time; the HVAC will then be required to supply a lower power than the fixed temperature case in peak periods. The thermal inertia of the building will slowly "accompany" the building's temperature along a day and allow for the flexibilization of the HVAC system. This is represented in case b).
- The first two cases account for a flat electricity tariff throughout the day. An additional step can be made to flexibilize a building by providing a price signal to the operator. If the electricity tariff changes throughout the day, the operation of the HVAC system in the building can be adapted to leverage the low price hours and consume less during high price ones. The need of storage manifests itself even more with this arrangement as low and high prices coincide with the low and high demand periods of a day. Due to this, the HVAC system has to be operated during low-price hours even when the demand of the building is not there. Storing cold water or electricity makes then possible to store operational potential<sup>1</sup> when there is no demand and use it when this increases. This case can be implemented both with or without flexible temperature in the zones (case a) and b)). In this thesis a flexible temperature is always considered. This is case c).

This thesis considers only the potential of implicit demand side flexibility, meaning that the savings harvest by implementing DSF are for the benefit of the operator of the building only. This does not involve any sale of the flexibility nor commitment to any market. For this reason, case c) is the only setup that allows for savings to be made with DSF. The reason lies in the difference between power and energy (electricity) tariff.

The peak power in the "Load" curves in Fig. 3.1 is the maximum level of the *ordinate* axis that the curve reaches. This tariff is defined as the Use-Of-System (UOS) tariff, which in

---

<sup>1</sup>This can be seen either like cooling potential in the form of cold water. In this case the water has been processed already through a chiller. Otherwise, the electricity stored is used in the chiller and the water is processed at the very time of the request.

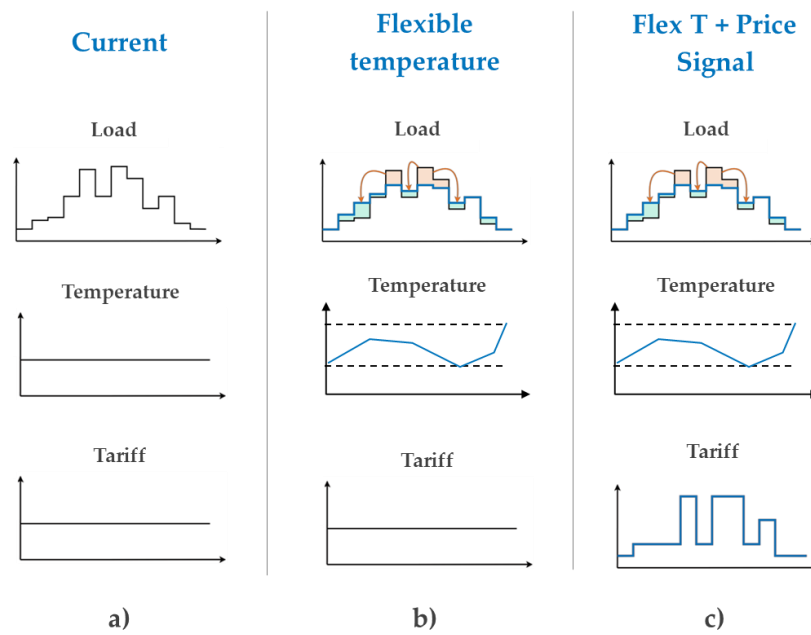


Figure 3.1: Possible setups for the operation of an HVAC of a building. The profiles for Load, temperature and tariff are qualitative and they do not reflect any real value.

Singapore is payable to SP group and is applied to recover the costs of transporting the electricity (Geneco, 2019). The UOS tariff depends on the voltage the customer receives the electricity (Fig. 3.3). This tariff is expressed in \$ per kW – or in general as money per unit of power.

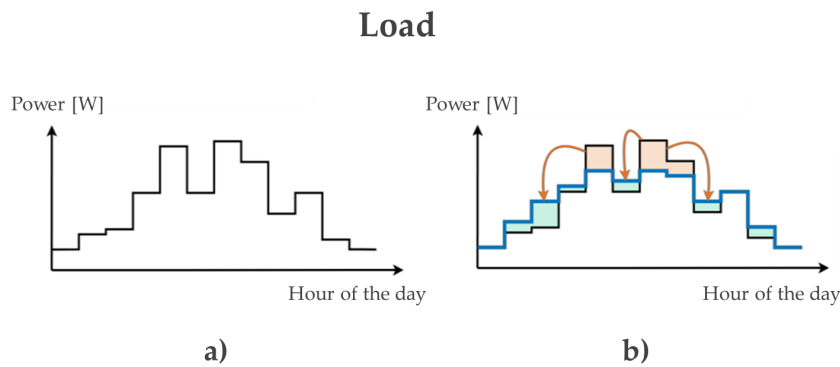


Figure 3.2: Examples of load curves. Detail of Fig. 3.1. Case a) is the non-flexible building, while b) is the flexible one.

	Contracted Capacity Charge (\$/kW/month)	Peak Period Charge (¢/kWh)	Off-Peak Period Charge (¢/kWh)	Reactive Power Charge (¢/kVAh)	Uncontracted Capacity Charge <sup>7</sup> (\$/kW/month)	Uncontracted Capacity Charge <sup>10</sup> (\$/kW/month)		
						CCS <sup>8</sup>	ECCS <sup>9</sup>	
							Tier 1	Tier 2
Ultra High Tension <sup>1</sup>	7.11	0.06	0.02	0.44	10.67	35.55	35.55	85.32
Extra High Tension <sup>2</sup>	7.87	0.08	0.03	0.48	11.81	39.55	39.55	94.44
High Tension - Large <sup>3</sup>	8.90	0.74	0.08	0.59	13.35	44.50	44.50	106.80
High Tension - Small <sup>4</sup>	8.90	0.96	0.09	0.59	13.35	44.50	44.50	106.80
Low Tension - Large <sup>5</sup>	-	5.44	4.12	-	-	-	-	-
Low Tension - Small <sup>6</sup>	-	5.44		-	-	-	-	-

Figure 3.3: Use-Of-System tariff depending on the voltage connection of the customer (Geneco, 2019)

Shaving the power peak by moving the energy demand from a peak hour to an off-peak one allows to reduce the expenses due to power peak tariff in such pricing model – Fig. 3.2 shows a detail of the load curve. For Low Tension customers – whether small (non contestable) or large (contestable, the case of office buildings in Singapore) – all the UOS tariffs are zero apart from the peak/off-peak ones. It was considered here that these tariffs are included into the wholesale and retail price signals. It can be concluded that when a time-varying price signals – wholesale or retailer – is provided to an office building operator, this is not urging a shift in the power peak of the building demand. The price signal does not reflect any price share related to the power peak.

Instead, the energy tariff depends on the amount of energy consumed by the consumer and is expressed in \$ per kWh – or in general money per unit of energy. When a consumer is provided with a price signal, shifting the energy consumption to low-tariff hours of the day entails a reduction of the overall energy costs as less energy is used at high fee time. Looking at Fig. 3.2 b), this strategy is rolled-out by moving the red energy blocks to lower peak hours – the red block become green blocks. It is very important to underline that the blocks are *moved* and not *deleted*. This is because the energy consumption of the building is considered to remain unvaried.

The electricity tariff is then key for the implicit DSF of the building to be accomplished. Implementing storage at the building level allows for a much bigger potential for flexibility – i.e. for moving much bigger red block in Fig. 3.2 enabling for thicker savings. In Section 4.4 it will be shown how linear optimization will be used as a tool to define the size of the storage installed in a building – using the CREATE Tower as a test case – and how the investment cost of the storage is assessed, defining whether it is economically feasible in terms of discounted payback time.

## 3.2 Control-oriented Building Model

The Control-oriented Building Model (CoBMo) developed in TUM CREATE is a framework modelling the thermal behaviour of a building and is designed to be suitable for the formulation of MPC problems. The mathematical model at the base of the CoBMo is a white-box approach, linear modelling.

The white-box approach is chosen because among the three methods available to model a convex problems for a building – black, grey and white (Section 2.3) – it is the only one that allows for a complete modelling process in the planning phase – i.e. in districts and neighbourhoods not yet built. This feature is best when it one wants to estimate not only the economic savings related to the building's operation with an MPC, but also the investment of the distribution system that connects the building, or the district (group of buildings), to the grid. For the planning of districts where flexible loads are constructed a white-box approach is required.

The linear characteristic of the CoBMo is also a very important and distinctive feature of this model. Although linear models can involve a higher number of assumptions on the system modelling side, their use is extremely beneficial for the numerical optimization, whose efficiency increases a lot with Linear Programming (LP) and is possible to be performed even with low computational power, which also means lower costs on simulation. Additionally, as presented in the literature review, a low computational power a necessity for running MPC on the multi-zone level, as the CoBMo does. The linear formulation makes an optimization problem convex by definition. Considering the recent advances in DSF on distributed control and the need of distributed control frameworks of running on a convex problem formulation, its linearity positions CoBMo in an even more advantageous position when looking a the future of MPC and DSF (Troitzsch et al., 2018).

### 3.2.1 The thermal model

The CoBMo represents a powerful tool that can be used to model the physical behaviour of a building and estimate the potential of its flexibility. CoBMo is expressing the relationship between the indoor air conditions with the electric load required by to keep this conditions stable. The thermal building systems – i.e. the Air Handling Unit (AHU) and the (TU) – need to supply thermal power to counterbalance the effects that surrounding external environment, occupants and appliances have on the building thermal conditions. Fig. 3.4 offers an overview of the CoBMo thermal model, highlighting the interactions between the building and all the elements that influence its thermal and comfort conditions.

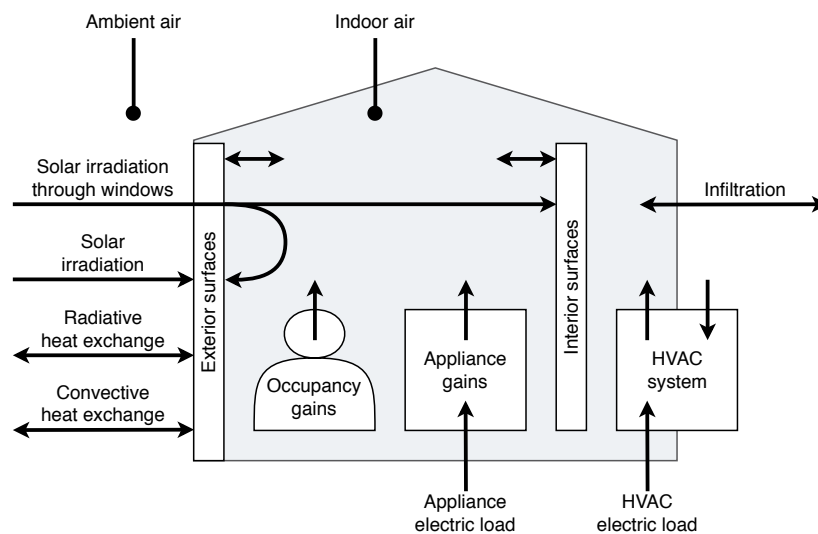


Figure 3.4: Overview of the CoBMo thermal model.

The focus of the thermal model is on meeting the comfort requirements of the occupants of the building. The demand of the building can be divided into two sub-categories. A fixed base thermal demand is required by the building and is represented by the gains caused by occupancy and appliances (such as lights and other devices). This base load is related to the type of building – hence scenario – which is considered. For instance, commercial and residential buildings will have very different occupancy profiles throughout the day, as well as different types and usage of lighting system and appliances. Sided to this base load is the supply from the HVAC system. Sided to this fixes load is what is supplied by the HVAC to meet the cooling and heating demand of the building.

### 3.2.2 Indoor Air Quality (IAQ) model

Next to the thermal model, the IAQ represents an important part of the CoBMo. As was presented in the Chapter 2, DSF is allowed by softening the constraints on some targeted variables allowing their charge, yet restricted between some predefined bounds. Besides the indoor air temperature – which is key to DSF in buildings – also the outdoor airflow requirement to meet IAQ standards can be flexibility. The CoBMo makes a further leap by implementing Demand Controlled Ventilation (DCV) and allowing this air flow to vary flexibly, shifting even more the load of the building. Even though in the past DCV was already used to reduce energy consumption by adapting the air flow to the current building and room quality requirements, new strategies further allow for shifting the load related to meet the IAQ.

### 3.2.3 State-Space formulation

The building model is constructed with a state-space formulation approach, where the model variables are put into vectors and the parameters into matrix. The formulation is firstly expressed in the continuous domain with differential equations that govern the behaviour of the chosen variables over time. Then a zero-order hold (ZOH) discretization is done to translate the system into the discrete domain.

The system equations in the state-space formulation in the conscious domain are arranged as follows (eq. (3.1)).

$$\dot{\mathbf{x}} = \mathbf{A}^{cnt} \mathbf{x} + \mathbf{B}^{u,cnt} \mathbf{u} + \mathbf{B}^{v,cnt} \mathbf{v} \quad (3.1a)$$

$$\mathbf{y} = \mathbf{C} \mathbf{x} + \mathbf{D}^u \mathbf{u} + \mathbf{D}^v \mathbf{v} \quad (3.1b)$$

$\mathbf{x}$ ,  $\mathbf{u}$ ,  $\mathbf{v}$ ,  $\mathbf{y}$  are the state, control, disturbance and output vectors;  $\mathbf{A}^{cnt}$ ,  $\mathbf{C}$  are the state and output matrix;  $\mathbf{B}^{u,cnt}$ ,  $\mathbf{D}^u$ ,  $\mathbf{B}^{v,cnt}$ ,  $\mathbf{D}^v$  are the input and feed-through matrices, on the control and disturbance vector respectively. Tables 3.1 and 3.2 presents the details for all the elements in the above equations. Consider that the subscripts  $z$  and  $s$  indicate the zone and surface belonging to  $\mathcal{Z}$  and  $\mathcal{S}$ , which are the sets of zones and surfaces.

Table 3.1: Description of the vectors that appear in the state space formulation

Element in the equation	Meaning
$\mathbf{x}$	<p>This is the state vector. It contains all the variables that describe the physics of the building and whose change in time is influenced by controls and disturbances. In the CoBMo this contains three main variables.</p> $\mathbf{x} = [T_z, T_s, c_z^{\text{CO}_2}]^\top$
$\dot{\mathbf{x}}$	<p>This is the vector containing the first derivative in time of the state variables.</p> $\dot{\mathbf{x}} = \left[ \frac{dT_z}{dt}, \frac{dT_s}{dt}, \frac{dc_z^{\text{CO}_2}}{dt} \right]^\top$
$\mathbf{u}$	<p>This is the control vector containing the variables that are used to control the state variables.</p> $\mathbf{u} = [\dot{Q}_z^{\text{gen}}, \dot{V}_z^{\text{ahu}}, \dot{V}_z^{\text{tu}}]^\top$ <p>For the case of CoBMo these are two types of variables: the generic heat <math>\dot{Q}_z^{\text{gen}}</math> is the generic thermal flow towards zone <math>z</math> and accounts for all the thermal supply systems whose models have not been implemented in detail; <math>\dot{V}_z^{\text{ahu}}</math> is the air volume supplied by the AHU to the zone <math>z</math>.</p>
$\mathbf{v}$	<p>This vector contains the disturbances that act on the system (building).</p> $\mathbf{v} = [T^{\text{amb}}, \dot{q}_d^{\text{irr}}, \dot{q}_z^{\text{occ}}]^\top$ <p>The outside ambient temperature, the irradiation heat flows and the occupancy heat flow are considered as disturbances in the building model. These influence the state variables but are not controllable.</p>
$\mathbf{y}$	<p>This is the output vector. As (Rowell, 2002) states, the output vector contains all variables that are of direct engineering interest, which doesn't necessarily mean all of them.</p>

Table 3.2: Description of the matrix that appear in the state space formulation

Element in the equation	Meaning
$A^{cnt}$	It contains the combination of parameters related directly to the state variable used to build the differential equation.
$B^{u,cnt}, B^{v,cnt}$	These contain the combination of parameters related directly to the control and disturbance variables used to build the differential equation .
$C$	This is the output matrix containing the conversion parameters to display the output.
$D^u, D^v$	Feed-through matrix on the control and disturbance.

Applying then the zero-order hold discretization, the matrix are transformed as follows:

$$A = e^{A^{cnt} \Delta t} \quad (3.2a)$$

$$B^u = (A^{cnt})^{-1} (A - I) B^{u,cnt} \quad (3.2b)$$

$$B^v = (A^{cnt})^{-1} (A - I) B^{v,cnt} \quad (3.2c)$$

$A, B^u, B^v$  are the discrete-time instances of  $A^{cnt}, B^{u,cnt}, B^{v,cnt}$ , while  $C, D^u$  and  $D^v$  are equivalent in discrete-time as these matrices do not describe a differential equation.

It is finally possible to write the discretized form of the building model as:

$$x_{t+1} = Ax_t + B^u u_t + B^v v_t \quad (3.3a)$$

$$y_t = Cx_t + D^u u_t + D^v v_t \quad (3.3b)$$

### 3.2.4 Thermal flexibility of buildings

A building is characterized by some thermal inertia. This inertia is allowed by the mass of air inside the building and by the mass of the walls the building is constructed with. In this sense, one can flexibilize a building already by letting the inside temperature  $T_z$  to

vary withing a range instead of keeping it constant, making the HVAC system to pre-cool or pre-heat in hours of low peak.

Since the comfort inside the building is measured with the internal temperature of the zones, the model is based on relationships between the state variable and the control and disturbances that influence these variables, namely the HVAC load (control), the local weather conditions and the internal gains (disturbances). The addition of storage is adding up to this already existing flexibility of the building system to further shift the peak consumption of the HVAC and provide even more DSF. A great difference though between the two methods is that the first one – flexibilizing by way of using the building inertia – does not require any investment cost<sup>2</sup>; installing the storage involves instead a significant investment, which has to be paid back by the additional savings.

### 3.2.5 The thermal model in the CoBMo

Hereby, an overview of the equations used to model the CoBMo is provided. For the purpose of this work it was assumed sufficient to build the state vector with only two state variables as shown above, whose other variables relative to the storage will be appended (Chapter 4 in the CoBMo).

$$\mathbf{x} = [T_z, T_s]^T$$

As said before, the indication of the comfort in the building is the indoor temperature of the zone  $z$ ; hence the thermal relationship between this temperature and the controls and disturbances has to be expressed. The differential equations 3.4 are show this relationship on a general level.

$$\frac{dT_z}{dt} = \frac{\dot{Q}_z}{C_z^{thm}}, \quad \forall z \in \mathcal{Z} \quad (3.4a)$$

$$\frac{dT_s}{dt} = \frac{\dot{Q}_s}{C_s^{thm}}, \quad \forall s \in \mathcal{S} \quad (3.4b)$$

$C_z^{thm}$  and  $C_s^{thm}$  are the thermal heat capacities of the zones<sup>3</sup> and the surfaces.

The core concept is that a global relationship has to be found that expresses the term  $\dot{Q}_z$  that influences the temperature of the zone. The single zone  $z$  can be surrounded by walls

<sup>2</sup>This is true when the building is already equipped with temperature sensors and controls for each zone of the building. When this is not the case, an investment has to be considered, which is very small when compared to a large storage facility – weather battery or thermal storage. We consider in this thesis that the buildings are already equipped with temperature sensors and individual temperature control for each zone.

<sup>3</sup>This is obtained according to ISO 13790

of different kind characterized by different thermal behaviours. To finally being able to account for the single heat exchange that is happening towards the zone  $z$ , the thermal behaviour of the whole system around that zone has to be modeled because it is having an influence of the zone itself. To present all the heat contributions coming from the different sections of the system in most clear way possible, a systematic approach is used. First, the global differential equation of  $T_z$  is presented where all the heat contributions are shown – but not made explicit. The detailed equations of each contribution are then shown. Two remarks have to be done before digging into the model. Firstly, for the sake of brevity the equations are presented directly in their final form, without showing all the maths steps needed to get to it. Secondly, the form the equations are shown is coherent with the state space formulation, meaning that the variables are isolated – state, control and disturbance – and parts multiplying the variables represent the coefficients of the matrix. This is done to ease the formulation of the state space matrix entries.

We consider the following equation to model the behaviour of the zone temperature in time.

$$\frac{dT_z}{dt} \cdot C_{th,z} = \left( \left( \sum_{s \in S_z} \dot{Q}_{s,z}^{cnv,int} \right) + \dot{Q}_z^{inf} + \dot{Q}_z^{occ} + \dot{Q}_z^{hvac} \right) \quad (3.5)$$

Where the right side of the equation represent the total heat transfer towards the zone ( $\dot{Q}_z$ ). The term  $\sum_{s \in S_z} \dot{Q}_{s,z}^{cnv,int}$  is the sum of all the convective heat transfers towards the zone;  $\dot{Q}_z^{inf}$  is the heat transfer due to infiltration;  $\dot{Q}_z^{occ}$  is connected to the occupancy of the zone; and  $\dot{Q}_z^{hvac}$  is the heat supplied from the HVAC thermal system. Each heat contribution is defined per zone  $z$ , except the convective one which is defined between a surface  $s$  and a zone  $z$ . Each term of eq. (3.5) will be expanded below.

### Exterior surfaces

$\dot{Q}_{s,z}^{cnv,int}$  represents the convective heat transfer from the surface  $s$  to the zone  $z$  and is part of a balance which is done on the surfaces of the building. Considering the external surfaces first, the heat balance on the surface can be written on the exterior and interior sides of the wall, as in eq. (3.6).

$$\dot{Q}_s^{cnv,ext} + \dot{Q}_s^{irr,ext} - \dot{Q}_s^{ems,sky} - \dot{Q}_s^{ems,gnd} = \dot{Q}_s^{ext,int} \quad (3.6a)$$

$$\dot{Q}_s^{ext,int} = \dot{Q}_{s,z}^{cnv,int} - \dot{Q}_s^{irr,int} \quad (3.6b)$$

It can be seen the common term between the equations,  $\dot{Q}_s^{ext,int}$ , and the term present in eq. (3.5),  $\dot{Q}_{s,z}^{cnv,int}$ . On the external side of the wall, the convection heat transfer can be expressed as

$$\dot{Q}_s^{cnv,ext} = A_s h^{ext} (T^{amb} - T_s^{sur,ext}) \quad (3.7)$$

Being  $A_s$  the area of the external surface and  $h^{ext}$  the exterior heat transfer coefficient, given according to ISO 6946.  $T_s^{sur,ext}$  is the temperature of the external surface of the wall.

The irradiation term is defined as

$$\dot{Q}_s^{irr,ext} = A_s \alpha_s \dot{q}_d^{irr,ext}, \quad d = d(s) \quad (3.8)$$

With  $\alpha_s$  being the absorption coefficient of the surface and  $\dot{q}_d^{irr,ext}$  the total incident irradiation onto a surface oriented towards direction  $d \in \{N, E, S, W, H\}$ .

The exterior emission heat transfers are directed towards the sky and the ground and expressed as

$$\dot{Q}_s^{ems,sky} = A_s h_s^{sky} (T_s^{sur,ext} - T^{sky}) \quad (3.9a)$$

$$\dot{Q}_s^{ems,gnd} = A_s h_s^{gnd} (T_s^{sur,ext} - T^{amb}) \quad (3.9b)$$

$h_s^{sky}$  and  $h_s^{gnd}$  are the sky and ground heat transfer coefficients which are defined as

$$h_s^{sky} = 4\sigma\varepsilon_s F_d^{sky} \left( \frac{T_s^{sur,ext,lin} + T^{sky,lin}}{2} \right)^3 \quad (3.10a)$$

$$h_s^{gnd} = 4\sigma\varepsilon_s F_d^{gnd} \left( \frac{T_s^{sur,ext,lin} + T^{amb,lin}}{2} \right)^3 \quad (3.10b)$$

$\sigma$ ,  $\varepsilon_s$  and  $F_d^{sky}$  are the Stefan-Boltzmann constant, the surface emission coefficient of surface  $s$  for long-wave radiations and the view factor of direction  $d(s)$  towards the sky. The temperatures  $T_s^{sur,ext,lin}$  and  $T^{sky,lin}$  are linearization constants that are defined as the average values of  $T_s^{sur,ext}$  and  $T^{sky}$ .

The interior convective heat transfer is expressed as

$$\dot{Q}_s^{env,int} = A_s h_d^{int} (T^z - T_s^{sur,int}) \quad (3.11)$$

with  $T_s^{sur,int}$  being the temperature on the interior surface (analogously to what said for the exterior one).  $h_d^{int}$  and  $T^z$  are the interior heat transfer coefficient and the zone air temperature. The interior heat transfer coefficient  $h_d^{int}$  depends on the surface's direction  $d(s)$  and is defined from ISO 6946.

The interior irradiation contribution is actually the radiation entering the zone from the windows and is expressed as

$$\dot{Q}_s^{irr,int} = A_s \alpha_s \dot{q}_z^{irr,int}, \quad d = d(s) \quad (3.12)$$

with  $\dot{q}_z^{irr,int}$  being defined as

$$\dot{q}_z^{irr,int} = \frac{\sum_{w \in \mathcal{W}_z} A_w \tau_w \dot{q}_{d(w)}^{irr,ext}}{\sum_{s \in \mathcal{S}_z} A_s} \quad (3.13)$$

The coupling term is

$$\dot{Q}_s^{ext,int} = A_s h_s^{ext,int} (T_s^{sur,ext} - T_s^{sur,int}) \quad (3.14)$$

At this point it is possible to write an expression of the term  $\dot{Q}_s^{cnv,int}$  which we need to use in eq. (3.5) in its first term. This is done by solving the over-determined system of equations from eq. (3.6) to eq. (3.14). The last form of the interior convective heat transfer is

$$\begin{aligned} \dot{Q}_s^{cnv,int} = & \dot{q}_d^{irr,ext} \cdot \alpha_s A_s \left( 1 + \frac{h^{cnv,ext} + h_s^{gnd} + h_s^{sky}}{h_s^{cnv,int}} + \frac{h^{cnv,ext} + h_s^{gnd} + h_s^{sky}}{h_s^{cnd}} \right)^{-1} \\ & + T^{amb} \cdot (h^{cnv,ext} + h_s^{gnd}) \\ & \cdot A_s \left( 1 + \frac{h^{cnv,ext} + h_s^{gnd} + h_s^{sky}}{h_s^{cnv,int}} + \frac{h^{cnv,ext} + h_s^{gnd} + h_s^{sky}}{h_s^{cnd}} \right)^{-1} \\ & + T^{sky} \cdot h_s^{sky} A_s \left( 1 + \frac{h^{cnv,ext} + h_s^{gnd} + h_s^{sky}}{h_s^{cnv,int}} + \frac{h^{cnv,ext} + h_s^{gnd} + h_s^{sky}}{h_s^{cnd}} \right)^{-1} \\ & + T_z(-1) \cdot A_s \left( \frac{1}{h^{cnv,ext} + h_s^{gnd} + h_s^{sky}} + \frac{1}{h_s^{cnv,int}} + \frac{1}{h_s^{cnd}} \right)^{-1} \\ & + \dot{q}_z^{irr,int} \cdot \alpha_s A_s \left( 1 - \left( 1 + \frac{h_s^{cnv,int}}{h^{cnv,ext} + h_s^{gnd} + h_s^{sky}} + \frac{h_s^{cnv,int}}{h_s^{cnd}} \right)^{-1} \right) \end{aligned} \quad (3.15)$$

Eq. (3.15) is written so that the first term of each line is a system variable, either state, control or disturbance, and the multiplied term is the coefficient that will be insert in the respective matrix in the state-space formulation (Section 3.2.3).

### Infiltration

The heat transfer towards the zone due to infiltration is expressed as

$$\dot{Q}_z^{inf} = \dot{V}_z C^{th,air} n_z^{inf} (T^{amb} - T_z) \quad (3.16)$$

Where  $V_z$  is the volume of zone  $z$ ,  $C^{th,air}$  is the heat capacity of air and  $n_z^{inf}$  is the infiltration rate.

### Interior and Adiabatic

For the sake of brevity the explanation for Adiabatic and Interior surfaces is not presented hereby as it is analogous to the exterior surfaces one.

### Occupancy

The occupancy gain is calculated as

$$\dot{Q}_z^{occ} = A_z \dot{q}_z^{occ} \quad (3.17)$$

Where  $A_z$  is the area of zone  $z$  and  $\dot{q}_z^{occ}$  is the specific thermal gain due to occupancy

### HVAC

The heat contribution from the HVAC system represents what can be controlled and used to modify act on the system. This heat contribution is define as

$$\dot{Q}_z^{hvac} = -\eta_b^{hvac} P_z^{hvac} \quad (3.18)$$

Where  $\eta_b^{hvac}$  is the efficiency factor of the HVAC system of the building  $b$  and  $P_z^{hvac}$  is the electric power consumption of the HVAC system associated with the zone  $z$ . The HVAC system is modeled in the same way for both the heating and cooling cases.

## 3.2.6 CREATE Tower test case

### Thermal model parameters

The geometric information of zones and surfaces are derived from the architectural drawings of the test case. Based on the building documentation, the thermal building model parameters in Table 3.3 are defined. The number of occupants  $\dot{n}_z^{occ}$  and occupancy gains  $\dot{q}_z^{occ}$  have been recorded for the test period.

### Weather data

Weather data is obtained from a nearby weather station at the campus of the National University of Singapore (NUS). The sky temperature  $T^{sky}$  is defined by an approximation for tropical climate as  $T^{sky} = T^{amb} - 13 \text{ K}$  according to ISO 52016-1.

### Comfort constraints

The thermal comfort and IAQ constraints are given in Table 3.5. For DCV strategies, also refer to the respectively defined constraints above.

Table 3.3: Thermal model parameters.

Parameter	Value
$h_s^{cnd}$ (ext./int. surf. type 1)	$0.54 \text{ W K}^{-1} \text{ m}^{-2}$
$h_s^{cnd}$ (ext./int. surf. type 2)	$3.85 \text{ W K}^{-1} \text{ m}^{-2}$
$\alpha_s$ (all surfaces)	0.3
$\varepsilon_s$ (all surfaces)	0.87
$\tau_w$ (ext. windows)	0.2
$C_z^{thm}$	$1.21 \text{ kJ K}^{-1} \text{ m}^{-3}$
$C_s^{thm}$ (ext./int. surf. type 1)	$91.5 \text{ kJ K}^{-1} \text{ m}^{-3}$
$C_s^{thm}$ (ext./int. surf. type 2)	$810 \text{ kJ K}^{-1} \text{ m}^{-3}$
$n_z^{inf}$	$0.2 \text{ h}^{-1}$

Table 3.4: Thermal model linearization parameters.

Parameter	Value
$\eta^{hvac}$	4
$T_s^{sur,lin}$	$35 \text{ }^\circ\text{C}$
$T_s^{sky,lin}$	$13 \text{ }^\circ\text{C}$
$T_s^{amb,lin}$	$30 \text{ }^\circ\text{C}$

Table 3.5: Comfort constraints.

Parameter	Min. value	Max. value
$c_z^{CO_2}$	-	700 ppm
$T_z$	$18 \text{ }^\circ\text{C}$	$25 \text{ }^\circ\text{C}$

### 3.3 Modelling of TES

As the thermal storage models have to be implemented into the CoBMo, which is a white-box model – this leads to the straightforward need to define clear mathematical models that can approximate the real behaviour of storage systems. This section presents the modelling approaches selected for TES systems.

In this work the TES has been modeled with different increasing steps of difficulty. First, a model was developed which considers the relation between the storage, the load and the heating/cooling system only via thermal flows. Then, more detailed models are developed which also account for the temperature of the storage. The reason why this approach was used is related to the chronological development of the models. At the beginning, a simple modelling which could be used to understand the basic behaviour of the system was designed. This helped building a fundamental optimization algorithm in Python. Then, upgrades have been done as over time adding details to the fundamental model and expanding it.

#### 3.3.1 Thermal flows Model

The first and most simple approach is to model the thermal storage by considering only the thermal flows in the system, hence not calculating the temperature of the storage.

Fig. 3.5 provides a representation of a system considering thermal storage. Superscripts are descriptive for the physical quantity, while subscripts indicate an indexing. In the figure it can be seen that there are two main sides: Supply (chillers) and Demand (Load). The supply side is the one providing the thermal potential. The Demand side is the one making use of the thermal potential provided by the Supply side. The storage is in between the two.

A balance of the system in terms of thermal flows can be written as:

$$\begin{cases} \dot{Q}^{demand} &= \dot{Q}^{dchrg} + \dot{Q}^{sup} \\ \dot{Q}^{chiller} &= \dot{Q}^{chrg} + \dot{Q}^{sup} \Rightarrow \dot{Q}^{sup} = \dot{Q}^{chiller} - \dot{Q}^{chrg} \end{cases} \quad (3.19)$$

Hence the balance can be rewritten in form of one equation only as:

$$\dot{Q}^{demand} = \dot{Q}^{chiller} - \dot{Q}^{chrg} + \dot{Q}^{dchrg} \quad (3.20)$$

Where  $\dot{Q}^{chiller}$  is the thermal flow supplied from the chillers;  $\dot{Q}^{chrg}$  is the thermal flow charging the storage;  $\dot{Q}^{sup}$  is direct contribution from the chiller to the demand;  $\dot{Q}^{dchrg}$  is the thermal flow discharging the to supply the demand;  $\dot{Q}^{demand}$  is the total demanded

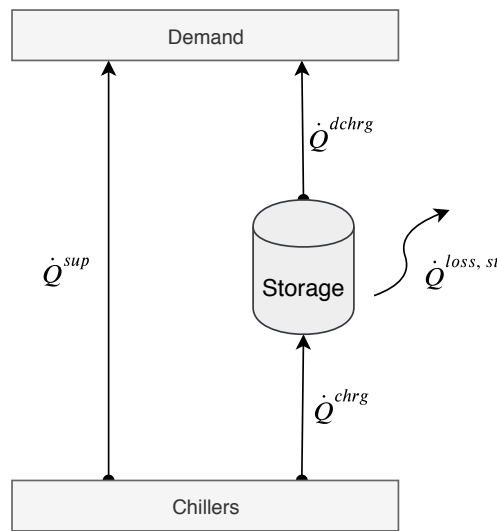


Figure 3.5: Simplified representation of a system including thermal storage. The parts involved are supply, demand and storage.

thermal flow . The charging and discharging processes are carried out to control the storage level and leverage the storage thermal potential when needed.

This modelling approach is made coherent with the multi-zone structure of CoBMo. Fig. 3.6 shows the representation of the thermal flows model for a multi-zone building model.

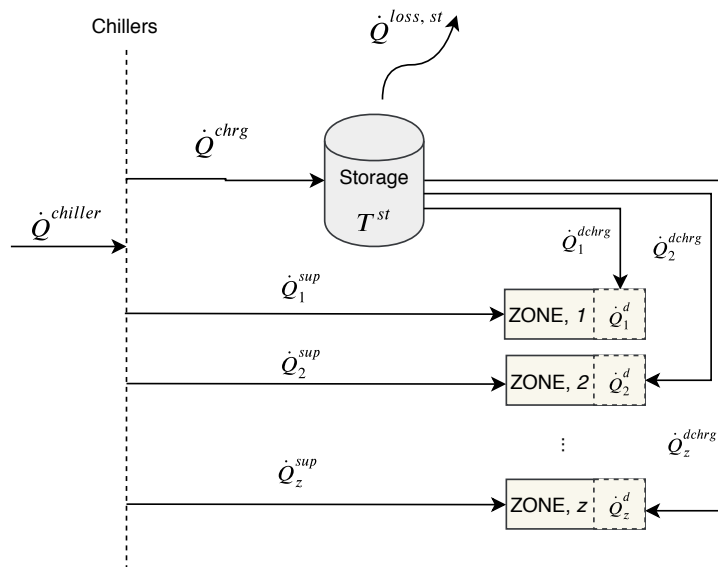


Figure 3.6: Thermal-flows model adapted to the multi-zone modelling approach.

This model is adapted to be made coherent with the multi-zonal approach CoBMo is based on. As done in eq. (3.19) we write the balance equations for the system.

$$\left\{ \begin{array}{l} \dot{Q}_z^{demand} = \dot{Q}_z^{sup} + \dot{Q}_z^{dchrg} : \\ \dot{Q}^{demand,tot} = \sum_{z=1}^Z [\dot{Q}_z^{dchrg} + \dot{Q}_z^{sup}] \\ \dot{Q}^{chiller} = \dot{Q}^{chrg} + \sum_{z=1}^Z [\dot{Q}_z^{sup}] \Rightarrow \sum_{z=1}^Z [\dot{Q}_z^{sup}] = \dot{Q}^{chiller} - \dot{Q}^{chrg} \end{array} \right. \quad (3.21)$$

The global balance can be then written as:

$$\dot{Q}^{demand,tot} = \sum_{z=1}^Z [\dot{Q}_z^{dchrg} + \dot{Q}_z^{sup}] - \dot{Q}^{chrg} \quad (3.22)$$

### 3.3.2 Single Temperature Tank Model

The model has evolved towards accounting for the temperature change of the storage tank. The temperature of the storage  $T^{st}$  represents the thermal potential that the storage can release and hence represents the level of the storage. An important remark has to be made before presenting the modelling approach. In cooling grids it is the priority to keep the chiller operation at its efficiency peak since the operational expenses related to the chiller account for almost 95%. For this reason the chillers supplies water at the fixed temperature of 4°C, which is the same temperature at which the demand is supplied. Changing the supply temperature of the chillers and demand leads to major changes in the operation of the cooling grid and to high inefficiencies. Is for this reason that the water storage tank for chilled water is designed to preserve the stratification of water and to always have available water at both the temperatures of supply and return of the chiller and demand – 4°C and 12°C. So said, in the model presented in this section the temperature of the storage is considered *only* as a potential, and not as the actual temperature at which the heat flows are delivered from the storage to the demand nor from the chiller to the storage. In fact, ff this was the case, since the *single* storage temperature is let varying between 4°C and 12°C, the operation of the cooling grid would be highly jeopardized.

#### Remark

The one-temperature model of the storage tank works well for tanks where heat exchangers are used to transfer heat to the storage. This process does not involve any direct mass exchange between the chiller and the tank and the water inside the tank is kept at homogeneous temperature conditions. When instead water is exchanged directly with the tank the temperature profile inside the tank is strongly not homogeneous due to the formation of a thermocline. The stratification of water forms two layers: warm and cold. Since in this thesis the cooling case is the one investigated, a the expansion of the single temperature model into a two-layers stratified one is done.

Acknowledged this remark it is possible to proceed with the description of the single-temperature model. Fig. 3.7 shows a sketch of the system.

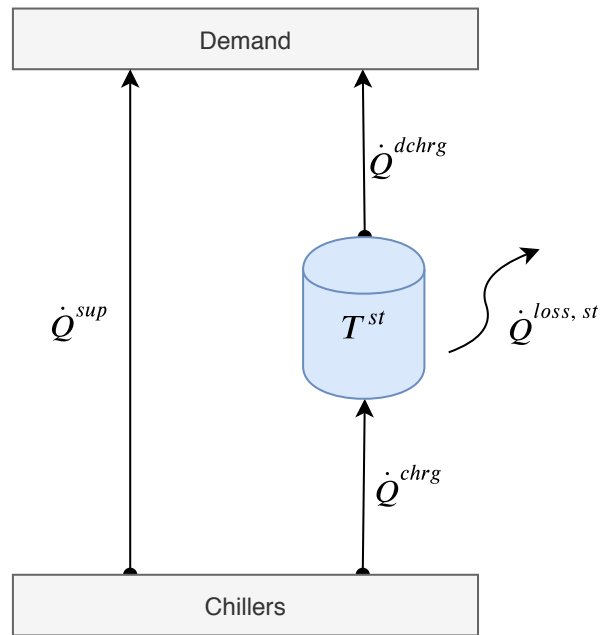


Figure 3.7: Sketch of the single-temperature modelling approach

The storage temperature is ruled by the following differential equation:

$$(mc_p)^{st} \cdot \frac{dT^{st}}{dt} = \dot{Q}^{chrg} - \dot{Q}^{dchrg} - (UA)^{st} (T^{st} - T^{amb'}) \quad (3.23)$$

eq. (3.23), which is proposed by (Duffie and Beckman, 2013) (see Section 2.6.1), is expressing the temperature change in time as dependent on three heat contributions: storage charge  $\dot{Q}^{chrg}$ ; storage discharge  $\dot{Q}^{dchrg}$ ; thermal losses towards the environment surrounding the tank  $(UA)^{st} (T^{st} - T^{amb'})$ <sup>4</sup>.  $(mc_p)^{st}$  is the thermal capacity of the storage tank ( $C^{st}$ );  $(UA)^{st}$  is the overall heat transfer coefficient of the tank and depends on the materials choice for the tank construction and the convection heat transfer coefficient on the air and water side.

Over time the temperature of the storage changes depending on the charge/discharge schedule imposed. If the storage is left unused for a long period of time, a linear decrease in temperature will occur due to the presence of thermal losses, consisting in a depletion of the thermal potential of the storage. The losses of the storage depend on the combination of the materials chosen to construct the tank. Many options are available, but information that were provided by Singapore authorities operating several district cooling grids have confirmed that these losses are very small and often irrelevant.

<sup>4</sup>As said in Section 2.6.1,  $T^{amb'}$  is the ambient temperature perceived by the tank, which might differ from the external one

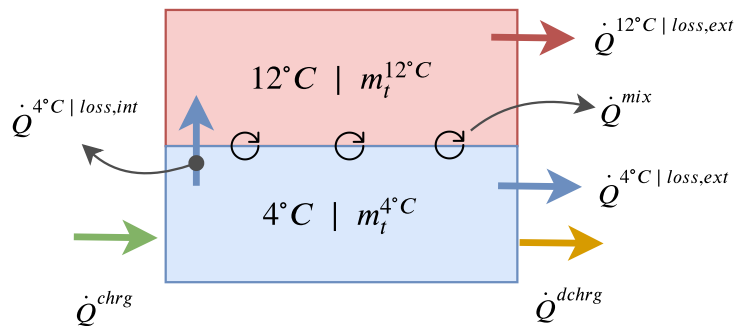


Figure 3.8: Sketch of the two-layer storage tank and the heat.

### 3.3.3 Two layers storage model

As mentioned before, it is important to keep the model of the storage linear for mainly two reasons: having a computational power required; keeping the model coherent with the CoBMo LP modelling approach. Hereby we propose a modelling approach that takes into consideration the stratification of the storage tank, though imposing some assumptions that are necessary to make the keep the model linear. A summary of the assumptions is shown in the box below.

The storage is considered to be a two-layers stratified tank, whose layers are set at the supply and demand temperatures of the chiller and the load, respectively 4°C (bottom layer) and 12°C (top layer). During charging, the bottom layer increases in mass while the top layer decreases; during discharging the opposite happens. This is coherent with what happens in reality, as was found also from industry sources (ARANER, 2018a). The two layers are divided by a mixed body of water called thermocline, which is not modelled in this thesis.

The differential equations expressing the change of the layers mass over time is in equations eq. (3.24) and eq. (3.25) and figure Fig. 3.8 shows a representation of the heat contribu-

#### Assumption

The stratification of a storage tank happens with multiple levels of temperatures, where only the bottom and top layers are at the temperatures of 4°C and 12°C respectively. When more than two layers are considered, the warm water that is returned to the chiller to be cooled down has to be withdrawn from the warmest layer. On the algorithm level, this involves the need of a binary variable that gives an information of the selected layer from which the water is being withdrawn. This is not desirable since a LP model has to be implemented and the presence of only two layer is the necessary condition to make the problem suitable for a linear approach. Additionally, the dynamic behaviour of the thermocline is not modelled.

tions in the equations.

$$\begin{aligned} \frac{dm^{4^\circ C}}{dt} \cdot (c_w \Delta T^{layers}) &= \dot{Q}^{chg} - \dot{Q}^{dchg} \\ &\quad - \dot{Q}^{4^\circ C | loss, amb} \\ &\quad - \dot{Q}^{4^\circ C | loss, int} \end{aligned} \quad (3.24)$$

$$\begin{aligned} \frac{dm^{12^\circ C}}{dt} \cdot (c_w \Delta T^{layers}) &= -\dot{Q}^{chg} + \dot{Q}^{dchg} \\ &\quad + \dot{Q}^{4^\circ C | loss, amb} \\ &\quad + \dot{Q}^{4^\circ C | loss, int} \\ &\quad - \dot{Q}^{12^\circ C | loss, amb} \end{aligned} \quad (3.25)$$

Both the equations above are rewritten by making explicit the losses terms. For the bottom layer:

$$\begin{aligned} \frac{dm^{4^\circ C}}{dt} &= \frac{\dot{Q}^{chg} - \dot{Q}^{dchg}}{c_w \Delta T^{layers}} \\ &\quad - f(m^{4^\circ C}) \frac{(UA)^{ext} (T_{amb}' - 4^\circ C)}{c_w \Delta T^{layers}} \\ &\quad - \frac{(UA)^{int} (\Delta T^{layers})}{c_w \Delta T^{layers}} - \frac{\dot{Q}^{loss, mixing}}{c_w \Delta T^{layers}} \end{aligned} \quad (3.26)$$

and top layer:

$$\begin{aligned} \frac{dm^{12^\circ C}}{dt} &= \frac{-\dot{Q}^{chg} + \dot{Q}^{dchg}}{c_w \Delta T^{layers}} \\ &\quad + f(m^{4^\circ C}) \frac{(UA)^{ext} (T_{amb}' - 4^\circ C)}{c_w \Delta T^{layers}} \\ &\quad + \frac{(UA)^{int} (\Delta T^{layers})}{c_w \Delta T^{layers}} + \frac{\dot{Q}^{loss, mixing}}{c_w \Delta T^{layers}} \\ &\quad + f(m^{12^\circ C}) \frac{(UA)^{ext} (T_{amb}' - 12^\circ C)}{c_w \Delta T^{layers}} \end{aligned} \quad (3.27)$$

The terms in the equations are presented in detail in Table 3.6.

Table 3.6: Explanatory table for the elements in the equations eq. (3.26) and eq. (3.27)

Element in the equation	Meaning
$\frac{\dot{Q}^{chg} - \dot{Q}^{dchg}}{c_w \Delta T^{layers}}$	This mass increase is caused by the charge and discharge heat flows.
$f(m^{4^\circ C}) \frac{(UA)^{ext}(T_{amb}' - 4^\circ C)}{c_w \Delta T^{layers}}$	This is a loss influencing the bottom layer and is caused by heat exchange between the 4°C layer towards the external environment. These losses depend on the mass of the 4°C layer with respect to the total mass, hence $f(m^{4^\circ C})$ . This is called the mass factor and is the share of the bottom layer mass over the total tank mass. The temperature potential of the loss is the temperature difference between the ambient and the storage fluid, $T_{amb}'$ and 4°C.
$\frac{(UA)^{int}(\Delta T^{layers})}{c_w \Delta T^{layers}}$	This is a loss influencing the bottom layer and caused by the conductive heat transfer that happens due to the temperature difference between the bottom and top layers, namely $\Delta T^{layers} = 12 - 4 = 8^\circ C$ . This type of loss is just dependent on the internal overall heat transfer coefficient $(UA)^{int}$ .
$\frac{\dot{Q}^{loss, mixing}}{c_w \Delta T^{layers}}$	This term represents the losses due to mixing between the bottom and top layers. This loss is the dominant one in thermal storage tanks (ARANER, 2018a) and is usually the only one that is not neglected. To account for this loss the concept of Figure Of Merit (FOM) is introduced in the next section.
$f(m^{12^\circ C}) \frac{(UA)^{ext}(T_{amb}' - 12^\circ C)}{c_w \Delta T^{layers}}$	This loss is caused by heat exchange between the 12°C layer towards the external environment. The model would require an additional layer at a temperature higher than 12°C that could host the mass transfer caused by this loss term. This layer is not modeled; instead, this loss will be accounted as an additional thermal power share required from the chiller to compensate for the loss Chapter 4.

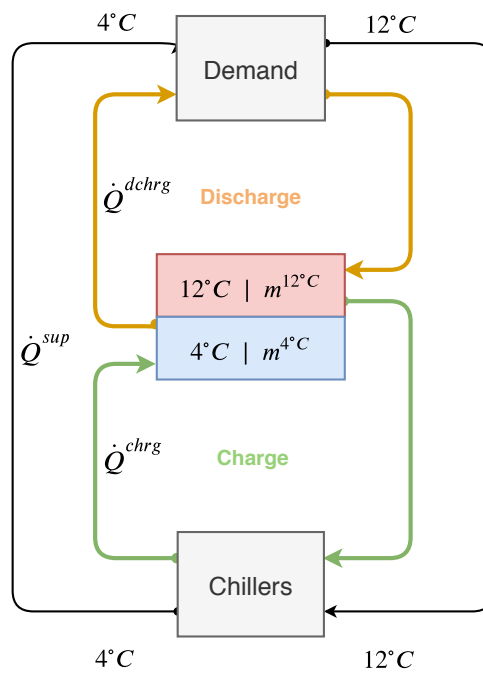


Figure 3.9: Representation of the system in the two-layer modelling approach for TES.

### 3.3.4 Mass flows model

It is of interest for this thesis to model obtain the mass flows besides the only heat flows related to the charge, discharge and direct supply process. The most usual approach to model the charge/discharge operation of a storage tank was shown in (Deng et al., 2015), where a binary variable is used to define whether the tank is charging or discharging. Though, the use of a binary variable makes the problem a Mixed Integer Linear Problem (MILP), which for the case of this thesis has to be avoided to stay coherent with the CoBMo. The system is then modeled in a different way to overcome the need of using MILP and remain in the LP domain. The mass flows model is developed starting from the two-layer model presented in the section before and the hereby explanation will be done for the cooling case, as for the two-layers one.

This model recalls what was proposed by (Deng et al., 2015), although a relevant difference was introduced. In the model formulated for this thesis there are two separate cycles for charge and discharge, in contrast with the (Deng et al., 2015) formulation. The system is modelled by keeping the two operations independent in terms of mass flows, meaning that the flow related to charge runs through a different – and totally independent – path than for discharge.

The supply and demand temperatures at the demand side are kept constant and equal to 4°C and 12°C respectively. As for the two-layer tank formulation, these operational information were gained during discussions with cooling grid operators in Singapore – not disclosed here – and is moreover coherent with the typical practices adopted in cooling grids. Fig. 3.10 shows a sketch of this model.

#### Assumption

No thermal losses are considered along the pipes. This was found both in the literature and during meetings with a cooling grid operator in Singapore who confirmed that real plants have negligible losses in the pipes.

It is assumed that the charge and discharge cycles are isolated one from the other. In this sense, the charge and discharge processes could theoretically happen at the same time. This is avoided in the optimization algorithm by adding a very small penalty for charging and discharging at the same time. This penalty is not affecting the final cost, but is allowing for a proper functioning of the optimization.

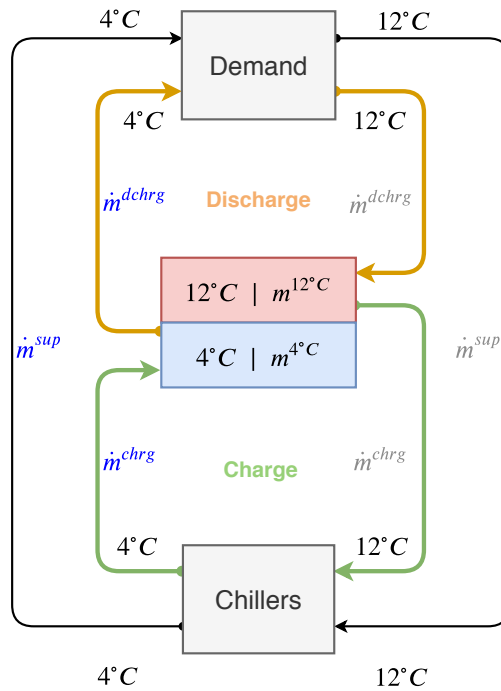


Figure 3.10: Sketch of the mass flows model highlighting the charge and discharge loops.

In the figure it is visible how the two loops, charge and discharge, are isolated one from the other. The charge and discharge mass flows –  $\dot{m}^{chrg}$  and  $\dot{m}^{dchrg}$  – flow in the two loops and assure that the conservation of mass is verified into the tank. The temperatures of the mass flows are coherent with the ones of supply and return of the chiller and demand.

Equations 3.24 and 3.25 can then be rewritten in eq. (3.29) and eq. (3.30) accounting explicating the mass flows into the charge and discharge terms (as expressed in eq. (3.28)).

$$\dot{Q}^{chrg} = \dot{m}^{chrg} \cdot c_w \Delta T^{(S-D)} \quad (3.28a)$$

$$\dot{Q}^{dchrg} = \dot{m}^{dchrg} \cdot c_w \Delta T^{(S-D)} \quad (3.28b)$$

Where the  $\Delta T^{(S-D)} = \Delta T^{layers}$  and is 8°C as 4-12 °C.

$$\begin{aligned} \frac{dm^{4^\circ C}}{dt} \cdot (c_w \Delta T^{layers}) &= (\dot{m}^{chrg} - \dot{m}^{dchrg}) \cdot c_w \Delta T^{(S-D)} \\ &\quad - \dot{Q}^{4^\circ C | loss, amb} \\ &\quad - \dot{Q}^{4^\circ C | loss, int} \end{aligned} \quad (3.29)$$

$$\begin{aligned}
\frac{dm^{12^\circ C}}{dt} \cdot (c_w \Delta T^{layers}) &= (-\dot{m}^{chg} + \dot{m}^{dchg}) \cdot c_w \Delta T^{(S-D)} \\
&+ \dot{Q}^{4^\circ C | loss, amb} \\
&+ \dot{Q}^{4^\circ C | loss, int} \\
&- \dot{Q}^{12^\circ C | loss, amb}
\end{aligned} \tag{3.30}$$

### 3.4 Modelling of BES

The modelling of the Battery Storage System (BES) is done in a more straightforward way when compared to TES. The reasons are multiple. Firstly, in the literature it was seen that when the modelling of BES is done to develop an MPC optimization problem, even treating the batteries as a black box has provided satisfying results for the main purpose of the research. Since the goal of this thesis is to model storage to show its effectiveness in DSF applications, it was not meaningful to spend excessive time digging into the chemistry of the batteries and producing a detailed model for the behaviour of different battery technologies. Another reason is that the interest of this thesis is rather to couple different storage technologies and see what the optimal result is in terms of DSF. Lastly, it was decided not to go with a detailed model of the batteries due to time constraint. Including the BES as a white box in this thesis would have meant to make a wide and deep research on the different models used to study the behaviour of a battery, for the different technologies (e.g. li-ion, lead acid, flow batteries) and this would have required a long and wide learning process for the author. Since previous studies in the literature have shown that good quality results can be achieved even with a black box approach, this was chosen as modelling method.

Fig. 3.11 shows a representation of the system including the BES. The sketch simplifies the system with only TES represented in Fig. 3.10 and adds two elements: *BES* and electric grid (*Grid*). In blue are highlighted the paths where thermal supply is flowing, while in black those carrying electric demand.

It can be seen from the sketch that in the model it is assumed that the BES is used to supply only the chillers and no other electric demand of the building. This is done for two reasons. On one hand, by far the most dominant

#### Assumptions

The BES is used to supply only the HVAC demand, without considering any other electric demand of the buildings (e.g. lighting, appliances, etc.).

The BES is modeled as a black-box, meaning that the internal functioning of the battery is not modeled. The chemistry does not influence the model here presented.

The round-trip efficiency ( $\eta^{RT}$ ) is considered as a DC-to-DC one. This means that the inverter is assumed as ideal and having an efficiency of 100%.

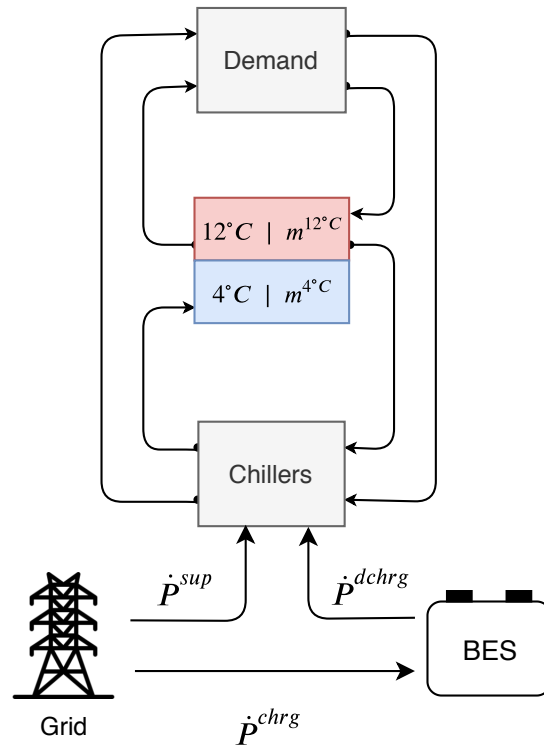


Figure 3.11: Sketch of the system with both TES and BES.

element in the electricity consumption of commercial buildings in Singapore is HVAC. HVAC is the consumption category in buildings really responsible for the creation of the peak and for this is the one targeted by this study. On the other hand, it was found not worth to further looking into the modeling of other kind of electric demands into commercial buildings – i.e. lighting, equipment, etc. – since this would have represented a large amount of work for a small impact on the final result – as said, HVAC is by far the dominant share of consumption.

Hereby the differential equation 3.31 defining the charge level of the BES is provided.

$$\frac{dE^{BES}}{dt} = (P^{chrg} - P^{dchrg}\eta^{RT}) \quad (3.31)$$

$$DoD^{min} \cdot E^{BES,tot} \geq SoC \leq 100\% E^{BES,tot}$$

Table 3.7: Explanatory table for the elements in the equations eq. (3.26) and eq. (3.27)

Element in the equation	Meaning
$\frac{dE^{BES}}{dt}$	Is the variation of the energy content of the BES over time in the continuous domain. The term $dE^{BES}$ is energy and can be expressed either in J or kW h (paying attention to the proper conversions).
$P^{dchrg} \cdot \eta^{RT}$	Is the actual electric power discharged by the BES, given by the power the BES would discharge in the ideal case multiplied by the round-trip efficiency $\eta^{RT}$ . The round-trip efficiency is defined as the ration between the energy output (kW h) to the energy input (kW h) of a storage system and is here considered as DC-to-DC, meaning that the inverter is not accounted in this value. This definition is adopted to remain coherent with (IRENA, 2017).
$P^{chrg}$	Is the actual electric power withdrawn form the grid used to charge the BES.
$SoC$	Is the state of charge of the BES. This state of charge is kept between a minimum depth of discharge ( $DoD^{min}$ ) and 100% of the storage capacity. This limitation of the state of charge of the battery is set due to considerations made on the influence of the Depth of Discharge (DoD) on the battery's health. It was widely discussed in the literature review that the DoD has a strong influence on the number of cycles that a battery can stand, meaning the lifetime of the battery. Here it was chose to limit the DoD to a maximum of 80% of the energy capacity of the battery.

### Summary of Modelling Assumptions

#### Thermal Storage

- Tank modeled with two layers, the cold (bottom) one at 4°C, the top (hot) one at 12°C. These temperature set-points were chosen to be coherent with the usual working conditions of Singapore district cooling systems.
- The thermocline – the thin layer dividing the cold and hot layers, where a high gradient of temperature happens – is not modeled.
- The performance of the thermal storage is accounted in a simplified manner by way of considering a round-trip-efficiency. In the literature it was found that the most relevant losses in a storage tank happen due to mixing. A figure for the efficiency is taken accordingly to the literature.

#### Battery Storage

- The battery storage is modeled as a simple black-box. It does not include the dynamics inside the battery cell nor in the battery management system. Neither the type of cell – e.g. lead acid or lithium-ion – nor the chemistry have an impact on the model. The choice of the type of battery influence only the inputs in terms of: round-trip-efficiency, depth of discharge, and cost (see Section 5.1.2 for more).
- No aging model is considered. The lifetime of the battery storage is not influenced by the operation of the cell nor the ambient temperature. Though, the condition of 1 cycle per day is respected to guarantee a correct choice of lifetime assumptions from the IRENA tool (IRENA, 2017) (see Section 5.1.2 for more).
- The influence of the temperature on the battery storage is not considered. The BES can actually be considered as what (Lazard, 2018) call the Energy Storage System (EES), which includes the battery management system, the thermal management, and the inverter.

### 3.5 Modelling storage into the CoBMo

In terms of state-space formulation, the presence of TES and BES storage leads to the addition of terms to the state and control variable vectors, while the disturbances vector remains unvaried.

$$\mathbf{x} = [T_z, T_s, c_z^{\text{CO}_2}, m^{4^\circ}, E^{PCM}, E^{BES}]^\top \quad (3.32a)$$

$$\mathbf{u} = \left[ \dot{Q}_z^{\text{gen}}, \dot{V}_z^{\text{ahu}}, \dot{V}_z^{\text{tu}}, \dot{Q}_z^{\text{chrg,ahu}}, \dot{Q}_z^{\text{dchrg,ahu}}, \dot{Q}_z^{\text{dchrg,tu}}, \right. \\ \left. P^{BES,\text{chrg}}, P_z^{BES,\text{dchrg,ahu}}, P_z^{BES,\text{dchrg,tu}} \right]^\top \quad (3.32b)$$

The terms  $m^{4^\circ}$ ,  $E^{PCM}$ ,  $E^{BES}$  are the state variable representing the state-of-charge of the storage respectively for sensible and latent TES and BES. These are the mass of the bottom layer of the storage tank in kg and the energy content of the storage for the PCM and battery in kW h.  $\dot{Q}_z^{\text{chrg,ahu}}$  is the thermal flow charging the TES – and is a power flow in the case of batteries ( $\dot{P}^{\text{chrg,grid}}$ ).  $\dot{Q}_z^{\text{dchrg,ahu}}$  and  $\dot{Q}_z^{\text{dchrg,tu}}$  are the storage discharge thermal flows that supply a zone instead of the ahu and tu respectively.

Before presenting how the storage is modeled into the CoBMo, it is first needed to deeper explain how the HVAC system is modeled. This is divided into Air Handling Unit (AHU) and the Terminal Units (TU).

The CoBMo considers one AHU per buildings which supplies all the zones. An AHU can supply a space with air at certain conditions to meet the comfort requirements of the space both in terms of temperature and humidity. The AHU draws fresh air from the outside. This means that an AHU is required to meet two types of thermal demands: *sensible* and *latent*. Sensible thermal demand is related to the dry bulb temperature condition in a room/zone; latent thermal demand concerns the humidity conditions inside the room, and is related to the total amount of water present in the air – called absolute humidity,  $x$ , and measured in kg of water per kg of air ( $\frac{\text{kg}_{\text{water}}}{\text{kg}_{\text{air}}}$ ).

TUs are modeled in the CoBMo as one unit per zone, and these take air from the zones and supply air to meet only dry bulb temperature requirements of the zone. Terminal units then only contribute to meet the *sensible* thermal demand of a zone.

Both AHU and TU are supplied with water from a heating/cooling plant, with the supply and return conditions of the water depending on the heating/cooling case. Thus, considering a single building, the thermal supply of the AHU and the TUs is associated with a power consumption by way of a COP, which is the one of the power plant. Below the equations expressing the heat supply and power requirement of AHU and TUs are presented.

### 3.5.1 Air-Handling Unit (AHU)

Starting from the AHU, the heat transfer towards a zone can be expressed as:

$$\dot{Q}_z^{ahu} = \dot{V}_z^{ahu} C^{th,air} (T^{ahu} - T_z^{lin}) \quad (3.33)$$

$\dot{V}_z^{ahu}$  is the air flow supplied to the zone  $z$  by the AHU and represents the control variable related to the air handling unit;  $C^{th,air}$  is the heat capacity of air;  $T^{ahu}$  is the temperature set-point of the AHU (meaning the temperature at which the air is introduced into the zone  $z$ ).  $T_z^{lin}$  is the linearization point of the zone temperature and is a constant. It can be noticed how the zone temperature  $T_z$  is a variable and should be not constant in the expression. Although, as LP has to be performed, a linearization point for the temperature is taken in this case to avoid a bi-linear problem. The linearization point is 15 °C for the heating case and 25 °C for the cooling one.

Eq. (3.33) provides the expression of the thermal flow supplied to a zone which is influencing the temperature of the zone throughout the control variable  $\dot{V}_z^{ahu}$ . Isolating all the terms multiplied to  $\dot{V}_z^{ahu}$  in the right side of the equations one can achieve the entry of the control matrix  $\mathbf{B}^{u,cnt}$  in the continuous formulation related to the zones temperatures (state variables, hence the row of the matrix) and the air flow at each zone (control variables, hence the columns). Since, as said before, the AHU supplies both sensible and latent thermal power to the zone, the thermal flow in eq. (3.33) is not the only contribution making up for the electric power required by the AHU. Two more contributions have to be considered: the latent thermal flow and the fan electric consumption to move the air. Latent thermal flow is de-humidification in cooling condition – i.e. tropical climate – ad humidification in heating conditions. In order to calculate the total thermal power the AHU extracts/supplies to the air, the unit has to be broken down into its main parts. Hereby the cooling case will be used to explain the working principle of the AHU, as this thesis considers a test case in the Singapore tropical climate, where cooling is by far the biggest thermal demand. An AHU is composed of the following components (Fig. 3.12):

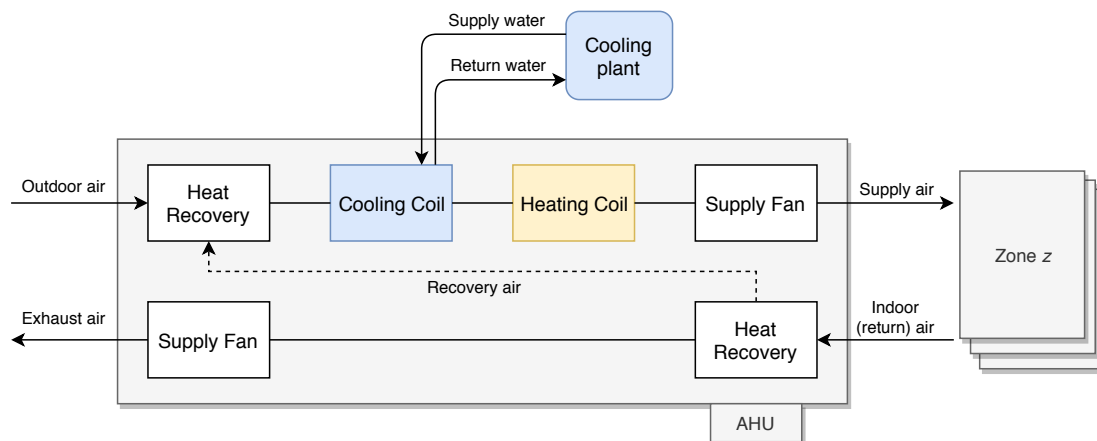


Figure 3.12: Representation of the AHU model in the CoBMo and the connections with the cooling/heating plant.

- **Heat recovery boxes.** These are air-to-air energy recovery equipment which (in the cooling case) aim to transfer heat from the outdoor temperature sucked by the AHU to the indoor return temperature which is extracted from the zone, heating the latter. Many types of air-to-air energy recovery are available<sup>5</sup>. Since is not of interest for the scope of this thesis to analyze this equipment, the reader is referenced to (Howell, 2017) for detailed knowledge.
- **Cooling coil.** This can be of different kinds (Howell, 2017). In this work is considered a cooling coil exploiting forced convection to transfer heat from the sucked outdoor air to cool water into the coil.
- **Heating coil.** My types also available (Howell, 2017), with the most diffused one those working with hot water and steam. In this work an electric cooling coil is considered.
- **Fans:** supply and exhaust. Are needed to move the air inside the AHU.

For more detailed information about the thermodynamics of an AHU see the follow-up box.

<sup>5</sup>Rotary devices, heat pipe heat exchangers, coil heat recovery loops, twin tower heat recovery loops, fixed plate exchangers, and thermosiphon heat exchangers (Howell, 2017)

### The thermodynamics of an AHU

Many process happen into an AHU. When it operates in cooling mode, both cooling and heating are done on the processed air. The cooling of air throughout a AHU is here explained using the psychometric chant in Fig. 3.13.

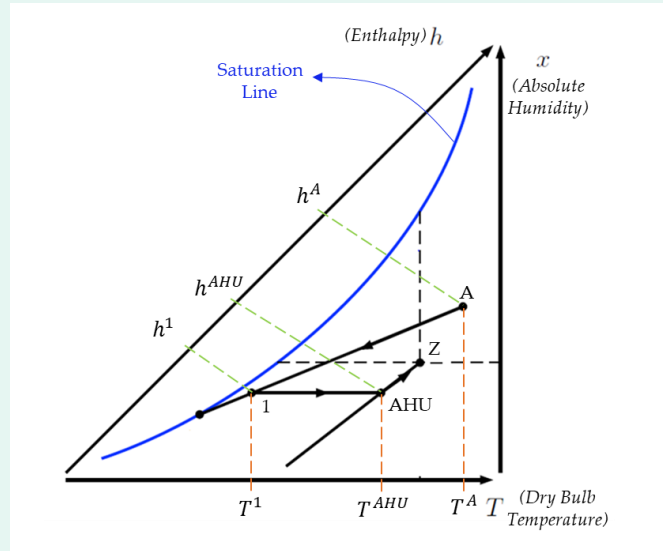


Figure 3.13: Psychometric chart representing the process of cooling air from the ambient (A) conditions to the zone (Z) conditions supplying air at the AHU conditions. The framework chart is rearranged from Spinelli (2015).

The air at conditions A is first dehumidified usually using a cooling battery where the air passes through a coil supplied with cold water. The water carried by the air flow is condensed and removed from the air flow, leading to a decrease in absolute humidity (y-axis). This process causes an inevitable reduction of the dry-bulb temperature of the air. The air is brought at the conditions in point 1. The enthalpic level of the air is reduced from  $h^A$  to  $h^1$ . Although, the air at point 1 does not meet the zone comfort conditions in terms of temperature (x-axis), while it does in terms of absolute humidity (y-axis). For this reason a re-heating process is needed to bring the air to the correct temperature set-point (AHU). The re-heating can be performed with multiple techniques and it is assumed to be electric heating in this thesis. Once the air is heated up to the AHU point, it is mixed with the air already inside the zone to meet the set zone comfort conditions (Z).

To calculate the electric power consumption of the AHU, the total thermal power supplied to the unit has to be considered. This can be calculated as the difference in enthalpy between the external air conditions and the supply conditions of the AHU. The enthalpy change provided by the heat recovery has to be subtracted by the total enthalpy jump. The total thermal power is expressed as follows:

$$\begin{aligned}\dot{Q}_z^{ahu,heat} &= \dot{V}_z^{ahu} (\Delta h^{ahu,heat} - \Delta h^{ahu,heat,rec}) \\ \dot{Q}_z^{ahu,cool} &= \dot{V}_z^{ahu} (\Delta h^{ahu,cool} - \Delta h^{ahu,cool,rec})\end{aligned}\quad (3.34)$$

To notice is that the heat share expressed in equation eq. (3.33) is included into the one of eq. (3.34), and the latter includes both latent and sensible thermal transfer.

And the total electric power to be supplied to the AHU is given by:

$$P_z^{ahu,tot} = \left( \frac{\dot{Q}_z^{ahu,cool}}{\eta^{cool}} + \frac{\dot{Q}_z^{ahu,heat}}{\eta^{heat}} \right) + \left( \dot{V}_z^{ahu} \Delta P^{ahu,fan} \eta^{el,ahu,fan} \right) \quad (3.35)$$

The first term is the electric power needed to provide the cooling, and the second term is related to the fan consumption.

#### Assumptions

The AHU is assumed to be the *only* equipment in the building being charging the storage, both TES and BES. In real life the charge of the TES is done with water coming from a cooling plant and the charge of BES by taking electricity from the grid, as shown in Fig. 3.14. Though, for modelling purposes, both the charging processes are considered to be an additional power to be supplied by the AHU – i.e. exiting the AHU. This is thermal power in the case of TES charge and electric power for the BES case. With this modelling expedient, the algorithm implementation is simplified.

The storage is introduced at two different levels of the AHU, depending on whether it is TES or BES. Fig. 3.14 provides an expansion of the AHU sketch to include storage.

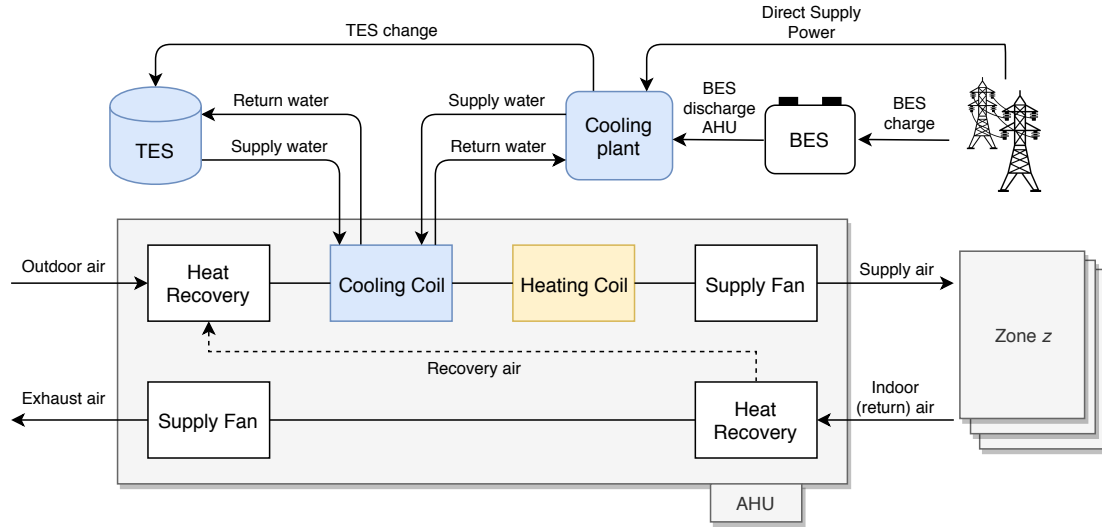


Figure 3.14: Addition of storage to the AHU model in the CoBMo.

TES can support the supply of cool water to the cooling coil of the AHU, reducing this way the total thermal supply required by the AHU in eq. (3.34). BES, instead, will act directly on the electricity level of the AHU and provides power to the cooling plant, being charged by electricity coming from the grid. Including the storage, eq. (3.35) can be rewritten expressing the AHU electric power as a total.

$$\begin{aligned}
 P_{ahu,tot} = & \sum_{z=1}^Z \left[ \left( \frac{\dot{Q}_z^{ahu,cool} - \dot{Q}_z^{dchg,ahu}}{\eta^{cool}} + \frac{\dot{Q}_z^{ahu,heat}}{\eta^{heat}} \right) + \left( \dot{V}_z^{ahu} \Delta P_{ahu,fan} \eta^{el,ahu,fan} \right) \right] \\
 & + \frac{\dot{Q}^{chg,ahu}}{\eta^{cool}} \\
 & + P^{BES,chg} - P^{BES,dchg,ahu}
 \end{aligned} \tag{3.36}$$

$\dot{Q}^{chg,ahu}$  is the charge thermal power flowing from the cooling plant to the TES;  $P^{BES,dchg}$  and  $P^{BES,chg}$  are the charge and discharge electric power that involve the BES.  $\dot{Q}_z^{dchg,ahu}$  is the discharge thermal power from the storage. Attention must be paid to the last term. Although one AHU per building is considered, and although the TES interacts with the AHU throughout the cooling coil (which is also one per building), the discharge thermal flow from the TES ( $\dot{Q}_z^{dchg,ahu}$ ) is considered as a control variable per zone. This is because the control of the AHU in the CoBMo happens at the zone level, and although the physical system would not allow the TES to interact with each zone, the model has been developed this way to allow a simpler and more effective

implementation of the algorithm. A remark has to be done about the BES in the modelling approach. The BES power consumption depends on electricity supplied from the grid, process which in practice does not involve the AHU. Instead, in eq. (3.36) the term  $P^{BES,chg}$  is modeled as an additional power consumption from the AHU. This is done to simplify the approach and the algorithm implementation, as this approach does not change the overall result in total power consumption of the whole building.

### 3.5.2 Terminal Unit (TU)

The Terminal Unit (TU) is modeled similarly to the AHU, but some differences in the approach have to be highlighted. As was already pointed out in the assumptions made for the AHU modelling, the AHU is modeled so that the TU is not involved in the charging process of any storage type, neither TES nor BES. Instead, the TUs do benefit from storage discharge.

Fig. 3.15 shows a sketch of the TU without storage implemented. It can be seen that one TU per zone is considered, and that the cool water supplied to each TU comes from a cooling plant.

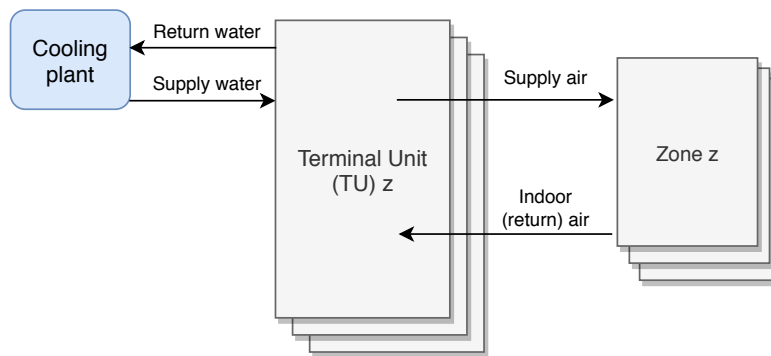


Figure 3.15: Representation of the TU model in the CoBMo and the connections with the cooling/heating plant.

The addition of storage modifies the system as shown in Fig. 3.16, where no charge is involved and only discharge flows are considered.

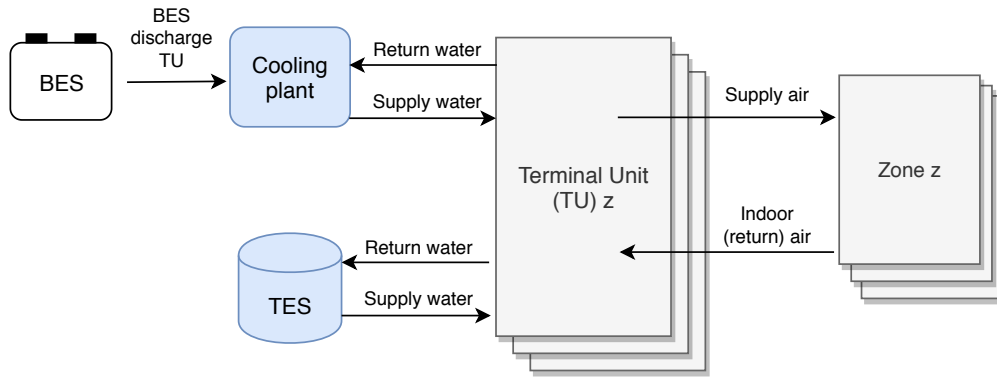


Figure 3.16: Addition of storage to the TU model.

The heat transfer towards the zone coming from the TU (eq. (3.37)) is expressed similarly to the AHU. To remember is that the TUs suck air from the zone and not from the external environment, making the thermal contribution of this unit type only in terms of sensible heat.

$$\dot{Q}_z^{tu} = \dot{V}_z^{tu} C^{th,air} (T^{tu} - T_z^{lin}) \quad (3.37)$$

Where  $\dot{Q}_z^{tu}$  is the heat transfer per zone and  $\dot{V}_z^{tu}$  is the control variable for the TU.

The total electric power required by the TU can be expressed as:

$$P_{ahu,tot} = \sum_{z=1}^Z \left[ \left( \frac{\dot{Q}_z^{tu,cool} - \dot{Q}_z^{dchrg,tu}}{\eta^{cool}} \right) + \left( \dot{V}_z^{tu} \Delta P^{tu,fan} \eta^{el,tu,fan} \right) \right] - P_z^{BES,dchrg,ahu} \quad (3.38)$$

Is important to underline the fact that in the case of TU, the term for battery discharge  $P_z^{BES,dchrg,ahu}$  is indexed per zone, unlike the AHU case.

Finally, the differential equations regulating the storage level can be written, accounting for the integration of the TES and BES with both the AHU and the TU. For the sensible TES (tank) the variation over time of the bottom 4°C layer is provided in eq. (3.39a). For

the BES, eq. (3.39b) provides the variation of the storage level (in kW h).

$$\begin{aligned}
\frac{dm^{4^{\circ}C}}{dt} = & + \dot{Q}^{chg,ahu} \\
& - \sum_{z=1}^Z \left[ \dot{Q}_z^{dchg,ahu} + \dot{Q}_z^{dchg,tu} \right] \\
& - f(m^{4^{\circ}C}) \frac{(UA)^{ext}(T_{amb}' - 4^{\circ}C)}{c_w \Delta T^{layers}} \\
& - \frac{(UA)^{int}(\Delta T^{layers}) + \dot{Q}^{loss,mixing}}{c_w \Delta T^{layers}}
\end{aligned} \tag{3.39a}$$

$$\begin{aligned}
\frac{dE^{BES}}{dt} = & P^{BES,chg} \cdot \eta^{RT} \\
& - \sum_{z=1}^Z \left[ P_z^{BES,dchg,tu} \right] - P^{BES,dchg,ahu}
\end{aligned} \tag{3.39b}$$

## 4 Optimization Problem

This section will present the second part of the methodology of this thesis, related to the development of an optimization problem for the optimal control of the storage. The chapter presents two distinct implementations. One is an independent framework which was designed from scratch to have a simple model of storage up and running without the building model involved. This model considers the building's thermal demand as an input and calculates the optimal scheduling of the storage as supplying the building instead of a central chiller. The chiller's operation is not modeled in detail.

A second framework is then presented related to the implementation of the optimization problem using the CoBMo. The framework uses the building model CoBMo improved with the storage. This second framework is the one on which the results presented in Chapter 5 are based.

Both the frameworks are explained in this methodology section in order to give the reader a double option on how to perform optimization with the storage models presented before. As it will be proposed, the independent framework considers the storage size as a parameter. Instead, when developing the optimization with the CoBMo the storage size is made a variable.

### 4.1 Implementation Approach

This thesis aims to evaluate the benefits of DSF in commercial buildings in Singapore. To do so, a numerical optimization problem is implemented to calculate the economic savings that the installation of storage could produce. Numerical optimization is a broad topic and includes many different methods and approaches to formulate a problem<sup>1</sup>.

The model in this work is formulated as a linear optimization problem with the following characteristics:

- The problem is formulated differently depending on the implementation:

---

<sup>1</sup>See Section 2.2 for an overview of mathematical programming

- A direct formulation in the continuous discrete domain is used for the framework developed independently from the building model. This is done by using simple Euler integration.
- When implementing the storage into the CoBMo, the problem is formulated in the continuous domain and then discretised via the state-space formulation.
- The problem is a constrained problem.
- The optimization problem seeks for a global optimum, meaning that it is convex. Linear programming has the natural characteristic of being a convex programming.

In this chapter three implementations of storage will be presented. One for the independent framework, one related to the CoBMo and one with the CONCEPT. This last is just an expansion of the CoBMo, as for the grid planning multiple building modelled with CoBMO are set up, where in each of them the storage is implemented.

### 4.1.1 Coding overview

The coding part of this thesis is done with Python as a programming language, while specifically in relation to the optimization problem formulation, Pyomo is used as framework and Gurobi as solver. The reason for using Python is that it is an open source, high-level efficient programming language, which benefits from the presence of a well-established and broad community online which can provides the single user with a broad aggregated help thanks to the volume of users worldwide.

### Pyomo

Pyomo (Python Optimization Modeling Objects) is a software package which allows to define and solve optimization problems in the Python scripting language. Pyomo can be used to set up many different problem types: linear programming, mixed-integer linear programming, non-linear mixed-integer models, as well as real-world problems involving even thousands of variables and constraints can be constructed in Pyomo (Hart et al., 2011).



Pyomo was developed to provide an open source platform that allows perform optimization using the high-level Python programming language, and at the same time allowing the users to enjoy a software designed for flexibility, extensibility, portability, and maintainability. At the same time Pyomo integrates the modern ideas in Algebraic Modeling Languages (AMLs) such as differentiation between abstract and concrete models (Hart et al., 2011). Extensive documentation can be found online on the package, like the official online documentation which is very often updated (here the June 2019 version (PYOMO, 2019)).

### Gurobi

Gurobi is a company that provides different products in the numerical solver sector, such as programming solver, tools for distributed optimization, optimization in the cloud, and also support (Gurobi, 2019a). Gurobi provides an optimizer claimed to outperform the competition thanks to years of experience and superior quality (Gurobi, 2019b). The optimizer is able to solve many optimization problem types – e.g. LP, MILP, QP, etc. – and is compatible with several programming languages – Python, Java, GAMS, C++, etc. For this thesis, the academic free version of the Gurobi optimizer was used.



## 4.2 Independent framework

The implementation in this section refers to the modelling approach presented in Section 3.3.4, meaning considering a two-layer model for the tank and a black box approach for battery storage.

The objective function of the optimization problem aims to minimize the operational costs given by the power consumption of the HVAC system multiplied by the electricity tariff. This is subject to multiple constraints:

- Demand constraint: the demand has to be always satisfied as a combination of storage discharge and direct supply from the chillers.
- Chiller constraints:
  - The chiller's total output is given by the sum of storage charge and direct supply thermal power. This is converted to electric power by using the COP<sup>2</sup>.
  - The chiller's operations are constrained within a range of 30% and 110% of the peak thermal demand. This is done to assure a real behaviour of the chiller in terms of COP.
- Constraint on the storage level: the storage level is constrained between zero and its maximum capacity. The capacity is the mass of the bottom layer for the sensible storage case and the maximum energy of the battery storage for the BES case.

The objective function can be expressed as follows (refer to Fig. 3.9):

$$\min \left\{ \sum_{t=0}^{N_t} P_t^{el,tot} \cdot p_t \right\} \quad (4.1)$$

Where  $P_t^{el,tot}$  is the electric power supplied to the chillers at the timestep  $t$  and  $p_t$  is the electricity tariff at the timestep  $t$ .  $N_t$  is the set of timesteps, which for this problem is composed of the 24 hours. The electric power consumed by the chillers is proportional to the thermal power supplied to the load and to charge the storage, so that it can be expressed as:

$$P_t^{el} = \frac{Q_t^{chiller,tot}}{COP} \quad (4.2)$$

Where COP is selected to have a value of 4.

---

<sup>2</sup>Coefficient of Performance

The mathematical expression of the constraints of the problem is defined as:

$$\begin{aligned}
 s.t. \quad & P_t^{el,tot} = P_t^{ahu,tot} + P_t^{tu,tot} \quad \forall t \\
 & 0 \leq P_t^{ahu,tot} \leq 1.2 \cdot P^{ahu,baseline} \quad \forall t \\
 & T_t^z \leq 23^\circ C \quad \forall t \in [6 : 30AM ; 6PM] \\
 & DoD^{min} \leq E_t^{st} \leq C^{storage,tot}, \quad \forall t
 \end{aligned} \tag{4.3}$$

The first constraints defines the total electric power as the sum of the AHU and TU operations.

The second constraint is important to allow a sound behaviour of the optimization problem. As the charge of the storage involves only the AHU and not the TU, the AHU total electric power output is composed of a share of power to supply the zones and one to charge the storage. If a maximum operation of the AHU is not defined, the optimization algorithm will choose to fully charge the storage in a single timestep – i.e. the lowest tariff one – and discharge for the rest of the time horizon. The power cap of the AHU operation is defined as the baseline AHU power – the one coming from running the CoBMo without any storage – increased by a 20%.

The third constraint limits the indoor zone temperature between a minimum and a maximum, which are chosen according to the comfort requirements in Singapore. This constraints is key to allow flexibility of the building load. A fixed temperature set point is avoided and substituted with a range.

Finally, the fourth constraints limits the storage level (energy or mass) between zero and the storage size.

The code expressing the objective function is provided below.

```

def rule_objective_cost(
    model
):
    objective_cost = 0.0

    for timestep in model.set_timesteps:
        objective_cost += (
            model.power_electric_tot[timestep]
            * data_input[timestep]['tariff']
        )

    return objective_cost

```



### Constraining the operation of a chiller

The performance of a chiller depends by the operational point. In Fig. 4.1 the x axes represents the load as a parentage and the y-axes the efficiency as  $\text{kW t}^{-1}$ .

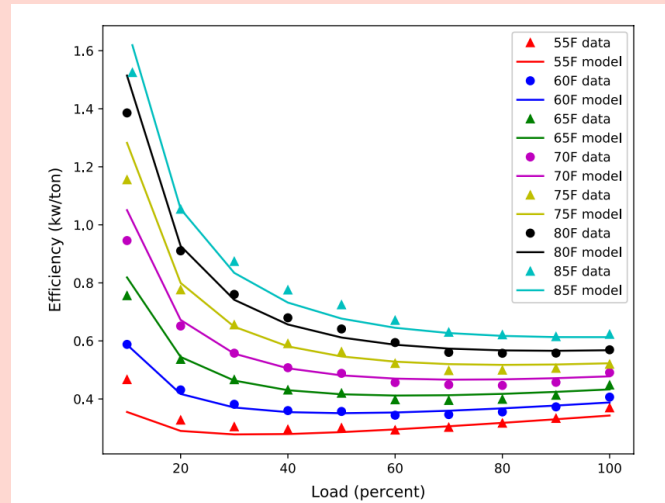


Figure 4.1: Behaviour of a chiller depending on the operational load. The figure  $\text{kW/ton}$  is expression of the efficiency and the load is indicated in percentage (%). The curves are parametric with the condensing temperature of the chiller (Blackburn et al., 2019)

It can be seen that the efficiency of a chiller does not experience great changes for a range between the 20/30% and 100% of the load. This means that if one has to linearize the curve in the figure around the point of maximum efficiency, the linearization would be meaningful if the load of the chiller is constrained not to go below 20% of the design conditions, as beyond this threshold a steep increase of the  $\text{kW/ton}$  value is seen.

What would be effective to do would be to limit the chiller's operation between 30% and 100% of the design load, *and* at the same time allow for a "switched-off" operation mode of the chiller. This would mean that the chiller could not operate in the region between 20% and 0% of load. Although this is an effective strategy and it has been adopted a lot in the literature, it involves the need of formulating the problem as a MILP, using an integer variable to define where the chiller's operation is on a curve such as the one in Fig. 4.1.

This is an important remark to be considered in the future work when implementing the operation of a centralized chiller supplying the building and charging the storage.

<sup>a</sup>This way of expressing the efficiency is typically used in large chillers and indicates the amount of electric power to supply a ton of refrigerant. Hence, opposite to the COP, the smaller this figure, the more efficient the equipment.  $\text{kW/ton}$  can be converted to COP as  $COP = \frac{3.517}{\text{kW/ton}}$  (Knot, 2011)

Referring to eq. (3.26) the below listing provides the algorithm section which defines the TES bottom layer.

```

def rule_bottom_layer_mass(
    model,
    timestep_int
):
    if timestep_int == 0:
        mass_bottom_layer = total_mass_tank * initial_share_bottom_layer
    else:
        mass_bottom_layer = (
            model.var_mass_bottom_layer[timesteps[timestep_int-1]]
            + (
                # Charge and discharge contributions
                (model.thermal_flow_charge[timesteps[timestep_int]]
                 - model.thermal_flow_discharge[timesteps[timestep_int]]
                 - model.thermal_flow_discharge[timesteps[0]])
                * 1000 / (cp_water*delta_temp_tot_layers)

                # Losses towards external environment
                - (
                    ua_ext * (
                        storage_ambient_temp_cooling
                        - temp_bottom_layer
                    )
                    * model.var_mass_factor_bottom[
                        timesteps[timestep_int]
                    ]
                    / (cp_water*delta_temp_tot_layers)
                )

                # Internal losses (included mixing)
                - (
                    ua_thermocline*delta_temp_tot_layers
                    / (cp_water*delta_temp_tot_layers)
                    * model.var_mass_factor_bottom[
                        timesteps[timestep_int]
                    ]
                )
            ) # losses between layers UM:[kg/s]

        ) * 3600

    return model.var_mass_bottom_layer[timesteps[timestep_int]] == mass_bottom_layer

```

The top layer mass is not a relevant information for the sake of the problem as, since the model of the TES tank has only two layers, the top mass will be equal to the total tank mass, minus the one of the bottom layer. Additionally, only one on the two layers is sufficient as state variable to represent the state of charge of the storage. Important to note is that the term `if timestep_int == 0:` includes the internal losses due to both conduction throughout the thermocline layer and the mixing losses. As it can be seen from the code, the storage level is initialized at a known level in the first timestep (`if timestep_int == 0:`), while for the timesteps following the first one the storage state of charge at the timestep  $t$  depends on the charge level at the previous timestep (`model.var_mass_bottom_layer[timesteps[timestep_int] -`

1]]). The total mass of the tank is not a variable and is given as an input of the problem (`total_mass_tank`).

Finally, as already presented in Section 3.3.4, the mass flows related to the charge and discharge of the storage tank are calculated afterwards the optimization problem is solved. The mass flows for charge, discharge and direct supply are calculated retrieving the value of the heat control variables at each time step ( $\dot{Q}_t^{sup}$ ,  $\dot{Q}_t^{chrg}$  and  $\dot{Q}_t^{dchrg}$ ) and are calculated considering the temperature difference between the two layers of the tank as follows:

$$\dot{m}_t^{sup} = \frac{\dot{Q}_t^{sup}}{c_w \Delta T^{layers}}; \quad \dot{m}_t^{chrg} = \frac{\dot{Q}_t^{chrg}}{c_w \Delta T^{layers}}; \quad \dot{m}_t^{dchrg} = \frac{\dot{Q}_t^{dchrg}}{c_w \Delta T^{layers}}; \quad (4.4)$$

In Fig. 4.2 are presented the demand curve from the CREATE tower and the electricity tariff used in the problem. The tariff represents the hourly wholesale market price in Singapore for May 28<sup>th</sup> 2019<sup>3</sup>.

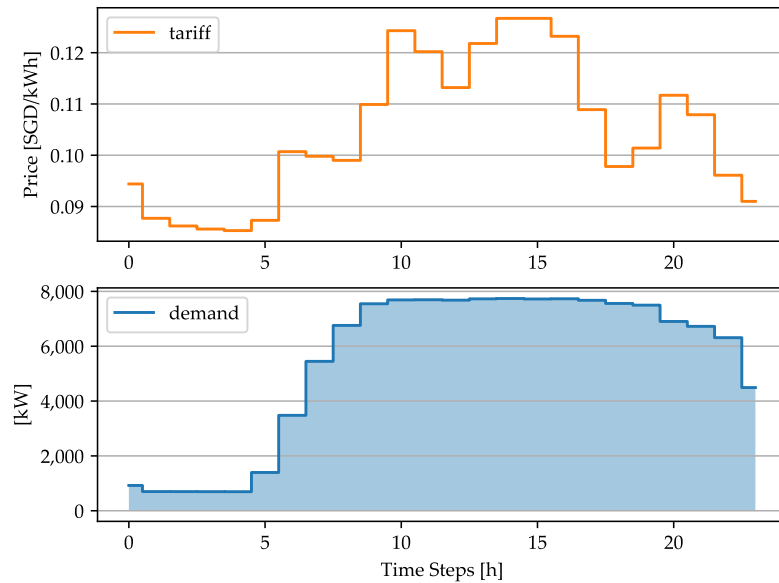


Figure 4.2: Hourly electricity tariff from the Singapore wholesale electricity market and demand curve of the CREATE Tower in NUS.

<sup>3</sup>The price is provided by (EMC, 2019c) as a half-hourly price. The hourly tariff is calculated as the average each two half-hours.

### 4.3 CoBMo optimization framework

This section will present the optimization framework used when implementing the storage technologies into the CoBMo. This differs from the previous independent framework as the thermal demand of the building is not an input of the problem, rather a result of the building model. In this section only few parts of the code will be presented, while the whole repository can be found at (TUMCREATE-ESTL, 2019).

The objective function is defined as follows:

$$\min \left[ \left( \sum_{t=0}^{N_t} P_t^{el,tot} \cdot p_t \right) \cdot d^{work} \cdot L^{storage} \right] + \left[ (S^{st} \cdot c^{st}) + (C^{power} \cdot P^{peak}) + C^{fixed} \right] \quad (4.5)$$

The term  $\left( \sum_{t=0}^{N_t} P_t^{el,tot} \cdot p_t \right)$  is alike what done in the previous section for the independent framework. This term represents the operational costs due to power consumption of the AHU and TU. This term though is extended through time along the lifetime of the storage –  $L^{storage}$  – considering only the working days in a year – since in office buildings the HVAC works only from Monday to Friday.

The second part of the objective function represents the investment for the storage. This investment is given by:

- Storage size: cost proportional to the installed size of the storage and the specific cost per unit of storage – \$/m<sup>3</sup> for sensible tank or \$/kWh for battery.
- Only for battery storage:
  - Cost of the inverter: this depends on the peak installed and the specific cost of the inverter – \$/kW.
  - Fixed cost: this includes the costs for housing, cooling, and periphery. This cost is estimated to 1760 \$ coming as an average of the data proposed by (Hesse et al., 2017). A further research about fixed costs for the battery storage would be needed to evaluate this contribution more accurately.

The two variables in the objective function are the total electric power consumption at each timestep  $P_t^{el,tot}$  and the storage size  $S^{st}$ . The reasoning behind the optimization is that the algorithm will evaluate if savings are achievable by installing storage or not along its lifetime. If over the lifetime the investment for the storage is not balanced out by the operational savings – made possible by exploiting the price difference during the day – the storage size will be set to zero.

The constraints are the same as the ones defined for the independent framework in eq. (4.3). It is worth highlighting how the constraint related to the storage level was implemented. Referring to the objective function defined above, the storage constraint is defined as

$$0 \leq E_t^{st} \leq S^{st}, \quad \forall t$$

In this constraint, both  $E_t^{st}$  and  $S^{st}$  are variables, being the first a state variable (the level of the storage) and the second the size of the storage, which is selected by the optimization algorithm. The storage level  $E_t^{st}$  will then change depending on the building operations – charge, discharge, direct supply – and the upper constraint will change representing the storage size and influencing the investment side of the objective function.

**Remark – Avoid singular matrix**

An important remark has to be done in relation to the state-matrix definition of the problem when including storage, and to the related discretization of the problem.

When considering the state-space formulation of Section 3.2.3, the values on the diagonal of state matrix  $A^{cnt}$  for the storage state variables represent the losses occurring in the storage. For the sensible storage tank, these depend on the losses towards the external environment; while for the battery storage, these might be losses due to self-depletion of the battery state-of-charge over time. Though, the modelling of the storage is done assuming negligible these two type of losses. This would mean that the term on the diagonal of the matrix  $A^{cnt}$  in the position of the storage level should be zero, as shown below:

$$A^{cnt} = \begin{bmatrix} \neq 0 & a_{12} & \dots & a_{1K} \\ \vdots & \neq 0 & & \\ \vdots & & \neq 0 & \\ a_{K1} & & & \textcircled{0} \end{bmatrix}$$

The problem with this matrix setup is that when the matrix  $A^{cnt}$  has to be inverted, it will not be possible to do so as it will be a singular matrix by having determinant equal to zero. To avoid this issue, is important to set each value on the diagonal of  $A^{cnt}$  to a very small number, though different that zero – the example below is using  $10^{-10}$ .

$$A^{cnt} = \begin{bmatrix} \neq 0 & a_{12} & \dots & a_{1K} \\ \vdots & \neq 0 & & \\ \vdots & & \neq 0 & \\ a_{K1} & & & 10^{-10} \end{bmatrix}$$

## 4.4 Economic Analysis and Optimization

The economic analysis is based on the optimization algorithm which considers the operation of the CREATE Tower for one day of the year: January the 2nd, 2017. The wholesale market prices are taken for the same day from (EMC, 2019c). Since by now the CoBMo has modelled only the 8th floor of create tower, the model is approximated for the whole tower assuming that all the levels of the building behave like the 8th storey.

To explain how the economic analysis is run, eq. (4.5) is proposed again to facilitate the explanation together with the flowchart in Fig. 4.3.

$$\min \underbrace{\left[ \left( \sum_{t=0}^{N_t} P_t^{el,tot} \cdot p_t \right) \cdot d^{work} \cdot L^{storage} \right]}_{\textcircled{A} / \textcircled{A}^{st}} + \underbrace{\left[ (S^{st} \cdot c^{st}) + (C^{power} \cdot P^{peak}) + C^{fixed} \right]}_{\textcircled{B}}$$

The economic analysis follows the process below.

1. Two optimization problems are run for the estimation of one storage setup – i.e. a certain technology.
  - a) The baseline CoBMo is run *without* the storage implemented. The results is an operational cost coming only from the part  $\textcircled{A}$  of the objective function. This result is influenced by the specific lifetime of the selected storage technology.
  - b) The CoBMo is run *with* the storage implemented. Now the part  $\textcircled{B}$  is included in the calculation. The optimization will install storage – i.e. select a storage size  $S^{st}$  different than zero – if the operational costs will be reduced at least as much as the investment for the storage itself. Otherwise, the storage size  $S^{st}$  will be kept equal to zero.
2. If the storage is not installed – ie if the optimization algorithm sets a storage size  $S^{st}$  equal to 0 – the selected setup is not economically feasible. Otherwise the discounted payback time is calculated for the storage installation  $S^{st}$ .
  - a) The yearly savings achieved thanks to the storage are calculated by comparing the parts  $\textcircled{A}$  and  $\textcircled{A}^{st}$  of the two optimization problems, the baseline and the storage one, both divided by the storage lifetime  $L^{storage}$ . The savings are given by

$$\Delta C = \left[ \left( \sum_{t=0}^{N_t} P_t^{el,tot} \cdot p_t \right) \cdot d^{work} \right]_{baseline} - \left[ \left( \sum_{t=0}^{N_t} P_t^{el,tot} \cdot p_t \right) \cdot d^{work} \right]_{storage}$$

These yearly savings are the ones that will be discounted.

- b) Once the yearly savings are achieved, the discounted payback time is calculated with the following algorithm. An interest rate of 6 % is used.

```

import numpy as np

interest_rate = 0.06
economic_horizon = 1000
cumulative_discounted_savings = np.zeros(economic_horizon)
yearly_discounted_savings = np.zeros(economic_horizon)

year = 0
while cumulative_discounted_savings[year] < investment_cost:
    year += 1

    discount_factor = (1 + interest_rate) ** (-year)
    yearly_discounted_savings[year] = savings_one_year * discount_factor
    cumulative_discounted_savings[year] = cumulative_discounted_savings[year - 1]
    + yearly_discounted_savings[year]

    if year == 70:
        print('\nDiscounted_payback_time_is_too_high._Reached_70_years.\n')
        year = 0
        break

```

The algorithm sums up the discounted savings over the years and stops in either two ways. When the accumulated savings exceed the initial investment (`investment_cost`): this means that the break even condition has been reached. Or when the payback time (the number of years) surpasses 70 years. This is done to avoid the while loop to run ad infinitum.

- c) Finally, the discounted payback time ( $y^{PB, disc}$ ) is compared with the lifetime of the storage ( $L^{storage}$ ). If the condition  $y^{PB, disc} < L^{storage}$  is verified, the storage installation is economically feasible. Otherwise, it is not.

The process presented above is at the base of the results that will be presented in Chapter 5.

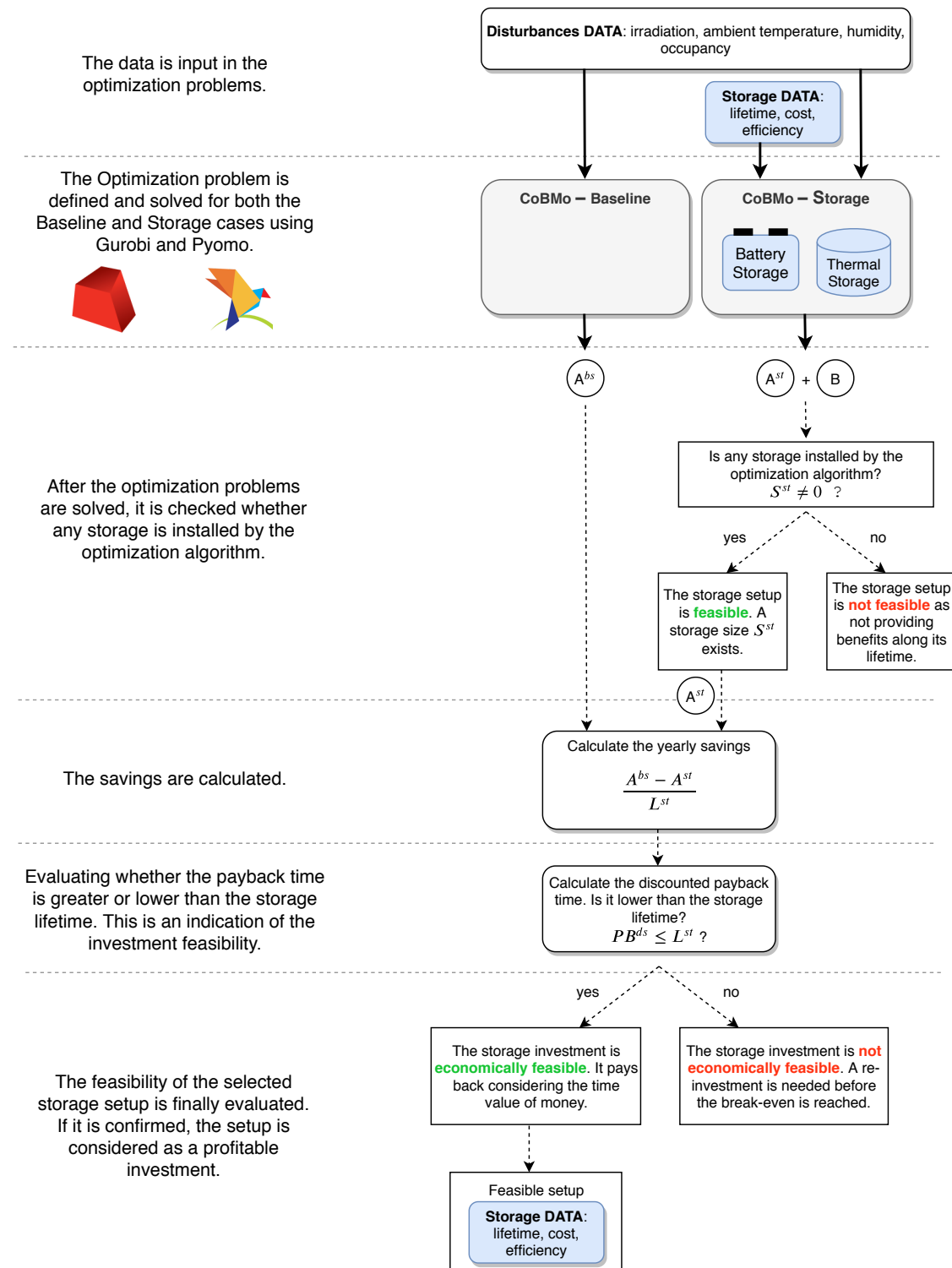


Figure 4.3: Flowchart describing the process defining the storage size (optimization algorithm) and evaluating whether installing storage is feasible or not.

### The baseline Scenario

The baseline scenario is defined as the building model (CoBMo) run without any storage implemented. This simulation considers the building as a flexibilized system already using the thermal mass of the building as storage and softening the constraint on the zone temperature. The electric power consumed by the HVAC is minimized still keeping the indoor zone temperature within a certain comfort range – instead of setting it to a fixed point.

In this regard, all the results coming from the economic analysis concerning the payback time are related to the savings that the storage case is able to make *relative to an already flexible building*. The analysis is thus conservative. If the non-flexible building – which is the case for CREATE tower today – would be used in the simulation, the savings would be higher and the payback lower.

## 4.5 Economic Analysis: theory and approach

The economic analysis aims to define whether it is worth or not installing storage for implicit demand-side flexibility purposes. This means that the flexibility will generate savings exploiting the price differences along a day, consuming electric power in periods of lowest prices and discharging the storage in high-tariff hours. This behind-the-meter operation does not involve any sale of flexibility on the market whatsoever.

The reasoning behind the economic is whether the storage technology will payback the investment with operational savings only or not. The payback time is defined as the year when the investment breaks even, meaning that the accumulated revenues equal the initial investment.

Two types of payback times can be defined: simple and discounted. The simple payback time is linear and can be expressed as below:

$$y^{PB,simp} = \frac{C^{invest}}{S_y} \quad (4.6)$$

$y^{PB,simp}$  is the year at which the investment will break even considering the savings constant along the years. The year is calculated as ratio between the investment  $C^{invest}$  – in \$ – and the yearly savings  $S_y$  in – \$/year.

The discounted payback time is another type of payback and considers the time value of money: money in the future are worthless than money in the present due to an interest

rate. The discounted payback time is the year that satisfies the following condition:

$$\begin{aligned}
 y^{PB,disc} : \quad & \sum_{y=1}^{L^{st}} \left[ S_y \cdot \frac{1}{(1+i)^y} \right] \geq C^{invest} \\
 & S_y \cdot \underbrace{\sum_{y=1}^{L^{st}} \left[ \frac{1}{(1+i)^y} \right]}_{\text{Discount Factor (DF)}} \geq C^{invest} \quad (4.7) \\
 & S_y \cdot \underbrace{\left( \frac{1 - (1+i)^{L^{st}}}{i} \right)}_{\text{Present Value Annuity Factor (PVAF)}} \geq C^{invest}
 \end{aligned}$$

$\frac{1}{(1+i)^y}$  is the discount factor (DF) which depends on the interest rate – constant along the years – and the year considered.  $S_y$  are the yearly savings, alike to the simple payback formulation in eq. (4.6).  $\frac{1-(1+i)^{L^{st}}}{i}$  is the Present Value Annuity Factor (PVAF) and is defined as the summation of all the DF along the years. As can be seen, the lifetime of the storage is directly used in the calculation of the discounted payback time as it affects the PVAF.

A graphical representation of the simple and discounted payback time concepts is presented in Fig. 4.4<sup>4</sup>. The proposed graph aims to give an idea of the theory behind the economic of payback time using mock numbers. The y-axis represents money which do not relate to any result of this thesis.

<sup>4</sup>Note: the numbers in this graph are mock and not related to any result.

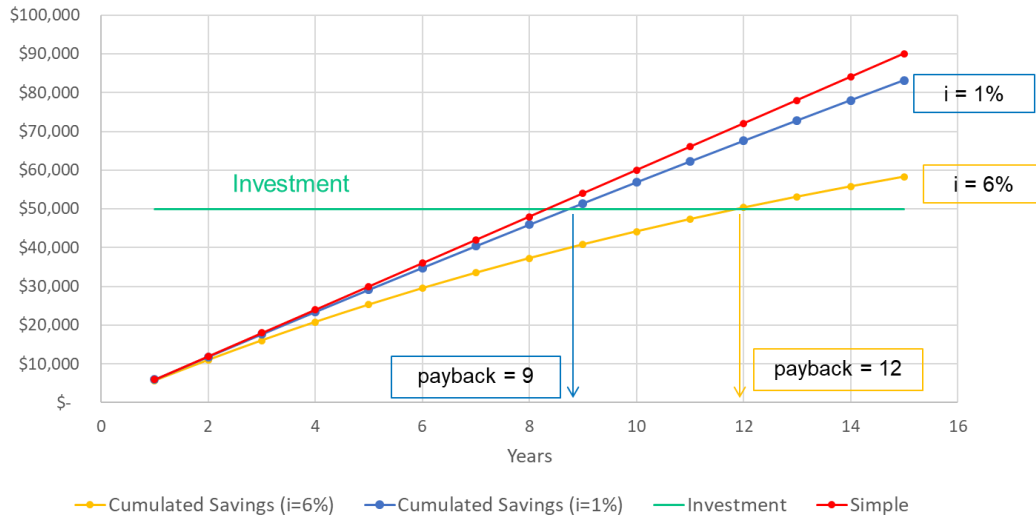


Figure 4.4: Graphical representation of simple and discounted payback time.

The green line is the investment, which occurs in year 0 and is kept constant make the crossing of the investment and the accumulated savings visible. The red line represents the simple payback time. It is linear as the yearly savings are constant along the years. The blue and yellow lines represent the accumulated savings done along the years with a lifetime of 15 years with an interest rate of 1% and 6% respectively. It is visible as already using an interest rate of 1% make the savings curve bend forward, crossing the investment line further in the future, this leading to a higher payback time. This behaviour is Even more emphasized with an interest rate of 6%.

What has to be grasped from the explanation above is that, in order to make a conservative analysis, the discounted payback time reasoning has to be used, in order to take into account the time value of money.

Whether the discounted payback year is lower of greater than the storage lifetime makes up for the economic feasibility of the technology – feasible in the first case and unfeasible in the second.

# 5 Results

This chapter presents the results coming from this thesis work, including both an economic analysis of the storage technologies and an optimal scheduling of their operation. Once again, it is important to underline that the optimization algorithm developed in this thesis was used to define a day-ahead optimal scheduling and not the operation of a Model Predictive Control (MPC). For the second, in fact, the presence of a real system to be controlled – a building in this case – is needed.

This chapter will present in sequence the cost assumptions and the results of the economic analysis first for the TES then for the BES. Finally, the optimal scheduling of both storage technologies is proposed.

## 5.1 Cost assumptions of storage

The results coming from the economic analysis are affected by the assumptions done on the modelling side as much as for the cost considered for the storage technologies. In this thesis different costs have been taken from the literature for both TES and BES. This section presents these assumptions.

### 5.1.1 TES cost assumptions

The costs for the sensible thermal storage are taken from two sources. The first one is (DeForest et al., 2014). In this paper the authors estimate a turnkey cost of 31.80 USD per kWh for a chilled water thermal sensible energy storage tank. The scope of the specific cost includes materials, installation costs and control system costs. This source is particularly interesting as it draws a the cost from a linear interpolation of real TES projects in the US since the early 2000. Fig. 5.1 shows the interpolation.

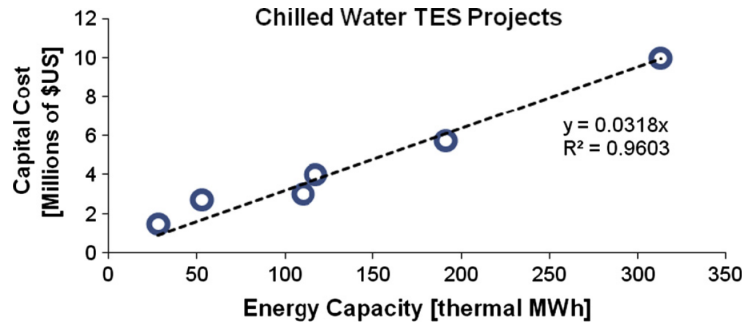


Figure 5.1: Linear interpolation of past TES projects in the US (DeForest et al., 2014).

To be noticed that the investment cost is given per kWh, meaning per unit of thermal energy stored in the water tank.

A second source is (Comodi et al., 2016) who provides a value of 212 USD per  $\text{m}^3$ , with the scope including the cost for vessel, the hydraulic system, the compact heat exchanger and the civil works. This cost goes with the volume of the tank instead of the energy stored.

To compare the effect of the two cost assumption, the two cost units have to be made coherent. It was decided to use SGD per  $\text{m}^3$  as base cost unit. Regardless the currency conversion, a less trivial conversion has to be done to transform USD per kWh in USD per  $\text{m}^3$ . To do so, the basic formula ruling the exchange of heat – energy – is proposed below:

$$Q = m \cdot c_p \cdot \Delta T \quad (5.1)$$

Where the heat  $Q$  is in J; the mass  $m$  kg; the specific heat  $c_p$   $\text{J kg}^{-1} \text{K}^{-1}$ ; and the temperature difference between cold and hot layer  $\Delta T$  in K. The reasoning at the base of the conversion is that, once the temperature difference  $\Delta T$  is defined, and water is used as fluid in the tank, a certain mass represents a certain amount of storable energy. Though, assuming being water as an incompressible fluid, the mass can be easily converted into a volume via its density –  $1000 \text{ kg m}^{-3}$  in the case of water. The goal is then to convert for example one  $\text{m}^3$  of water into its thermal potential at a temperature difference of  $\Delta T = 12 - 4 = 8^\circ\text{C}$ . This can be expressed as follows:

$$1m^3 \rightarrow V\rho \cdot c_p \cdot \Delta T = \left(1'000 [kg] \cdot 4'186 \left[\frac{J}{kgK}\right] \cdot 8 [^{\circ}C(K)]\right) \cdot 2.778 \cdot 10^{-7} \left[\frac{kWh}{J}\right]$$

$$1 \cdot m^3 \rightarrow 9.3 \cdot kWh$$

$$\frac{1}{kWh} \rightarrow 9.3 \cdot \frac{1}{m^3}$$

$$\frac{\$}{kWh} \rightarrow 9.3 \cdot \frac{\$}{m^3}$$

Hence, the conversion factor with the proposed assumptions is 9.3 to go from USD per kWh to USD per  $m^3$ . The cost proposed by (DeForest et al., 2014) of 31.80 USD per kWh can be converted into 296 USD per  $m^3$ .

## 5.1.2 BES cost assumptions

### The choice of the technologies

For the battery storage (IRENA, 2017) was used as main source. The reason is that IRENA not only is proposing an excellent report with the market trends of several battery technologies, but is including also an Excel tool which can be used to calculate the cost of storage for personalized cases. The tool shows the cost assumptions for the battery storage in terms of "Energy installation cost" – in USD/kWh –, power installation cost – in USD/kW which represents the cost of the inverter – and also includes estimations for the lifetime and round-trip efficiencies of many technologies. All the figures are provided over four years – 2016, 2020, 2025 and 2030 – with each year including a reference, a best and worst case. Fig. 5.2 shows a snapshot of how the data are provided in the tool.

Energy Storage Unit	2016			2020			2025			2030			unit
	best	worst	ref	best	worst	ref	best	worst	ref	best	worst	ref	
NaNiCl													
Cycle life	7500.0	1000.0	3000.0	8441.3	1125.5	3376.5	9785.8	1304.8	3914.3	11344.4	1512.6	4537.8	equivalent full-cycles
Calendar life	22.0	8.0	15.0	24.8	9.0	16.9	28.7	10.4	19.6	33.3	12.1	22.7	a
Depth of discharge	100.0	100.0	100.0	100.0	100.0	100.0	100.0	100.0	100.0	100.0	100.0	100.0	%
Round-trip efficiency	92.0	80.0	84.0	93.1	81.0	85.0	94.2	81.9	86.0	95.3	82.9	87.0	%
Self-discharge	0.1	15.0	5.0	0.1	15.0	5.0	0.1	15.0	5.0	0.1	15.0	5.0	% per day
Energy installation cost	315.0	488.0	399.0	243.2	376.8	308.0	176.0	272.7	222.9	127.4	197.3	161.3	USD / kWh
Power installation cost	105.0	290.0	155.4	80.3	221.7	118.8	57.4	158.5	84.9	41.0	113.3	60.7	USD / kW

Figure 5.2: Snapshot of the IRENA battery cost tool (IRENA, 2017)

(IRENA, 2017) analysis several battery technologies, namely lead acid, lithium-ion and flow batteries, accounting for different chemistry combinations. Between each technology and chemistry, the costs, lifetime and efficiency of the cells changes.

Only few technologies appearing in the IRENA tool were included into this analysis. The selection process followed the reasoning of selecting a battery storage type that could be used in the future also for grid services, such as arbitrage, frequency regulation, and others. As widely stated, this thesis does not include any grid application nor the flexibility market into its analysis. Nevertheless, it was chosen to narrow the scope of the present – behind-the-meter – analysis to those battery solutions that could be converted in the future into other applications.

In (IRENA, 2017) the competitiveness of all the considered battery technologies is assessed in several applications. This is based on specific literature like (Müller et al., 2017) who propose a certain suitability each battery technology is for the different applications. The choice can be simply represented graphically in Fig. 5.3, where the set of the offered technologies is crossed with those suitable for behind-the-meter applications and grid services.

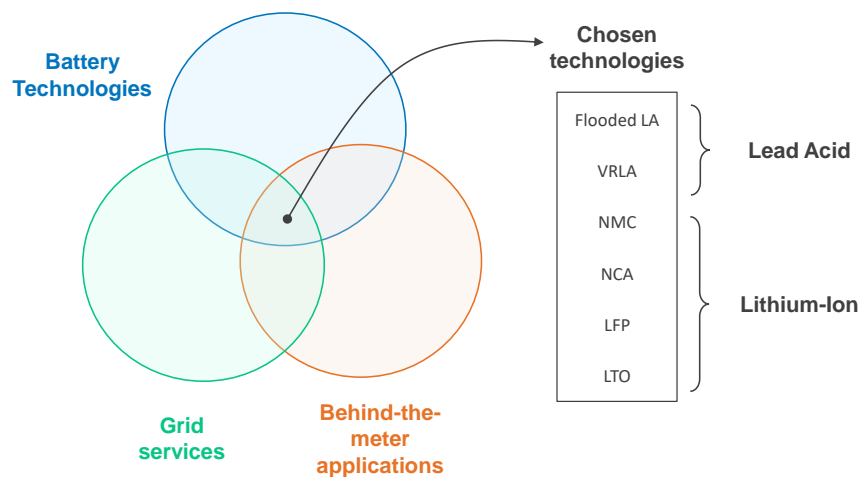


Figure 5.3: Representation of the reasoning used to select the battery storage technologies.

All the applications proposed by IRENA are the following:

- Grid Services
  - Enhanced Frequency Response
  - Frequency Containment Reserve
  - Frequency Restoration Reserve
  - Energy Shifting / Load Levelling
- Behind-the-meter applications

- Self-consumption
- Community Storage
- Increased Power Quality
- Peak Shaving
- Time-of-use
- Off-grid
  - Nano Off-Grid
  - Village Electrification
  - Island Grid

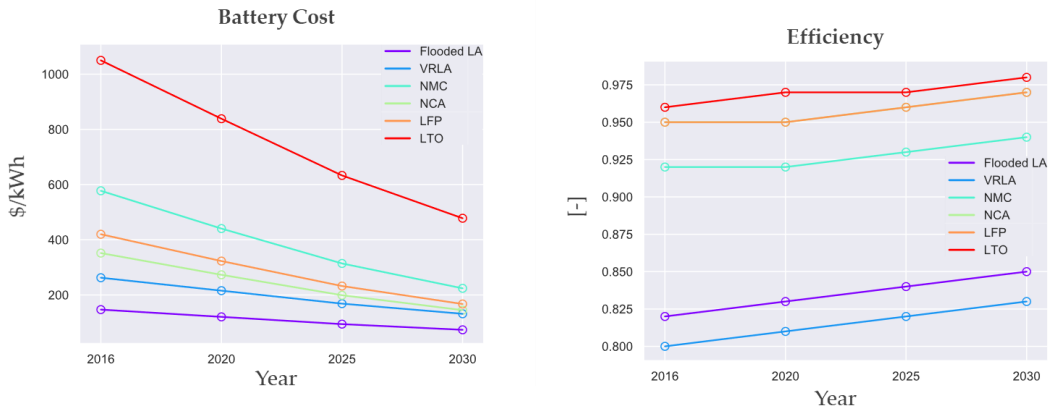
When considering commercial office building in Singapore, the application can be selected as either Peak Shaving, Time-of-Used, or Self-Consumption. The technologies that display a high suitability for these applications and also for all the grid services ones are 6, 2 lead acid and 4 lithium-ion:

- Flooded Lead Acid (Flooded LA)
- Valve-regulated Lead Acid (VRLA)
- Li-Ion Nickel-manganese Cobalt (NMC)
- Li-Ion Nickel Cobalt Aluminium Oxide (NCA)
- Li-Ion Phosphate (LFP)
- Li-Ion Titanate (LTO)

These are then the technologies selected for the economic analysis in this thesis.

### **Battery Cost, lifetime and efficiency**

Of the six selected battery technologies, what is of interest to be selected is particularly three parameters: the energy installation cost (in USD/kWh), the efficiency and the lifetime of the technology (in years). These are taken for all the 4 years – 2016, 2020, 2025, 2030 – proposed by IRENA. The data used for the economic analysis are the reference values proposed by IRENA. The data is presented in Fig. 5.4a, Fig. 5.4b and Fig. 5.5.



(a) Battery Cost – Energy installation Cost in \$/kWh

(b) Efficiency

Figure 5.4: Battery (energy installation) cost and battery efficiency (rearranged from (IRENA, 2017)).

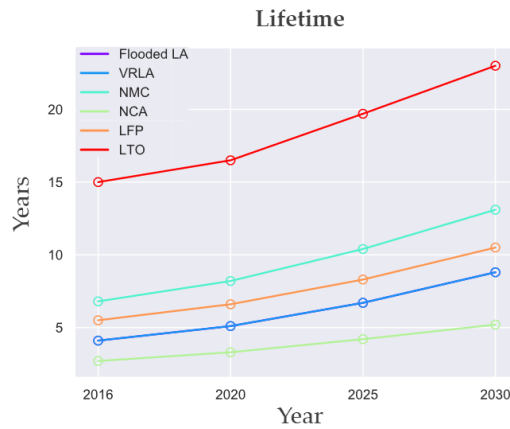


Figure 5.5: Battery lifetime (rearranged from (IRENA, 2017)).

It is visible how the efficiency and lifetime of all the battery technology is increasing over time due to projected improvements in R & D development of battery storage. In contrast, the costs of the battery (as energy installation) is projected to decrease for the same reason.

## 5.2 Price signals

Two different price signals have been used: the wholesale market price and the retailer market price. The wholesale market price in Singapore – Wholesale Electricity Prices (WEP) – changes every half hour and is provided by the Energy Market Company (EMC) (EMC, 2019c)<sup>1</sup>. For the retailer market price, the peak/off-peak pricing package KNIGHT by Képpel Electric was used (KE, 2019). This package provides two tariffs along a day:

- Peak period (7 AM - 11 PM): 20.20 cSGD/kWh
- Off-peak period (11 PM - 7 AM): 16.16 cSGD/kWh

The two price signals are represented in Fig. 5.6.

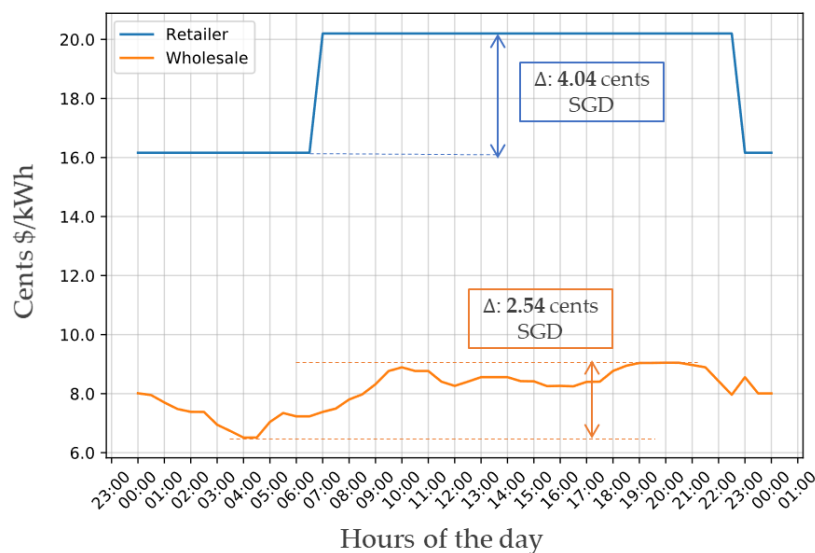


Figure 5.6: Wholesale and retail price signals from (EMC, 2019c) and (KE, 2019). The peak-to-peak distance is highlighted as a  $\Delta$ .

In the figure it is highlighted for both the price signals the distance peak-to-peak as a  $\Delta$ . It can be seen how although the retail price scheme has only two tariffs in a day, it offers a higher  $\Delta$  than the wholesale market price. Although the absolute price of the retailer is

<sup>1</sup>A deeper guide to electricity prices in Singapore can be found at (EMC, 2019b).

higher (is the top one in the figure), what matters from a payback perspective is this  $\Delta$ , because it represents the savings potential when shifting the energy consumption during a day using storage. It can be said that the "price leverage" is bigger for the retail price scheme. This behaviour will be observed in the results section.

### 5.3 Results: Economic Analysis

The results of the economic analysis are shown in this section first for the TES and later for the BES. The two are presented in a different way. The TES results are provided with a graphical representation according to what proposed in Fig. 4.4. This is done to show how the discounted payback theory looks like with a real simulation case. Results are shown for both the TES costs assumptions presented in Section 5.1.1.

For the BES results a different approach is used. Many more cases have been simulated for the BES, all coming from the cost assumptions in Section 5.1.2. It was considered not substantial to present a graph like Fig. 4.4 for each case since it would be uselessly long. Instead, a mapping of the cases is done in terms of discounted payback time first and considering the yearly savings then. The results for the BES economic analysis are presented in the framework presented in Fig. 5.7.

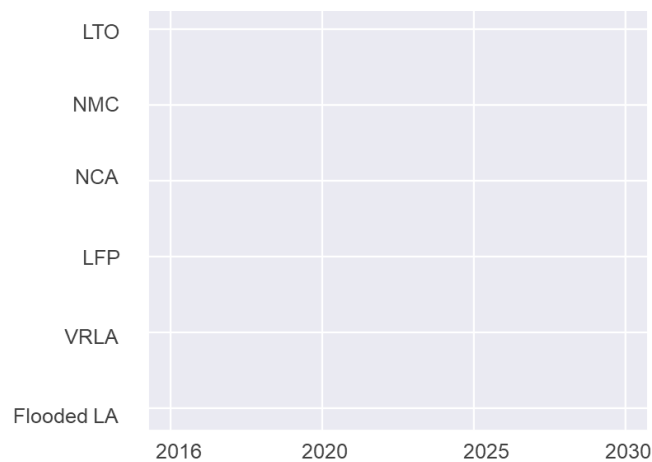


Figure 5.7: Framework used to present the results of the BES economic analysis.

Each intersection of the grid represents a result which, as presented in Section 4.4, comes from running two optimization problems, one for the baseline case and one for the storage case. A "bubble" appears only when the condition  $\gamma^{PB, disc} < L^{storage}$  is respected – in other words when the storage is feasible from a discounted payback time perspective. The size of the bubble is proportional to the value of the solution, whether

it is the payback number of years or economic savings. It must be underlined the fact that although the graphs might display few bubbles, the optimization problems for each intersection is run. The generation of the results for a single BES setup comes then from running a total of 56 optimization problems – 7 technologies, over 4 years, for both baseline and storage cases. In the generation of these results it is visible how the linearity of the model influences the computational time. In fact, to calculate the 56 results the TUM CREATE server takes about 6 minutes of computational time. Although this time can vary depending on the hardware employed to run the simulation, it is clear how the linear models allow for a fast and efficient simulation, which provides one of the major values of the CoBMo.

### 5.3.1 TES Economic Analysis

The TES economic analysis results come from running the model with the following assumptions:

- Interest rate of 6%
- Two different cost assumptions: 291 SGD per m<sup>3</sup> (212 USD per m<sup>3</sup>); and 407 SGD per m<sup>3</sup> (296 USD per m<sup>3</sup>).
- Efficiency of the storage of 80%.
- Lifetime of the storage 15 years<sup>2</sup>.

The result of the TES economic analysis for both the investment cost assumptions are presented in Fig. 5.8.

---

<sup>2</sup>Different sources state different lifetimes for the sensible water storage tank technology Some of these include (ASHRAE, 2013) and (Werner, 2017). 15 years is taken as reference value.

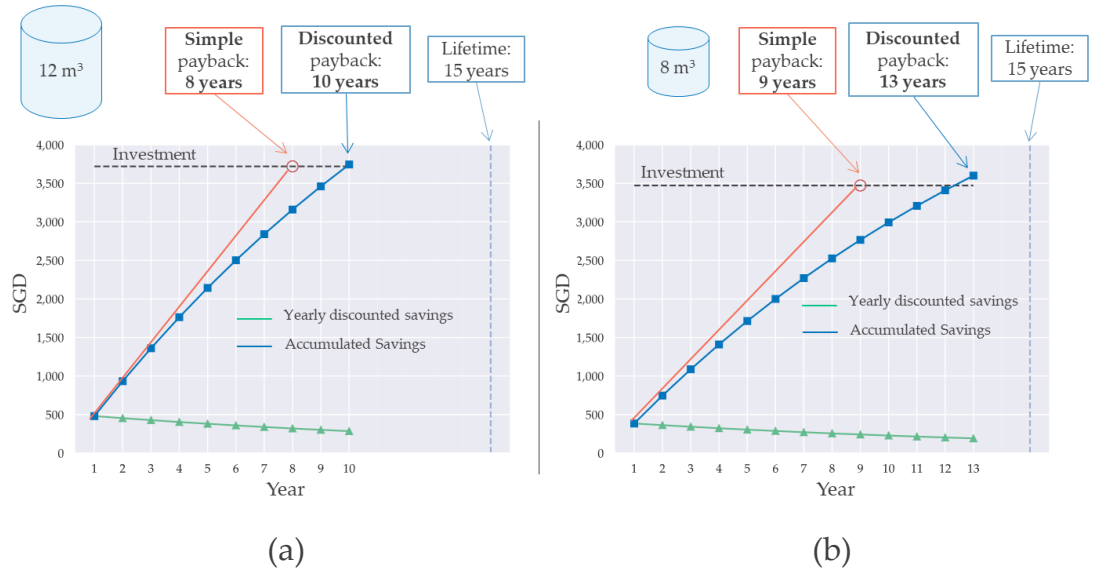


Figure 5.8: TES Economic Analysis results using an overall efficiency of 80%. Figure (a) is the result using 291 SGD per m<sup>3</sup> as cost. Figure (b) using 407 SGD per m<sup>3</sup>.

It can be noted that the lower investment cost case is better for multiple reasons. The discounted payback time is lower even though the investment is higher. This is possible thanks to a bigger storage installed (12 m<sup>3</sup> in case (a) against 8 m<sup>3</sup> in case (b)). A bigger storage means a higher savings potential thanks to a bigger potential for shifting the consumption of the building in low-tariff hours. Hence, a lower investment cost means that the storage will payback sooner and that after the project has reached the break-even it will generate more savings, namely 508 SGD for case (a) and 406 SGD for case (b).

By far the most relevant assumption in the TES case is the efficiency. 80% is in fact a very conservative value. As presented in Section 2.6.2, (Bahnfleth and Musser, 1998) has proved that thermal storage tanks can display an overall efficiency up to 92%. Fig. 5.9 shows the results for the TES economic analysis using the same cost assumptions and changing the efficiency to 92%.

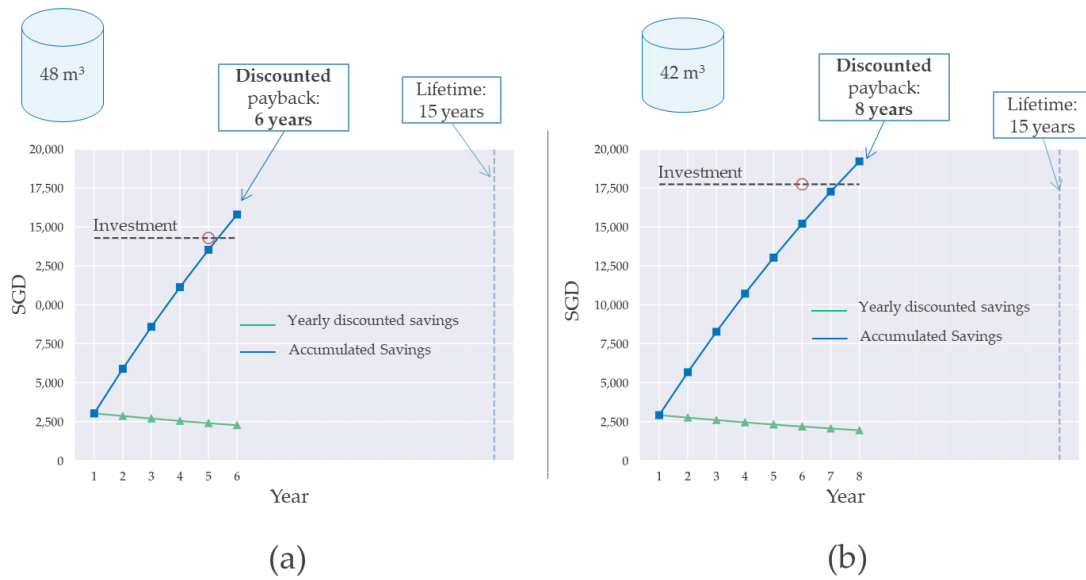


Figure 5.9: TES Economic Analysis results using an overall efficiency of 92%. Figure (a) is the result using 291 SGD per  $\text{m}^3$  as cost. Figure (b) using 407 SGD per  $\text{m}^3$ .

Once again, the lower the investment cost the better. But an improvement of efficiency by 12 points % leads to a great difference in the size of the storage. For case (a) the size is  $48 \text{ m}^3$ , while for case (b) is  $42 \text{ m}^3$ . The storage size for (a) and (b) are respectively 4 and 5.25 times higher. This also reflects what shown in Fig. 5.9. Although the investment cost for the 92% efficiency case is higher, the payback time is lower. This is possible due to the higher yearly savings the storage can bring, being the storage size bigger. The savings for cases (a) and (b) in the 92% efficiency case are respectively 3'200 and 3'100 SGD per year.

Concluding, even though both the cases with 80% and 92% efficiency payback the storage in discounted terms within its lifetime, the higher efficiency case is a far better option. Besides the lower payback time, the reason for this is that when the investment has reached break-even, the savings it will generate over time will be higher. It is then concluded that the efficiency is the parameter that has to be prioritized in the choice of the storage.

### 5.3.2 BES Economic Analysis

As introduced before, the results of the BES economic analysis will not be displayed by charting the detailed trend of the accumulated savings along the years. This is due to the high number of simulated cases (28, 7 technologies over 4 years) and it would be



Figure 5.10: BES Results: wholesale price signal. Discounted payback time.

uselessly long to show a figure like Fig. 5.8 and Fig. 5.9 for each of them. Instead, the results will be shown in the framework proposed in Fig. 5.7.

For the BES case, the simulations are run for both the price signals, wholesale and retailer, presented in Fig. 5.6.

### BES Economic Analysis: Wholesale price signal

The results of the discounted payback time are shown in Fig. 5.10.

With the wholesale price signal, no storage investment is paying back within the lifetime of the technology before the 2025 investment conditions. Then, only Li-Ion Nickel-manganese Cobalt (NMC) and Li-Ion Phosphate (LFP) batteries payback, with the first having a payback time of 7 years and the second of 10 years. To further compare these two investment possibilities (NMC and LFP in 2025), the yearly savings are displayed in Fig. 5.11.



Figure 5.11: BES Results: wholesale price signal. Yearly savings as percentage of baseline operational costs.

It can be seen how the optimization problem for the NCM case sizes the battery storage with 2025 conditions such that it provides 2.30% yearly savings with respect to the baseline scenario. For the LFP case, the savings are 1.3 %. This shows that NCM is a better option to be selected as battery storage to invest in as it not only pays back earlier, but over time it will allow higher yearly savings thanks to the bigger size of the storage.

### BES Economic Analysis: Retail price signal

The results for the discounted payback time for the retail price signal case are shown in Fig. 5.12



Figure 5.12: BES Results: retail price signal. Discounted payback time.

As it was foreseen, the retail price signal gives a bigger price leverage to the storage case to use, hence the savings are higher and the payback lower compared to the wholesale price case. The Li-Ion Nickel-manganese Cobalt (NMC) technology proves to payback again as one of the earliest together with the Li-Ion Titanate (LTO) technology. In the retail price case, the 2020 investment conditions are already suitable to have a break even of the investment within the lifetime of the storage.

As done for the wholesale price case, the yearly savings are shown in Fig. 5.13.



Figure 5.13: BES Results: retail price signal. Yearly savings as percentage of baseline operational costs.

The results for the yearly savings are more homogeneous than the wholesale case. Very small changes are observed along the years for the different technologies, and small variations also occurring technologies between each other.

To select a suggested technology and year to invest in, the break-even is used for the retailer case. Although for all the technologies the payback time is decreasing over time, the choice must be driven by the combination of the earliest break-even with a satisfactory amount of savings per year. This evaluation can be done observing Fig. 5.14.

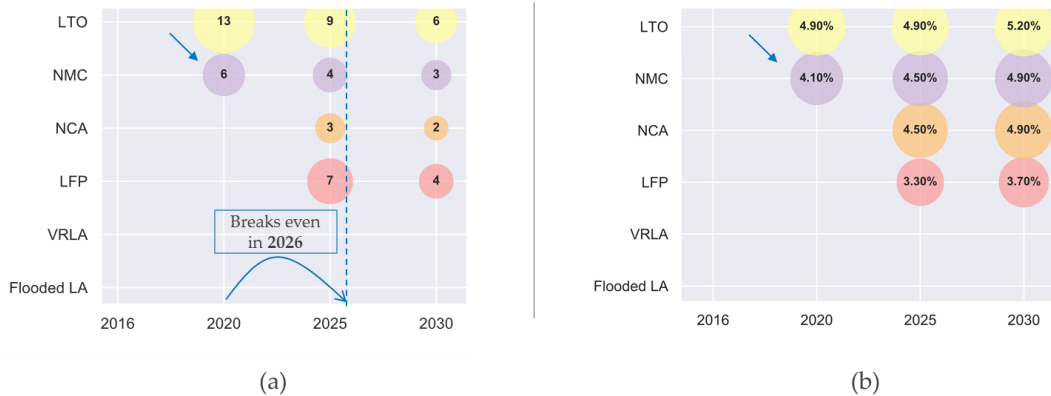


Figure 5.14: BES Results: retail price signal. Break-even evaluation.

The technology that breaks even the earliest is NCM investing in 2020, and this solution also displays yearly savings very close to the other solutions, even much further in the future (2025 and 2030). Hence, the investment suggestion for the retail price signal is NCM in 2020.

## 5.4 Results: Optimal Scheduling

The goal of this section is to show what is the optimal schedule of the storage operations for two storage simulations run to obtain the economic analysis results, one per storage type (sensible and battery). Although the scheduling changes depending on all the assumptions made for the problem, what is relevant here is to show the behaviour of the storage operations.

The schedule is shown over 24 hours, which is the considered time horizon for the optimization problem. The time step is half-hour, making up for 48 total timesteps in a simulation.

The optimal scheduling will be shown separately for the AHU and TU operation first, then putting them together and highlighting the storage charge-discharge cycle and the influence of the price signal on the charge electric power.

### 5.4.1 Optimal Scheduling: TES

The operation of the AHU and TU coming from the optimal scheduling simulation are presented in Fig. 5.15 and Fig. 5.16. This section presents the schedule of the results

presented in Fig. 5.8 (a). The storage state of charge (or storage level) (red dashed line) is also shown and referenced to the secondary right y axis.

The plots show that both the AHU and the TU supply the zones directly during most of the day. Only three timesteps over the 48 simulated involve the discharge of the storage. The operation of AHU and TU is reduced for both during the same period of time, 9.30 AM - 11 AM. The TU operation (Fig. 5.16) is brought to zero during two timesteps, when the storage discharge takes completely over. Instead, the AHU operation never goes to zero and is just decreased (by approximately 50%) during the same time window).

The level of the storage (measured in  $\text{m}^3$  of the bottom cold layer) reaches and keeps its maximum before discharging completely along the same 3-timesteps time period.

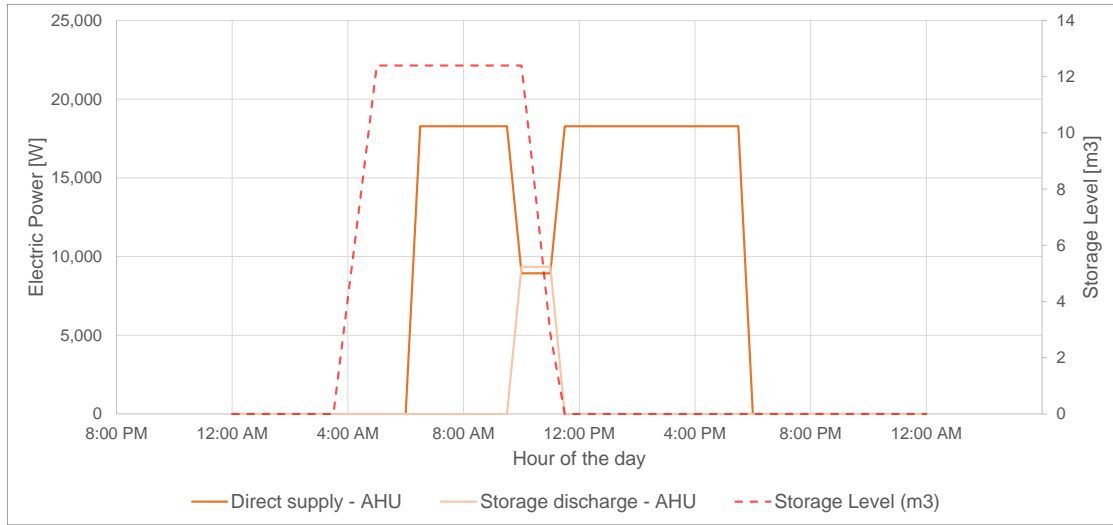


Figure 5.15: Optimal scheduling – TES – AHU operation.

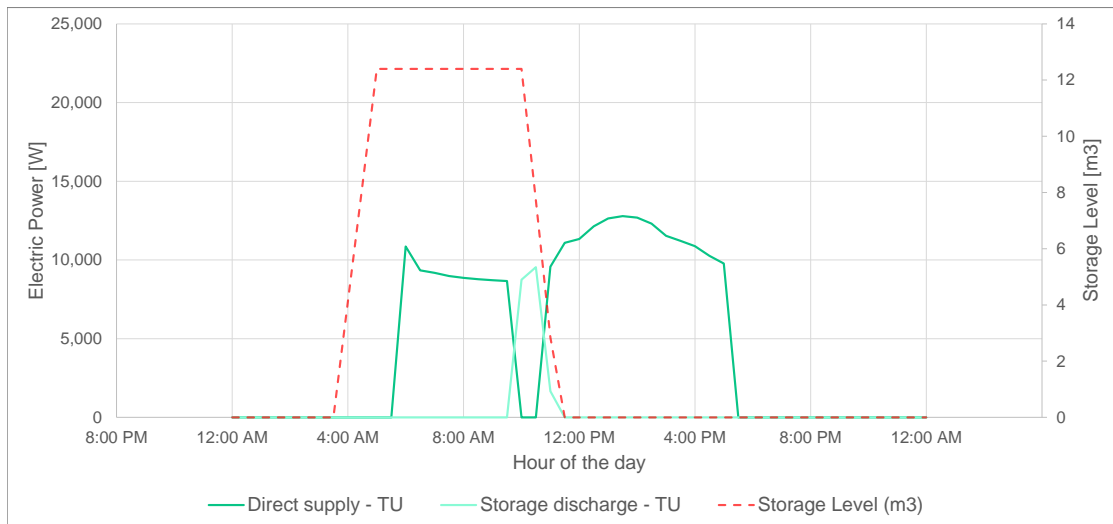


Figure 5.16: Optimal scheduling – TES – TU operation.

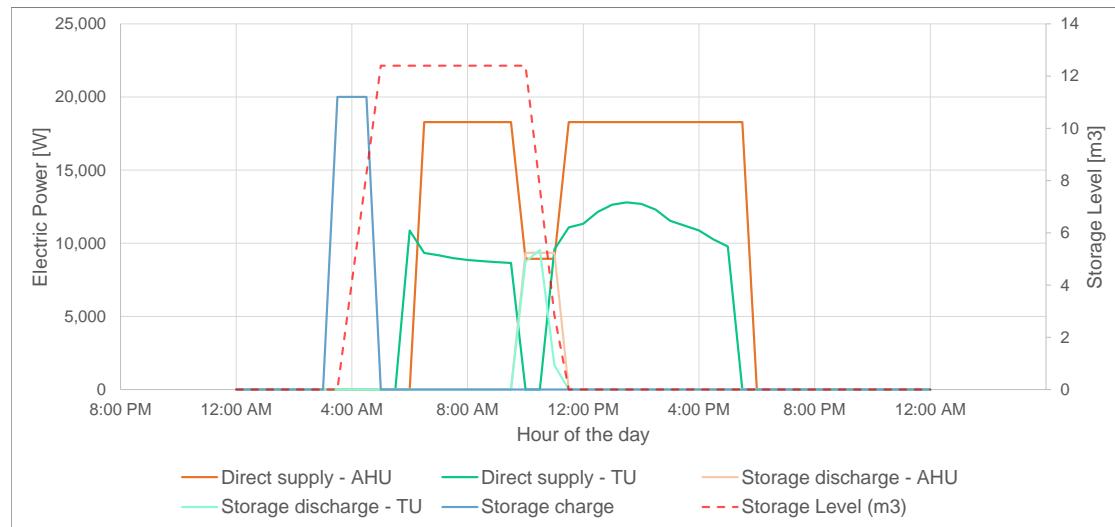


Figure 5.17: Optimal scheduling – TES – AHU and TU operation; storage level; charge electric power.

In Fig. 5.17, the AHU and TU are plotted in the same graph together with the storage level and the charge electric power (blue solid line). The charge power stays at its maximum for 3 timesteps and charges the storage up to its maximum.

Fig. 5.18 is alike to Fig. 5.17 showing the wholesale electricity price (referenced to the secondary y axis) instead of the storage level. This graph shows how the storage charge/discharge schedule reflects the price signal. The storage is charged in the moment of the day when the price is at its lowest point (3 AM to 4.30 AM) and discharged at one of its two peaks (9.30 AM to 11 AM). This shows how the optimization algorithm leverages the price difference in during the day to minimize the operational costs.

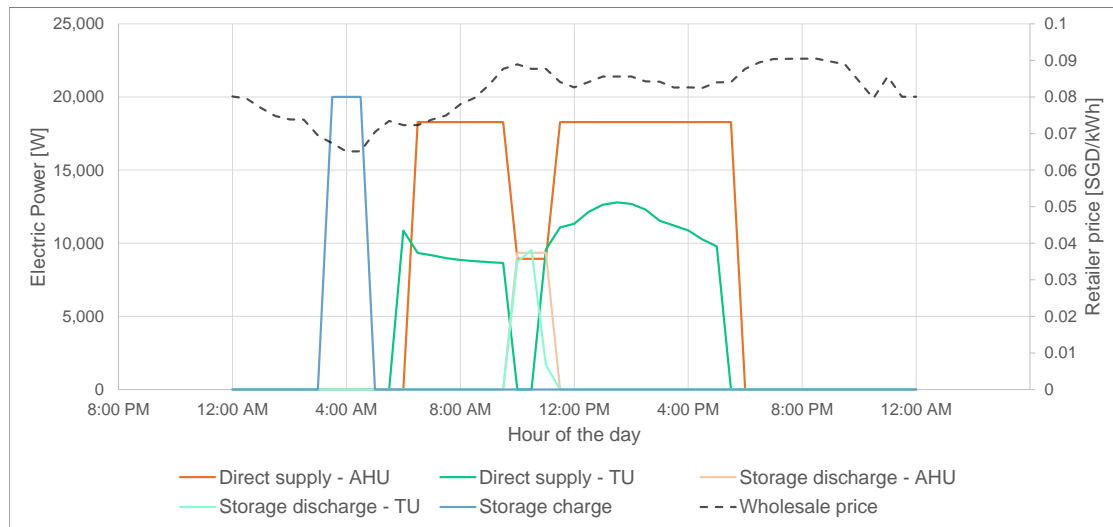


Figure 5.18: Optimal scheduling – TES – AHU and TU operations; wholesale electricity price; charge electric power.

### 5.4.2 Optimal Scheduling: BES

The optimal scheduling for the battery (BES) case is shown for the investment suggestion provided in Section 5.3.2: Li-Ion Nickel-manganese Cobalt (NCM) technology investing in 2020 (Fig. 5.14).

Fig. 5.19 and Fig. 5.20 show the optimal scheduling of the battery storage case for the AHU and TU operations respectively. It is noticed immediately how the BES case displays a wider range of storage operations with respect to the TES case. The storage discharge supplying the AHU happens between 7 AM and 10.30 AM (7 timesteps), while the TU one along 7 AM and 3.30 PM (17 timesteps). The storage level (red dotted line) reflects the discharge schedule. The storage is first charged and then immediately discharged, with the discharge path having two different steepness of the decreasing curve section. The first part is steeper as the storage discharges to supply both the AHU and the TU, while the second part is less steep by supplying only the TU.

Similar to the TES case, Fig. 5.21 shows the aggregated graph of the AHU and TU optimal schedule together with the storage level and the charge electric power. The battery storage is charged during 14 timesteps (from 12 AM to 6.30 AM).

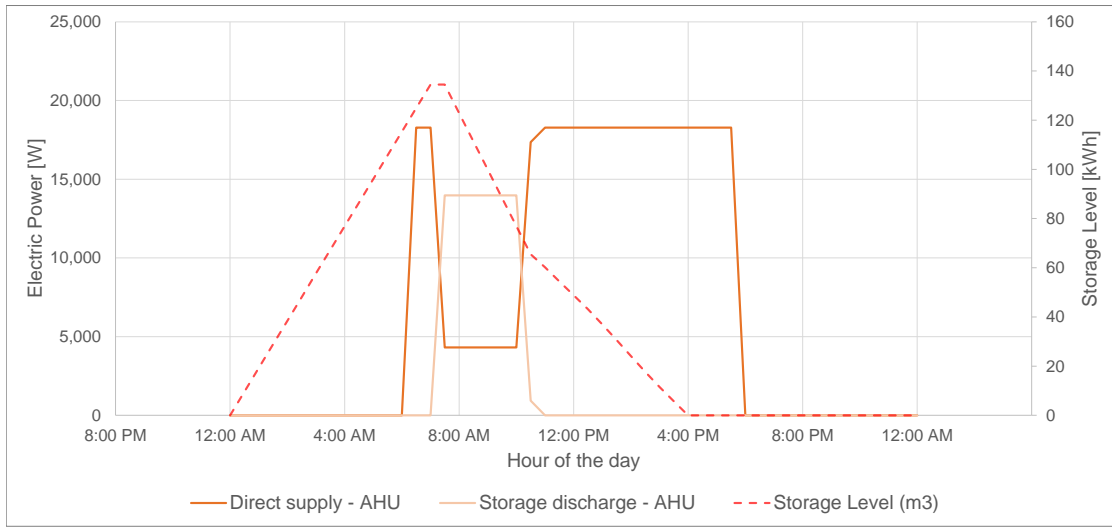


Figure 5.19: Optimal scheduling – BES – AHU operation.

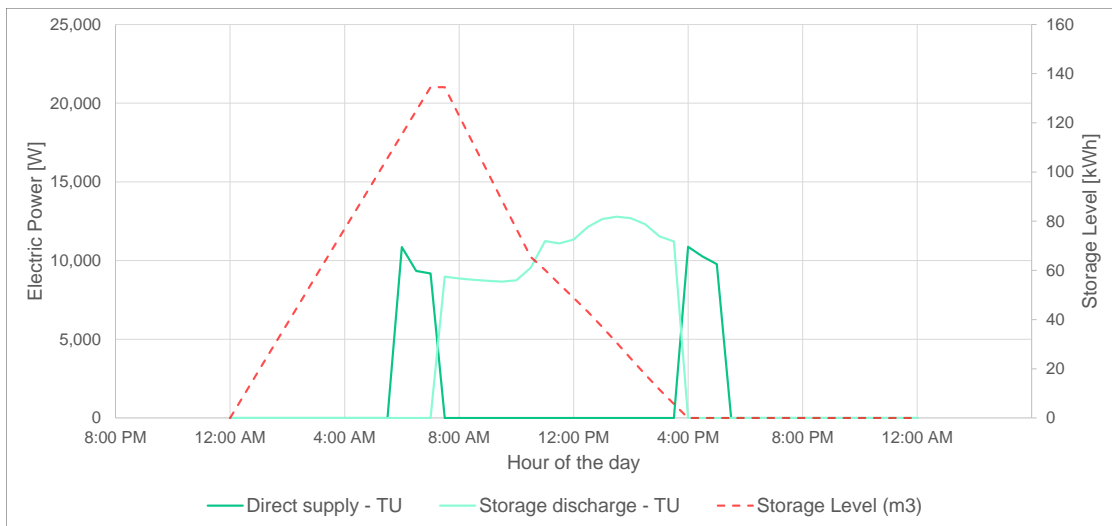


Figure 5.20: Optimal scheduling – BES – TU operation.

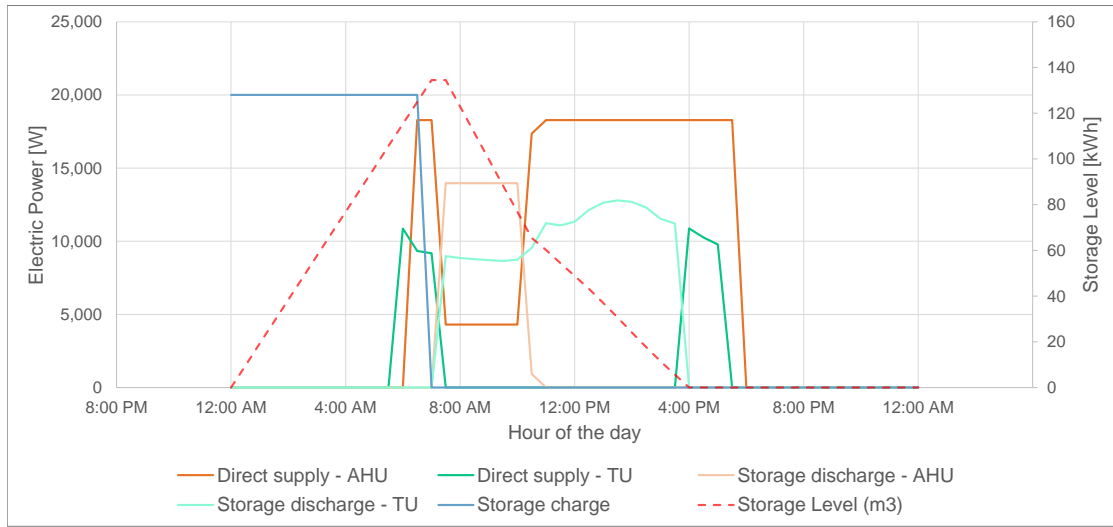


Figure 5.21: Optimal scheduling – BES – AHU and TU operation; storage level; charge electric power.

Fig. 5.22 shows the same information as Fig. 5.21 plotting the retailer electricity price signal instead of the storage level. It can be observed that the charge/discharge schedule reacts to the price signal as the storage charge happens during the off-peak tariff period. When the peak tariff takes place, the storage discharges until it is empty.

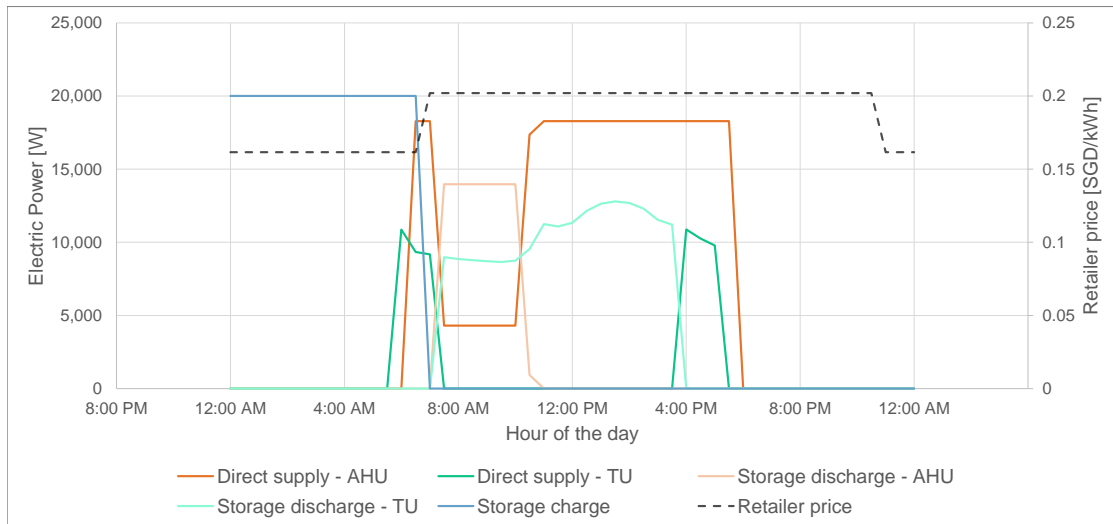


Figure 5.22: Optimal scheduling – BES – AHU and TU operation; retailer electricity price; charge electric power.

## 6 Discussion

This section discusses the results presented in Chapter 5 and underlines some limitations of the analysis.

### 6.1 Economic Analysis

The economic analysis results show that both TES and BES are feasible economically in terms of discounted payback time. For TES two cost assumptions were used and for both of them the payback time results are lower than the technical lifetime of the TES (15 years). This assures that the savings will generate profit before a re-investment is needed. What was noticed for the TES is that the results of the economic analysis are extremely sensible to the storage efficiency. When using a very conservative value for the round-trip efficiency (80%) the storage installation allows to achieve about 500 SGD per year in savings, paying back between 10 and 13 years – depending on the cost assumption. Though, when using an efficiency of 92% – value recommended by (Bahnfleth and Musser, 1998) – the payback time drops to 6 and 8 years. Besides the sooner break-even point of the investment, an importance difference the efficiency produces is the installed size of the storage, hence the savings per year: for both the TES cost assumptions the savings are around 3000 SGD per year. An higher value of efficiency allows not only for a break-even point closer in time, but also to being left with a storage facility which generates far more savings than the low-efficiency one. The recommendation for building operators in the TES case would then be to choose the value of efficiency carefully and invest in increasing this figure as much as possible.

The economic analysis results for the BES also show feasibility. As presented in Chapter 5, for the BES case many battery technologies were considered. The data that is input – energy installation cost, power installation cost, fixed costs, lifetime, efficiency and minimum depth of discharge – are taken from (IRENA, 2017). For the BES case the data for all the aforementioned parameters are considered at four different points in time (2016, 2020, 2025, 2030). An important point to underline is then that the analysis is then based on the data projections which IRENA has calculated which will be affected by a certain error factor. The BES case was tested with both the wholesale and retail

price signal. As foreseen, the latter produces a better case as the price leverage is higher – i.e. the difference between the maximum and minimum price in a day. The results show that the best investing option with the retail price signal is Nickel Manganese Cobalt oxide (NMC) battery technology with the 2020 conditions. The NMC technology is also the best option with the wholesale market price signal.

It must be raised again the fact that the BES model is a black-box one which does not account for the influence of external temperature and aging of the battery cells. For this reason the results coming from the economic analysis are considered to be an indication for the investment feasibility in BES, but not an instrument for final decision. The analysis should be broadened to deepen specific topics when considering the installation of a certain battery technology in an office building. Moreover, although this work considers the potential of BES only as a way to make savings by using electricity at low-tariff hours during the day, a further potential can be identified in the grid services the battery storage can provide. By way of performing frequency regulation, voltage control, arbitrage, and other grid services, the building operator – and owner of the BES – would see another revenue stream from selling these services to the grid. This potential is not accounted for in the present work, making the analysis conservative. A point of discussion for this expansion would be to which extent the installed BES could provide both behind-the-meter operations and grid services at the same time; and in case also to which extent it would be to shift from one to the other.

## 6.2 Optimal Scheduling

The results of the optimal scheduling make two important points arise. On one side it is visible that the optimal scheduling does not aim to shave the power peak of the building, but rather optimize the cost by leveraging the variable tariff during the day. This reflects the price structure implemented into the objective function in the optimization problem. In fact, in the objective function no term is implemented which affects the price depending on the power peak supplied to the building during a day. The reason for this is that being an office building in Singapore considered as a low-voltage consumer, the Use-of-System tariff does not include pricing section related to the power peak (see Section 3.1).

Another important point emerges when looking at the storage level in the optimal scheduling charts for both TES and BES. It can be observed that only 1 storage cycle per day is performed – meaning that the storage charges and discharges only once. This aspect has to be considered for example when selecting the lifetime of the storage facility. For the BES case, in the IRENA report different values of lifetime are provided depending on the cycles per day the battery storage has to supply. A change in the number of cycles per day leads to the need to check that the assumptions made for the storage are still valid.

### 6.3 Limitations of the Analysis

Finally some limitations of the analysis are here underlined. As widely explained during the report, the current analysis is done using linear models for the storage and linear numerical optimization. This is done as because the CoBMo is set as a linear model and consequently the storage was modeled accordingly. Due to this linearity, some linearization points are used in the modelling of the building in order to avoid bi-linearities. This includes for example using a fixed temperature – a linearization point – for the surface temperature in modelling the exterior surfaces' emission heat transfer; or for the zones temperature when modelling the AHU heat transfer. Another relevant simplification done via linearization is to assume a constant efficiency for the AHU: this value should be dependent on the load factor of the unit, but to avoid non linearities it is taken as a constant. The use of linear modelling and optimization brings the huge advantage of providing modelling frameworks which are fast and convex – meaning highly suitable also for commercial MPC in the future – but it leads to an inevitable decrease of accuracy in the physical model of the building.

Another limitation of the analysis is that the optimal scheduling is calculated over a 24-hours time horizon only, making the results of the economic analysis dependent of the conditions of the selected simulation day. This approximation is acceptable especially for Singapore where the weather conditions do not vary much over the year. Nevertheless, to improve the results of both the economic analysis and optimal scheduling a longer simulation time up to one week or even one month can set. The reason why this was not done in the current work is due to time limitations, as the computational time increases with the growing of simulation days.

A limitation is also the fact that although the results are related to the hole CREATE Tower, only the 8th storey – where TUM CREATE is located – is modelled. This is the scaled 14 times to make up for the remaining storeys in the building. An improvement of the model can come from modelling all the floors of the tower.

Finally a consideration has to be done on the fact that the BES results for the economic analysis come from putting together “today's prices” and "tomorrow's costs". The wholesale market price is taken from the EMA and the retailer one from a package Keppel Electric sells today. The assumptions related to the BES about costs, lifetime and efficiency are related to the future (2020, 2025 and 2030) and are projections coming from the study made by (IRENA, 2017). What should be improved is to estimate the change in the electricity price in the next years and adapt the analysis to this. A possible solution could be to run simulations for different weeks along a year and extrapolate a profile of the storage over a year in Singapore. Then scenarios can be build where the electricity tariff varies according to how the power system in Singapore might change. A strong increase in DSF in the island could for instance squeeze the wholesale market price

as the congestion is better managed; this squeeze would give a lower “price leverage” to the building operator, leading to a higher payback time. The same event of increase DSF could instead generate other peaks during the day – rebound effect – and the price would change its shape still providing a sufficient price leverage. All these different situations can be the subject of a further study analysing the feasibility of storage in a series of different political and technological scenarios that might evolve in Singapore.

## 7 Future Work

As the future work of this thesis it is recommended to benchmark the model of the storage, as well as expand the analysis into different paths that might provide interesting results.

The thermal storage model can be expanded including Phase-Change Material (PCM) thermal storage – e.g. ice storage. Ice storage is often used in district cooling systems as solution which displays high efficiency. The sensible storage tank model can be expanded by implementing a mathematical model of the thermocline into it to properly define its formation and better estimate the losses into the storage tank.

The benchmarking of the sensible storage modelling can be done via comparison with a Computational Fluid Dynamic (CFD) simulation of the storage tank. This was actually included into the scope at the beginning of the thesis but discarded due to time limitations. A potential methodology for performing a CFD benchmarking starts by defining a common simulation test case – e.g. a 1 m<sup>3</sup> water storage tank – agreeing on the physical and thermodynamic characteristics of the case, inputting these in both models. The first step would be to run the CoBMo on a 24-hours time horizon and retrieve the storage schedule, and particularly the mass flows which characterize every change and discharge timesteps (as show in Section 3.3.4). These mass flows can be input into a CFD model which, by simulates the fluid dynamics into the water tank can also provide the temperature profile in the tank along the time horizon. Comparing the two and repeating the process iterative the CoBMo model can be adjusted – i.e. changing the assumptions made or even expanding the modelling approach, for instance for what regards the losses. An example of CFD model is the one provided by Araner (ARANER, 2018b) <sup>1</sup>.

The CoBMo improved with the storage can be also benchmarked using industry-standards modelling frameworks which include the storage into them. The most famous among them is Energy Plus (US DoE, 2019c). This framework is being used at the time of this thesis for validating the CoBMo without storage, hence an expansion of the validation process can be done from this.

---

<sup>1</sup>Direct link to a video representation of the simulation result.

## 7. Future Work

---

A further extension of the analysis can be done towards electric grid planning. As the installation of storage at the building level can allow to decrease the overall consumption peak, at the planning stage this can result in investment savings on the grid planning side – i.e. lines, transformers, substations. If such consideration is included into an optimization framework, the model would provide an optimum which is not only considering the storage capital cost, but one of the whole distribution grid. On the planning side – i.e. before the construction of a district – this can be a powerful tool to analyze the potential of the storage for implicit DSF. As a tool modelling the distribution grid in Singapore district is already developed in TUM CREATE, this modelling expansion has been part of the scope of this thesis. Although, due to time constraint, it was removed and left as future work.

Finally, implementing a modelling framework for district cooling systems and connecting it with the CoBMo and the distribution electric grid one will result in having a framework which can estimate an optimum total cost with an even broader scope. This could be even larger by including for instance Electric Vehicles (EVs) at the electric grid side.

## 8 Conclusions

This work analysed the potential of energy storage on the Demand Side Flexibility (DSF) of commercial buildings in Singapore. Linear mathematical models of thermal sensible storage – in the form of a water storage tank – and battery storage are defined and implemented in Python.

This work extends the Control-oriented Building Model (CoBMo) developed in TUM CREATE, improving the modelling framework to include the storage. CoBMo is a linear model that simulates the thermal comfort and indoor air quality within a building subject to disturbances from the external environment and to the control of the HVAC system. CoBMo is a white-box model, meaning that the building is modeled implementing explicitly the physical equations governing its thermal behaviour. This modelling approach – an alternative to the black-box and grey-box approaches – is particularly useful when the flexibility of a building has to be evaluated in the planning phase, meaning when there are no data about the building's operation, while information on its physical characteristics are available. The goal of the thesis was to formulate and implement the storage models into CoBMo and to perform an economic payback analysis of the storage investment.

The models implemented for the storage, as well as the optimization problem, are linear. The optimization is a planning and operation problem. The optimal day-ahead schedule of the storage is defined while assuring the optimal operation of a building. CREATE Tower – the building hosting TUM CREATE among other research centers – is used as test case for the model. Besides the weather conditions in Singapore and the physical features of the building, the electricity price signals are provided as an input to the optimization algorithm. Furthermore, the impact of two different price signals is considered: the Singapore wholesale market price and the retail market price. Both are time-of-use prices. The wholesale market price changes half-hourly, while the retail price provides the customers with two tariffs only, peak and off-peak. The economic analysis evaluates the discounted payback time of a storage installation, where the storage size is obtained as output of the optimization algorithm. The economic analysis aims to provide an initial assessment of the feasibility of installing storage for behind-the-meter applications – i.e. for implicit DSF.

## 8. Conclusions

---

The results from the economic analysis prove that both thermal and battery storage are feasible for the test case. The payback of the sensible storage is extremely sensitive to the tank efficiency. However, even using a conservative value for the efficiency (80%), the discounted payback time was still calculated to be 13 years for the highest investment cost assumption, value that fulfills the technical lifetime requirements. The battery storage displays the best investment conditions for Li-Ion Nickel-manganese Cobalt (NMC) technology in 2020, with a payback time of 6 years. The findings prove the feasibility and potential of storage when installed at the building (distributed) level. The building operators have the opportunity of shifting the energy consumption of a building in low-tariff hours of the day, particularly leveraging the newly came open electricity market in Singapore to purchase electricity in retail offers or directly from the wholesale market. Expanding this study to the grid planning level, the use of storage can allow the municipality of Singapore to generate savings using storage to defer or avoid expansion costs of the distribution grid. The presence of storage in the building and the increased flexibility this investment creates can also give the opportunity to the building owner to participate in flexibility aggregation and be compensated for curtailing a part (or the whole) electric peak of the building in hours of high congestion in the grid.

The future work on this topic would be to validate the model, using either an industry standard building-modelling framework – e.g. Energy Plus – or even a comparisons with more detailed models – e.g. Computational Fluid Dynamics (CFD) for the thermal storage tank and other modelling frameworks for the battery storage to evaluate the different chemistries. Furthermore, it would be interesting to evaluate the potential revenues that can be gathered using the battery storage installed in the building to provide grid services – e.g. voltage support, arbitrage, frequency regulation, etc. Finally, CoBMo can be connected with a district cooling system model, considering the storage as centralized. In this case, the optimal operation point of the central chiller would affect the control of the building, the storage size and the investment payback time.

# Acknowledgments

I firstly wish to thank TUM CREATE for the opportunity of developing my master thesis with this amazing institution based in Singapore. It has been a life-changing experience for sure, and the support from TUM CREATE has been a key in my professional growth. But special gratitude goes to my supervisor Sebastian Troitzsch. His patience, especially at the beginning of the thesis, allowed me to find my path. By leaving me great freedom he gave me the opportunity to prove to myself what my abilities are, and grow independently and with confidence. Although having very different styles, I am glad to say that we developed a complicity during the period spent in TUM CREATE which enriched my experience even more. My gratitude is also to my supervisors in KTH and UPC; Miroslav Petrov and Andreas Sumper, who provided me with valuable feedback during the work. But if my academic experience in Singapore brought great change in my professional life, so has it in my personal one. The people who filled my time and life with laughter, adventures, travels, food and lots, lots of talks have turned this experience into a life-changing one. Misha, Sabrina, Tim, Shikar, Alex, Hanna, Yvonne, Daniel, Helena, Damien, Rodrigo, Syahidah, Moritz, and all the others that passed by. You have all contributed to make this time memorable, and I will always be thankful for your friendship. Well, some people must be mentioned as well that were not in Singapore at the time. All the friends I found during the masters have lit new lights in my life. And I owe a particular thank you to Chris “Coffee” Menos and Fabio “Basically” Giunta for the very bad influence they had on me. Thank you, Janis, for compensating on the other side.

Thanks to my parents, who have sustained me and always believed in me. Counterbalancing your great esteem and affection by also spurring me on to face my responsibilities; a great present. You always acknowledged my feelings and yours, allowing my emotional sensibility to develop sharper, and you have never put your needs in front of mine. Questioning yourselves as parents allowed me to grow as a son and a man.

Lucia, thank you. In retrospect, I am impressed by how well you could pretend to understand what I was working on during my thesis. “Ha Ha Ha :)”. I guess laughter and bad jokes are kind of our style. But all kidding aside, I start realizing that your love has been the key ingredient in the last years to succeed in what I am doing. And contrary to what thermodynamics states, it feels like an endless source of energy (recall? 2nd principle of Thermodynamics? We spoke about it and you were like “aah yes yes I know what you are talking about!”). Seriously, I hope it never ends.

To conclude, let’s get into fiction and give my gratitude to Wes Montgomery, who kept me company in a parallel life, lived in a black-and-white tape from the 60’s where, eventually, I can play jazz guitar - I really wanted the last word on this work to be *guitar* and not *storage*. ... opssss

# Bibliography

Zeineb Abdmouleh, Adel Gastli, Lazhar Ben-Brahim, Mohamed Haouari, and Nasser Ahmed Al-Emadi. Review of optimization techniques applied for the integration of distributed generation from renewable energy sources. *Renewable Energy*, 113:266–280, 2017.

ARANER. Thermal energy storage tes tank reference e-book. <https://content.araner.com/ebook-thermal-storage-tank>, January 2018a.

ARANER. Computational fluid dynamics uses for tes design in district cooling design computational fluid dynamics for tes design of district cooling design. <https://www.araner.com/blog/computational-fluid-dynamics/>, 2018b.

ASHRAE. *District Heating and Cooling Guide*. 2013.

Ercan Atam and Lieve Helsen. Control-oriented thermal modeling of multizone buildings: methods and issues: intelligent control of a building system. *IEEE Control Systems Magazine*, 36(3):86–111, 2016.

William P Bahnfleth and Amy Musser. Thermal performance of a full-scale stratified chilled-water thermal storage tank. *TRANSACTIONS-AMERICAN SOCIETY OF HEATING REFRIGERATING AND AIR CONDITIONING ENGINEERS*, 104:377–388, 1998.

Landen Blackburn, Aaron Young, Pratt Rogers, John Hedengren, and Kody Powell. Dynamic optimization of a district energy system with storage using a novel mixed-integer quadratic programming algorithm. *Optimization and Engineering*, 20(2): 575–603, 2019.

British Petroleum BP. Energy demand by sector. <https://www.bp.com/en/global/corporate/energy-economics/energy-outlook/demand-by-sector.html>, 2019.

Kathryn R Bullock. Lead/acid batteries. *Journal of power sources*, 51(1-2):1–17, 1994.

- Johannes Büngeler, Eduardo Cattaneo, Bernhard Riegel, and Dirk Uwe Sauer. Advantages in energy efficiency of flooded lead-acid batteries when using partial state of charge operation. *Journal of Power Sources*, 375:53–58, 2018.
- Luisa F Cabeza. *Advances in thermal energy storage systems: Methods and applications*. Elsevier, 2014.
- Climate Action Tracker CAT. Singapore – current policy projections. <https://climateactiontracker.org/countries/singapore/current-policy-projections/>, 2019.
- Vikas Chandan, Anh-Tuan Do, Baoduo Jin, Faryar Jabbari, Jack Brouwer, Ioannis Akrotirianakis, Amit Chakraborty, and Andrew Alleyne. Modeling and optimization of a combined cooling, heating and power plant system. In *2012 American Control Conference (ACC)*, pages 3069–3074. IEEE, 2012.
- Carbon Market Watch CMW. Pricing carbon to achieve the paris goals. [https://carbonmarketwatch.org/wp-content/uploads/2017/09/CMW-PRICING-CARBON-TO-ACHIEVE-THE-PARIS-GOALS\\_Web\\_spread\\_FINAL.pdf](https://carbonmarketwatch.org/wp-content/uploads/2017/09/CMW-PRICING-CARBON-TO-ACHIEVE-THE-PARIS-GOALS_Web_spread_FINAL.pdf), September 2017.
- Gabriele Comodi, Francesco Carducci, Balamurugan Nagarajan, and Alessandro Romagnoli. Application of cold thermal energy storage (ctes) for building demand management in hot climates. *Applied thermal engineering*, 103:1186–1195, 2016.
- Charles D Corbin, Gregor P Henze, and Peter May-Ostendorp. A model predictive control optimization environment for real-time commercial building application. *Journal of Building Performance Simulation*, 6(3):159–174, 2013.
- Peter Cramton. Electricity market design. *Oxford Review of Economic Policy*, 33(4): 589–612, 2017.
- Nicholas DeForest, Gonçalo Mendes, Michael Stadler, Wei Feng, Judy Lai, and Chris Marnay. Optimal deployment of thermal energy storage under diverse economic and climate conditions. *Applied energy*, 119:488–496, 2014.
- Kun Deng, Yu Sun, Sisi Li, Yan Lu, Jack Brouwer, Prashant G Mehta, MengChu Zhou, and Amit Chakraborty. Model predictive control of central chiller plant with thermal energy storage via dynamic programming and mixed-integer linear programming. *IEEE Transactions on Automation Science and Engineering*, 12(2):565–579, 2015.
- John A Duffie and William A Beckman. *Solar engineering of thermal processes*. John Wiley & Sons, 2013.
- Energy market authority EMA. Demand side management. [https://www.ema.gov.sg/Demand\\_Side\\_Management.aspx](https://www.ema.gov.sg/Demand_Side_Management.aspx), 2015.

- Energy market authority EMA. Clarification on eligibility for participation in the demand response programme. [https://www.ema.gov.sg/cmsmedia/Electricity/Demand\\_Response/Demand%20Response%20Clarification%20Information%20Paper.pdf](https://www.ema.gov.sg/cmsmedia/Electricity/Demand_Response/Demand%20Response%20Clarification%20Information%20Paper.pdf), February 2016a.
- Energy Market Authority EMA. Policy framework for energy storage in singapore – consultation paper. [https://www.ema.gov.sg/ConsultationDetails.aspx?con\\_sid=20161021EB8aXV2UZsAp](https://www.ema.gov.sg/ConsultationDetails.aspx?con_sid=20161021EB8aXV2UZsAp), October 2016b.
- Energy Market Authority EMA. Launch of singapore’s first utility-scale energy storage system. [https://www.ema.gov.sg/media\\_release.aspx?news\\_sid=20171023Q2Ay3V8ycW9P](https://www.ema.gov.sg/media_release.aspx?news_sid=20171023Q2Ay3V8ycW9P), October 2017.
- Energy Market Authority EMA. Energy storage system for singapore – policy paper. <https://www.ema.gov.sg/cmsmedia/Final%20Determination%20Paper%20-%20ESS%20vf.pdf>, 2018a.
- Energy market authority EMA. Singapore energy statistics, 2018. [https://www.ema.gov.sg/Singapore\\_Energy\\_Statistics.aspx](https://www.ema.gov.sg/Singapore_Energy_Statistics.aspx), 2018b.
- Energy Market Authority EMA. Energy storage system (ess). [https://www.ema.gov.sg/Energy\\_Storage%20System.aspx](https://www.ema.gov.sg/Energy_Storage%20System.aspx), 2019a.
- Energy market authority EMA. Power system operator (pso). [https://www.ema.gov.sg/Power\\_System\\_Operator.aspx](https://www.ema.gov.sg/Power_System_Operator.aspx), 2019b.
- Energy market authority EMA. Our roles. [https://www.ema.gov.sg/Our\\_Roles.aspx](https://www.ema.gov.sg/Our_Roles.aspx), 2019c.
- Energy Market Company EMC. Provision of regulation by batteries. <https://www.emcsg.com/f1380,101679/EMC321-EMA-JO.pdf>, August 2015.
- Energy Market Company EMC. About us. <https://www.emcsg.com/aboutus>, 2019a.
- Energy Market Company EMC. Guide to prices. <https://www.emcsg.com/marketdata/guidetoprices>, 2019b.
- Energy Market Company EMC. Price information. <https://www.emcsg.com/marketdata/priceinformation>, 2019c.
- European Union Emissions Trading Scheme EUETS. Demand-side flexibility (dsf). <https://www.emissions-euets.com/internal-electricity-market-glossary/1141-demand-side-flexibility-dsf>, 2006.
- S Furbo. Using water for heat storage in thermal energy storage (tes) systems. In *Advances in Thermal Energy Storage Systems*, pages 31–47. Elsevier, 2015.

- Linus Gelazanskas and Kelum AA Gamage. Demand side management in smart grid: A review and proposals for future direction. *Sustainable Cities and Society*, 11:22–30, 2014.
- Geneco. Use of system charge. <https://www.geneco.sg/business/faq/use-of-system-charges/>, 2019.
- Tomasz T Gorecki, Faran A Qureshi, and Colin N Jones. Openbuild: An integrated simulation environment for building control. In *2015 IEEE Conference on Control Applications (CCA)*, pages 1522–1527. IEEE, 2015.
- The Guardian. "just a matter of when": the \$20bn plan to power singapore with australian solar. <https://www.theguardian.com/environment/2019/jul/14/just-a-matter-of-when-the-20bn-plan-to-power-singapore-with-australian-solar>, June 2019.
- Gurobi. About gurobi. <https://www.gurobi.com/company/about-gurobi/#mission>, 2019a.
- Gurobi. Gurobi optimizer. <https://www.gurobi.com/products/gurobi-optimizer/>, 2019b.
- William E Hart, Jean-Paul Watson, and David L Woodruff. Pyomo: modeling and solving mathematical programs in python. *Mathematical Programming Computation*, 3(3): 219, 2011.
- Holger Hesse, Rodrigo Martins, Petr Musilek, Maik Naumann, Cong Truong, and Andreas Jossen. Economic optimization of component sizing for residential battery storage systems. *Energies*, 10(7):835, 2017.
- Housing and Development Board. Solarnova. <https://www.hdb.gov.sg/cs/infoweb/about-us/our-role/smart-and-sustainable-living/solarnova-page>.
- Ronald Hunter Howell. *Principles of Heating Ventilating and Air Conditioning: A Textbook with Design Data Based on the 2017 Ashrae Handbook Fundamentals*. ASHRAE, 2017.
- International Energy Agency IEA. Energy efficiency 2018. <https://www.iea.org/efficiency2018/>, 2018.
- International Energy Agency IEA. Total final consumption statistics. <https://www.iea.org/statistics/kwes/consumption/>, 2019.
- IRENA. Thermal energy storage - technology brief. <https://irena.org/publications/2013/Jan/Thermal-energy-storage>, 2013.
- IRENA. Electricity storage and renewables: costs and markets to 2030. *International Renewable Energy Agency: Abu Dhabi, UAE*, 2017.

- ISEA. Technology overview on electricity storage. 2012. URL [http://www.sefep.eu/activities/projects-studies/120628\\_Technology\\_Overview\\_Electricity\\_Storage\\_SEFEP\\_ISEA.pdf](http://www.sefep.eu/activities/projects-studies/120628_Technology_Overview_Electricity_Storage_SEFEP_ISEA.pdf).
- Akhila Jambagi, Michael Kramer, and Vicky Cheng. Energy storage within a multi-energy carrier optimisation framework. In *2016 IEEE International Energy Conference (ENERGYCON)*, pages 1–6. IEEE, 2016.
- Keppel Electric KE. Fact sheet for non-standard price plan – knight. [https://www.keppelectric.com/Signup/EMA?txt\\_PlanTitle=KNIGHT&CCBPlanVersion=2&txt\\_Payment=Others&Opt\\_idType=NRIC&txt\\_icColor=Pink&txt\\_PropertyTypeID=4](https://www.keppelectric.com/Signup/EMA?txt_PlanTitle=KNIGHT&CCBPlanVersion=2&txt_Payment=Others&Opt_idType=NRIC&txt_icColor=Pink&txt_PropertyTypeID=4), 2019.
- Power Knot. Cops, eers, and seers. <http://www.powerknot.com/2011/03/01/cops-eers-and-seers/>, 2011.
- Michael Kramer, Akhila Jambagi, and Vicky Cheng. A model predictive control approach for demand side management of residential power to heat technologies. In *2016 IEEE International Energy Conference (ENERGYCON)*, pages 1–6. IEEE, 2016.
- Lazard. Lazard’s leveled cost of storage analysis – version 4.0. <https://www.lazard.com/media/450774/lazards-levelized-cost-of-storage-version-40-vfinal.pdf>, November 2018.
- Gang Li, Yunho Hwang, and Reinhard Radermacher. Review of cold storage materials for air conditioning application. *International journal of refrigeration*, 35(8):2053–2077, 2012.
- John H Lienhard. *A heat transfer textbook*. Courier Corporation, 2011.
- Yudong Ma, Francesco Borrelli, Brandon Hancey, Andrew Packard, and Scott Bortoff. Model predictive control of thermal energy storage in building cooling systems. In *Proceedings of the 48th IEEE Conference on Decision and Control (CDC) held jointly with 2009 28th Chinese Control Conference*, pages 392–397. IEEE, 2009.
- Abhishek Malhotra, Benedikt Battke, Martin Beuse, Annegret Stephan, and Tobias Schmidt. Use cases for stationary battery technologies: A review of the literature and existing projects. *Renewable and Sustainable Energy Reviews*, 56:705–721, 2016.
- Bruce A McCarl and Thomas H Spreen. *Applied mathematical programming using algebraic systems*. Cambridge, MA, 1997.
- Ministry of Foreign Affairs MFA. Towards a sustainable and resilient singapore. [https://sustainabledevelopment.un.org/content/documents/19271Singapores\\_Voluntary\\_National\\_Review\\_Report.pdf](https://sustainabledevelopment.un.org/content/documents/19271Singapores_Voluntary_National_Review_Report.pdf), 2018.

- Marcus Müller, Lorenz Viernstein, Cong Nam Truong, Andreas Eiting, Holger C Hesse, Rolf Witzmann, and Andreas Jossen. Evaluation of grid-level adaptability for stationary battery energy storage system applications in europe. *Journal of Energy Storage*, 9:1–11, 2017.
- National Climate Change Secretariat NCCS. Singapore’s climate action plan - how a carbon tax works. <https://www.nccs.gov.sg/docs/default-source/default-document-library/how-a-carbon-tax-works.pdf>.
- National Climate Change Secretariat NCCS. A climate-resilient singapore, for a sustainable future. <https://www.nccs.gov.sg/docs/default-source/publications/a-climate-resilient-singapore-for-a-sustainable-future.pdf>, 2016a.
- National Climate Change Secretariat NCCS. Take action today, for a carbon-efficient singapore. <https://www.nccs.gov.sg/docs/default-source/publications/take-action-today-for-a-carbon-efficient-singapore.pdf>, 2016b.
- National Climate Change Secretariat NCCS. Singapore’s fourth national communication and third biennial update report. <https://www.nccs.gov.sg/docs/default-source/default-document-library/singapore-s-fourth-national-communication-and-third-biennial-update-repo.pdf>, December 2018.
- Nordic Council of Ministers NCM. Demand side flexibility in the nordic electricity market. [https://www.nordicenergy.org/wp-content/uploads/2017/12/Demand-side-flexibility\\_-DSO-perspective.pdf](https://www.nordicenergy.org/wp-content/uploads/2017/12/Demand-side-flexibility_-DSO-perspective.pdf), 2017.
- Open Electricity Market OEM. Singapore’s market overview. <https://www.openelectricitymarket.sg/about/market-overview>, 2019.
- Noshin Omar, Mohamed Abdel Monem, Yousef Firouz, Justin Salminen, Jelle Smekens, Omar Hegazy, Hamid Gaulous, Grietus Mulder, Peter Van den Bossche, Thierry Coosemans, et al. Lithium iron phosphate based battery–assessment of the aging parameters and development of cycle life model. *Applied Energy*, 113:1575–1585, 2014.
- Samuel Prívar, Zdeněk Váňa, Dimitrios Gyalistras, Jiří Cigler, Carina Sagerschnig, Manfred Morari, and Lukáš Ferkl. Modeling and identification of a large multi-zone office building. In *2011 IEEE International Conference on Control Applications (CCA)*, pages 55–60. IEEE, 2011.
- PYOMO. Pyomo documentation release 5.6.7.dev0. <https://buildmedia.readthedocs.org/media/pdf/pyomo/latest/pyomo.pdf>, June 2019.

- James B Rawlings, Nishith R Patel, Michael J Risbeck, Christos T Maravelias, Michael J Wenzel, and Robert D Turney. Economic mpc and real-time decision making with application to large-scale hvac energy systems. *Computers & Chemical Engineering*, 114:89–98, 2018.
- RDP Red Dot Power. Red dot power partners with ema to launch project optiwatt. <https://www.reddotpower.com.sg/in-the-news/2016/11/8/red-dot-power-partners-with-ema-to-launch-project-optiwatt>, November 2016.
- Michel Rieutord. *Fluid dynamics: an introduction*. Springer, 2014.
- Michael J Risbeck, Christos T Maravelias, James B Rawlings, and Robert D Turney. Closed-loop scheduling for cost minimization in hvac central plants. 2016.
- Michael J Risbeck, Christos T Maravelias, James B Rawlings, and Robert D Turney. A mixed-integer linear programming model for real-time cost optimization of building heating, ventilation, and air conditioning equipment. *Energy and Buildings*, 142: 220–235, 2017.
- Derek Rowell. State-space representation of lti systems. <http://web.mit.edu/2.14/www/Handouts/StateSpace.pdf>, October 2002.
- Diego Sandoval, Philippe Goffin, and Hansjürg Leibundgut. How low exergy buildings and distributed electricity storage can contribute to flexibility within the demand side. *Applied energy*, 187:116–127, 2017.
- Bruno Scrosati and Jürgen Garche. Lithium batteries: Status, prospects and future. *Journal of power sources*, 195(9):2419–2430, 2010.
- Smart Energy Demand Coalition SEDC. Explicit and implicit demand-side flexibility. <https://www.smartenergy.eu/wp-content/uploads/2016/09/SEDC-Position-paper-Explicit-and-Implicit-DR-September-2016.pdf>, September 2016.
- Gianluca Serale, Massimo Fiorentini, Alfonso Capozzoli, Daniele Bernardini, and Alberto Bemporad. Model predictive control (mpc) for enhancing building and hvac system energy efficiency: Problem formulation, applications and opportunities. *Energies*, 11(3):631, 2018.
- Claudia SOUSA MONTEIRO, Carlos Cerezo, André Pina, and Paulo Ferrão. A method for the generation of multi-detail building archetype definitions: Application to the city of lisbon. In *Proceedings of International Conference CISBAT 2015 Future Buildings and Districts Sustainability from Nano to Urban Scale*, number CONF, pages 901–906. LESO-PB, EPFL, 2015.

- SPGroup. About sp group. <https://www.spgroup.com.sg/about-us/corporate-profile>, a.
- SPGroup. Electricity tariffs. [https://www.ema.gov.sg/Residential\\_Electricity\\_Tariffs.aspx](https://www.ema.gov.sg/Residential_Electricity_Tariffs.aspx), b.
- Lorenzo Spinelli. *Principi di climatizzazione ambientale*. Technical report, Politecnico di Milano, 2015.
- Ana-Irina Stan, Maciej Świerczyński, Daniel-Ioan Stroe, Remus Teodorescu, and Søren Juhl Andreasen. Lithium ion battery chemistries from renewable energy storage to automotive and back-up power applications—an overview. In *2014 International Conference on Optimization of Electrical and Electronic Equipment (OPTIM)*, pages 713–720. IEEE, 2014.
- Joseph E Stiglitz, Nicholas Stern, Maosheng Duan, Ottmar Edenhofer, Gaël Giraud, Geoffrey M Heal, Emilio Lèbre la Rovere, Adele Morris, Elisabeth Moyer, Mari Pangestu, et al. Report of the high-level commission on carbon prices. 2017.
- Yongjun Sun, Shengwei Wang, Fu Xiao, and Diance Gao. Peak load shifting control using different cold thermal energy storage facilities in commercial buildings: A review. *Energy conversion and management*, 71:101–114, 2013.
- SunCable. Project overview. <https://www.suncable.sg/>, 2019.
- SUNSEAP. Sunseap to build one of the world’s first and largest sea water floating solar systems. <https://www.sunseap.com/sunseap-to-build-one-of-the-worlds-first-and-largest-sea-water-floating-solar-systems/>, November, 9 2019.
- Rui Tang, Shengwei Wang, and Lei Xu. An mpc-based optimal control strategy of active thermal storage in commercial buildings during fast demand response events in smart grids. *Energy Procedia*, 158:2506–2511, 2019.
- The Strait Times. Sun seeker at sea: One of the world’s largest offshore floating solar systems will soon be soaking up the rays along the strait of johor. <https://www.straitstimes.com/singapore/sun-seeker-at-sea>, 2019.
- Climate Action Tracker. Singapore emissions. <https://climateactiontracker.org/countries/singapore/>, June, 17 2019.
- N Tran, JF Kreider, and P Brothers. Field measurement of chilled water storage thermal performance. *ASHRAE transactions*, 95:1106–1112, 1989.
- Sebastian Troitzsch, Sarmad Hanif, and Thomas Hamacher. Distributed robust reserve scheduling in congested distribution systems. In *2018 IEEE Power & Energy Society General Meeting (PESGM)*, pages 1–5. IEEE, 2018.

- TUMCREATE-ESTL. Control-oriented building model. <https://github.com/TUMCREATE-ESTL/cobmo>, 2019.
- United Nations Framework Convention on Climate Change UNFCCC. Singapore's intended nationally determined contribution (indc) and accompanying information. <https://www4.unfccc.int/sites/ndcstaging/PublishedDocuments/Singapore%20First/Singapore%20INDC.pdf>, 2016.
- US Department of Energy US DoE. Introduction: Energyplus essentials — energyplus 9.1. <https://bigladdersoftware.com/epx/docs/9-1/essentials/title.html>, 2019a.
- US Department of Energy US DoE. Full documentation | energyplus. <https://energyplus.net/documentation>, 2019b.
- US Department of Energy US DoE. Energyplus™. <https://energyplus.net/>, 2019c.
- Universal Smart Energy Framework USEF. Flexibility value chain. <https://www.usef.energy/new-update2018-flexibility-value-chain/>, 2018.
- Rachel Warren. Environmental economics: Optimal carbon tax doubled. *Nature Climate Change*, 4(7):534, 2014.
- Sven Werner. International review of district heating and cooling. *Energy*, 137:617–631, 2017.
- MW Wildin and CR Truman. A summary of experience with stratified chilled water tanks. *ASHRAE transactions*, 91(1):956–976, 1985.
- Dinçer İbrahim and Rosen Marc A. *Thermal Energy Storage: Systems and Applications, Second Edition*. Wiley, 2010.